Scanning Theory with Application to High Definition Television (HDTV)

Gianfranco Cariolaro

Department of Information Engeneering, University of Padova, Italy

cariolar@dei.unipd.it

Abstract Given a time–varying image, or more generally a multi–dimensional source, a *scanning* process eventually produces a one–dimensional signal suitable for transmission or recovery. *Reproduction* is the converse process.
The paper deals with a signal theory approach to scanning and reproduction, in which such processes are decomposed into elementary operations, such as frame–limitation, sampling, change of signal dimensionality (3D to 1D and 1D to 3D), etc. To derive a general theory capable of including the different scanning formats of interest (continuous or discrete, progressive, interlaced or multiply interlaced) a unified signal theory is used, in which signals (and their Fourier transforms) are defined on Abelian groups.
A universal model of the scanning process is proposed, in which a specific format is uniquely specified by a 3D Abelian group. The remaining scanning parameters are then determined by the condition that the scanning process be invertible (by the reproduction process). The model is analyzed in the frequency domain with both deterministic and random inputs.
The theory is finally applied to multiplexing luminance and chrominance signals in HDTV systems.

This report was written in 1986 in the framework of the European project HD–MAC for high definition television.

1 Introduction

The *scanning process* may be regarded as a set of operations which, starting from a time–varying image, more generally from a multi–dimensional source, finally produces a one–dimensional signal (hereafter, the *video signal*), i.e. a signal suitable for transmission or recovery. The *reproduction process* consists of the inverse operations.

The television scanning theory began with television itself, with the fundamental work of Mertz and Gray [41], who introduced the *periodic model* of scanning. Later fundamental contributions were made by Robinson [37], Drewery [42], Tonge [43] [44] [45] and Dubois [39]. However, to the author's knowledge a systematic approach with an appropriate "signal formulation" has never been proposed. In fact, as will soon be evident, a "signal formulation" is essential for the kind of operations involved in scanning and reproduction.

To begin, let us consider the simplest form of scanning process, according to the *progressive 1:1 format*, with the aim of illustrating the nature and variety of the operations involved. The source image is spatially unlimited, so that the first operation is to limit the image to the *frame* (Fig.1), a rectangle $Q = [0, D_x) \times [0, D_y)$. The limited image is temporally sampled to capture pictures (or *fields*) every T_q seconds and each field is divided into N equally spaced *lines* (vertical sampling). Finally, the lines of each field are sequentially read to pick up a signal proportional

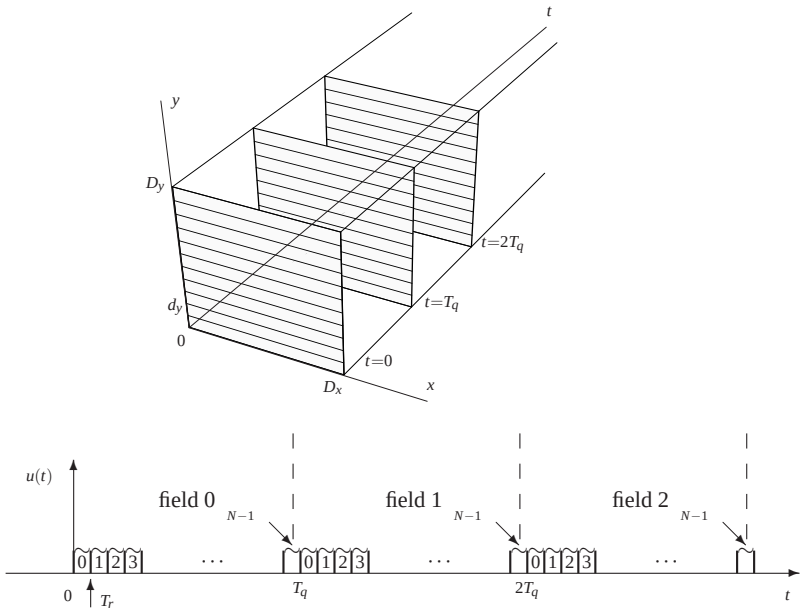

Fig. 1 The grating of progressive scanning (with memory) of a time–varying image and the corresponding *video* signal $u(t)$

to the image luminance (or chrominance). Thus, the video signal consists of replicas of the image signal portions limited by the line–field format.

The equations for the operations described are as follows. The time–varying source image is a 3D signal, which we write in the form

$$\ell(x,y,t)\,, \qquad (x,y,t) \in \mathbb{R}^3$$

where x, y and t are the horizontal, vertical and temporal coordinates, respectively. All three coordinates are continuous and unlimited, so that each takes a value from the set of real numbers $\mathbb{R}$. The frame limitation[1] is simply expressed by the relationship

$$\ell_Q(x,y,t) = w_Q(x,y)\,\ell(x,y,t)\,, \qquad (x,y,t) \in \mathbb{R}^3 \tag{1}$$

where $w_Q(x,y)$ is the indicating function of the frame Q. Hence, $\ell_Q(x,y,t)$ is set to zero outside the frame. The image domain after sampling, i.e. the subset of $\mathbb{R}^3$ consisting of the field–line format, can be written as the Cartesian product:

$$I_S = \mathbb{R} \times \mathbb{Z}(d_y) \times \mathbb{Z}(T_q) \tag{2}$$

where $\mathbb{Z}(d) \stackrel{\Delta}{=} \{nd \mid n \in \mathbb{Z}\}$, $d_y = D_y/N$ is the vertical line spacing, and T_q is the frame period. Hence, the sampling operation is given by

$$\ell_{QS}(x,y,t) = \ell_Q(x,y,t)\,, \qquad (x,y,t) \in I_S \tag{3}$$

where $(x,y,t) \in I_S$ states that $\ell_{QS}(\cdot)$ is obtained from $\ell_Q(\cdot)$ by a domain *restriction* from $\mathbb{R}^3$ to I_S.

The final 3D→1D conversion, which produces the video signal *by reading* the image along the I_S lines, can be written in the form

$$u(t) = \sum_{n=-\infty}^{+\infty} \sum_{k=-\infty}^{+\infty} \ell_{QS}\Big(v_x(t - nT_r - kT_q), nd_y, kT_q\Big)\,, \qquad t \in \mathbb{R} \tag{4}$$

where v_x is the horizontal velocity of the line reading operation and $T_r = T_q/N$ is the line period. In (4) n could be limited from 0 to $N-1$. However, after frame limitation the infinite summation would not add new contributions. Moreover, $\ell_{QS}(\cdot)$ could be replaced by $\ell_Q(\cdot)$ since in (4) it is automatically confined within I_S, but with this replacement we would lose the underlying sampling operation, with awkward consequences for the frequency domain analysis.

From the above simple formulation we can make the following observations. The scanning operation involves different kinds of signals: the source image is a 3D signal defined on $\mathbb{R}^3$, and remains so after frame limitation, the sampled image is defined on the 3D (*discrete*) *grating* I_S, given by (2), and the video signal is a continuous–time 1D signal defined on $\mathbb{R}$. If we pass from *continuous* scanning to *discrete* scanning, where even the horizontal coordinate becomes discrete, I_S be-

[1] The frame limitation is usually neglected in the literature. Its introduction, however, is essential for a correct formulation of the scanning process.

comes a 3D *lattice* of the form

$$I_S = \mathbb{Z}(d_x) \times \mathbb{Z}(d_y) \times \mathbb{Z}(T_q)\,, \tag{5}$$

where d_x is the horizontal spacing, so that the final video signal becomes a discrete–time signal whose domain is of the form $\mathbb{Z}(T_e)$, where T_e is the *pixel period*.

If we go from the 1:1 progressive format to the 2:1 interlace format, and to higher order interlace formats, we will find a variety of discrete gratings and lattices, with the novelty that they are no longer factorisable as in (2) and (5).

Finally, we note that the continuous 1:1 progressive scanning outlined above may be taken as an approximation to the real scanning process performed by conventional cameras, since we have tacitly assumed that the image fields are taken at the instants kT_q, $k \in \mathbb{Z}$, like film frames, and that the line scanning is performed on these fixed–time frames (Fig. 2a). This model will hereafter be called the *memory model*, since it implies image storage at field level. In conventional cameras, lines are not taken from a fixed–time frame since the image signal evolves during line scanning operations so that we have to write $\ell(\cdot,\cdot,t)$ rather than $\ell(\cdot,\cdot,kT_q)$. We then pass to the *instantaneous model* (Fig. 2b), where fields and lines are tilted with respect to the x,y plane and the grating must be modified to

$$I_S = \left\{ v_x(t - nT_r - kT_q),\, v_y(t - nT_r - kT_q) + nd_y,\, t \;\middle|\; n,k \in \mathbb{Z}\,,\; t \in \mathbb{R} \right\} \tag{6}$$

where v_x and v_y are the horizontal and vertical velocities, respectively.

In conclusion, a large variety of signals are involved in scanning theory, so that a unified signal theory approach is essential.

The paper is organized as follows. In Section II we give the signal theory preliminaries needed for a general formulation of the scanning theory. These are essentially: a unified formulation of signals and Fourier transforms based on Abelian groups, a

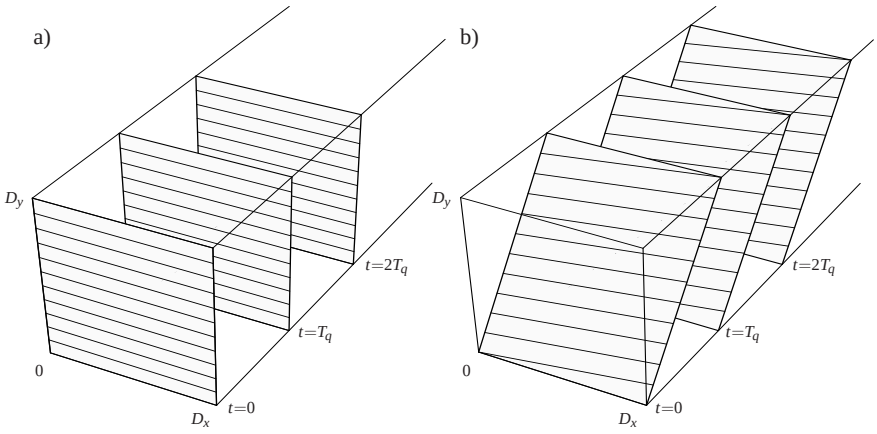

Fig. 2 The two fundamental models of scanning: a) the *memory* progressive scanning **M**(1:1) and b) the *instantaneous* progressive scanning **I**(1:1).

unified formulation of linear systems, which may include a change of signal dimensionality, and theorems concerning the possibility of signal recovery after sampling and dimensionality reduction.

Section IV deals with the *scanning group*, i.e. the subset of $\mathbb{R}^3$ on which the time–varying image is picked up.

Sections V and VI deal with the two universal scanning models (periodic and aperiodic), in which a given scanning process is completely specified by a scanning group. The remaining parameters are implied by the condition of invertibility, i.e. by imposing a correct recovery of the time–varying image from the video signal by the reproduction process. In Section VII and VIII these models are used for the frequency domain *analysis* of the scanning and reproduction processes.

In the final section the theory is applied to study the MAC multiplexing of luminance and chrominance components used in the European proposal for HDTV.

2 Unified Signal Theory

In this section we summarize the Unified Signal Theory [23] [22] [25], of which scanning theory is the most successful application to date. The fact that all signal domains are Abelian groups is the key to unification.

2.1 Abelian groups in $\mathbb{R}^m$

Only subgroups of $\mathbb{R}^m$, the additive groups of the m–tuples of real numbers, are considered. The 1D additive groups $\mathbb{R}$, $\mathbb{Z}$ and $\mathbb{O} \stackrel{\Delta}{=} \{0\}$, the *trivial* group, are used as a reference to construct multi–dimensional groups.

Definition 1. Let $\mathbf{J}$ be a non–singular $m \times m$ real matrix and let $H = H_1 \times \cdots \times H_m$, where H_i may be either $\mathbb{R}$ or $\mathbb{Z}$ or $\mathbb{O}$. An Abelian group in $\mathbb{R}^m$ specified by the pair $(\mathbf{J}, H)$ is the set

$$J = \left\{ \mathbf{Jh} \mid \mathbf{h} \in H \right\}, \tag{7}$$

where the matrix $\mathbf{J}$ is the *base* of the group, H is the *signature*, and the pair $(\mathbf{J}, H)$ is a *representation* of the group. □

By partitioning the base $\mathbf{J}$ into its column vectors, say $\mathbf{J} = [\mathbf{j}_1 \dots \mathbf{j}_m]$, we find that $\mathbf{j}_1, \dots, \mathbf{j}_m$ are linearly independent real vectors of the m–dimensional Euclidean space $\mathbb{R}^m$ (denoted by the same symbol as the corresponding group). Letting[2] $\mathbf{h} = (h_1, \dots, h_m)$, the compact form (7) becomes

$$J = \left\{ h_1\mathbf{j}_1 + \ldots + h_m\mathbf{j}_m \mid h_1 \in H_1, \dots, h_m \in H_m \right\}, \tag{7a}$$

[2] In matrix operations, m–tuples of the form $(h_1, \dots, h_m)$ denote column vectors.

which states that J is given by all the linear combinations of the vectors $\mathbf{j}_1, \ldots, \mathbf{j}_m$, where the i–th coefficient is real if $H_i = \mathbb{R}$, integer if $H_i = \mathbb{Z}$ and zero if $H_i = \mathbb{O}$.

The signature H states the nature of the group. If $H = \mathbb{R}^m$ the group J is $\mathbb{R}^m$ itself (the *continuous* m–dimensional group). If $H = \mathbb{Z}^m$ the group J is a *lattice* (a discrete m–dimensional group). If $H = \mathbb{R}^p \times \mathbb{Z}^{m-p}$ with $1 \leq p < m$ or a permutation of such factors, the group is a *grating* (a mixed m–dimensional group). The signature also states the dimension of the group: if H does not contain $\mathbb{O}$ the group is *full–dimensional*, otherwise *reduced–dimensional*.[3] More specifically, if H contains $\mathbb{O}$ $m-n$ times, the group is said to be *an n–dimensional group in $\mathbb{R}^m$*. Thus, if $m = 3$ and $H = \mathbb{Z}^2 \times \mathbb{O}$ the group is a two–dimensional lattice in $\mathbb{R}^3$. We shall always assume that signal domains are full–dimensional groups; reduced–dimensional groups will only be considered in connection with periodicity (see below).

A few examples of groups are illustrated in Fig.3: at the top we have a 2D grating

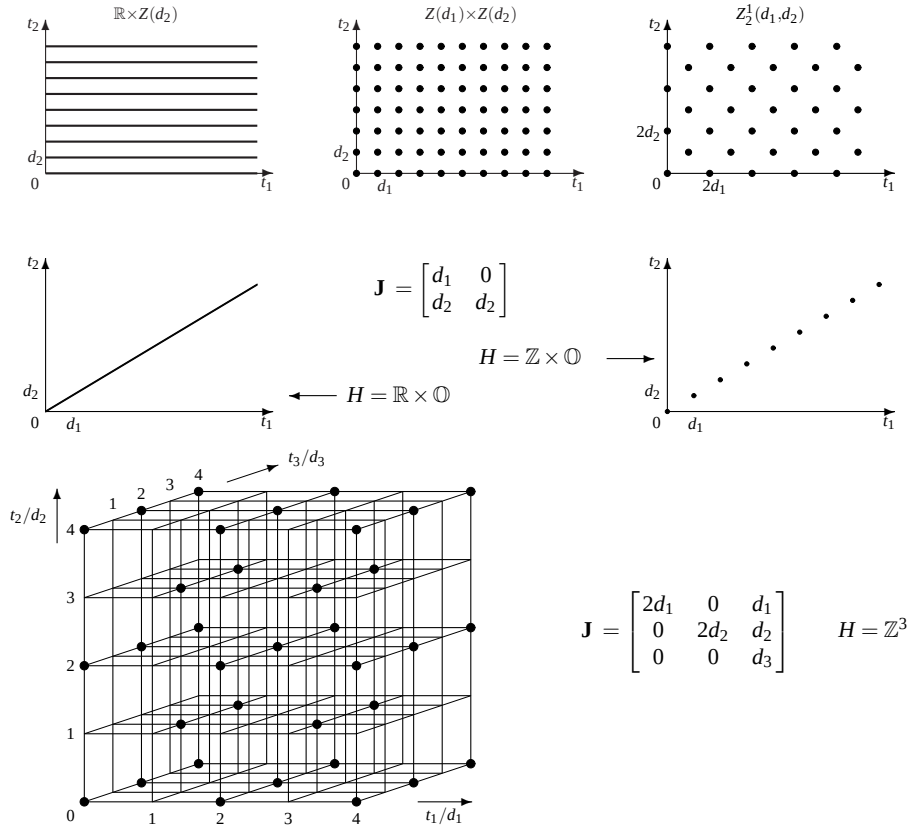

Fig. 3 Examples of groups in $\mathbb{R}^2$ and in $\mathbb{R}^3$.

[3] Reduced–dimensional groups could be introduced by letting the base matrix be singular, but we find it more convenient to work on the signature.

and two 2D lattices, at center a 1D grating and a 1D lattice in $\mathbb{R}^2$, and at bottom a 3D lattice. Note that Fig.2 gives two examples of 3D gratings with signature $\mathbb{R}\times\mathbb{Z}^2$.

The above is a generalization of the lattice definition [39]. Note that within the lattice class the signature specification is redundant; it is, however, essential for the present, more general class.

2.2 On group representations

The representation $(\mathbf{J},H)$ of a group J is not unique. Firstly, the combined permutation of the columns of $\mathbf{J}$ and of the factors of H yields the same group J. Hence, without loss of generality, the signature of an m–dimensional group can be written in the form $\mathbb{R}^p\times\mathbb{Z}^q\times\mathbb{O}^s$ with $p+q+s=m$ and $p,q,s\geq 0$. Secondly, for a fixed signature H, the base is not unique. In particular, for a full–dimensionality lattice J with base $\mathbf{J}$ any matrix of integers $\mathbf{E}$ such that $\det\mathbf{E}=\pm 1$, the matrix $\mathbf{EJ}$ provides another base for J [61]. For the continuous group $\mathbb{R}^m$ any non–singular matrix is a correct base. Finally, intermediate considerations hold for gratings (see below).

Hereafter, the notation $(\mathbf{J},H)\mapsto J$ stands for "the group J determined by the representation $(\mathbf{J},H)$".

Canonical representations. It is often convenient to refer to "canonical" (or "minimal") representations to economize on specification and to simplify comparisons. For full–dimensional groups the signature can be set to the standard form $\mathbb{R}^p\times\mathbb{Z}^q$, whereas the simplification of the base depends on the nature of the group. For the continuous group $\mathbb{R}^m$ the identity matrix is the canonical base.

Theorem 1. *For a grating with signature $\mathbb{R}^p\times\mathbb{Z}^q$ a canonical base has the partitioned form*

$$\mathbf{J}_\delta=\begin{bmatrix}\boldsymbol{\delta} & \mathbf{0}\\ \mathbf{E} & \mathbf{F}\end{bmatrix} \tag{8}$$

where $\boldsymbol{\delta}$ is the $p\times p$ identity matrix, $\mathbf{0}$ is $p\times q$, $\mathbf{E}$ is $q\times p$ and $\mathbf{F}$ is a non singular $q\times q$ matrix. □

Note that with such a base the scanning point on the grating can be written in the form $\mathbf{t}=(\mathbf{t}_r,\mathbf{t}_d)$ with

$$\mathbf{t}_r=\mathbf{r}\,,\qquad \mathbf{t}_d=\mathbf{E}\mathbf{r}+\mathbf{n}\,,\qquad \mathbf{r}\in\mathbb{R}^p\,,\ \mathbf{n}\in F \tag{9}$$

where F is the q–dimensional lattice $F=\{\mathbf{F}\mathbf{s}\mid\mathbf{s}\in\mathbb{Z}^q\}$.

The form (8) can be obtained by starting from an arbitrary representation [25]. We illustrate the procedure for the 3D grating of the instantaneous scanning model. The coordinates in (6) are given by

$$\begin{bmatrix}x\\ y\\ t'\end{bmatrix}=\begin{bmatrix}v_x & -v_xT_r & -v_xT_q\\ v_y & -v_yT_r+d_y & -v_yT_q\\ 1 & 0 & 0\end{bmatrix}\begin{bmatrix}t\\ n\\ k\end{bmatrix}\,,\quad t\in\mathbb{R}\,,\ (n,k)\in\mathbb{Z}^2\,.$$

Since $x \in \mathbb{R}$ we can set $x = r \in \mathbb{R}$ to get

$$\begin{bmatrix} x \\ y \\ t' \end{bmatrix} = \begin{bmatrix} 1 & 0 & 0 \\ v_y/v_x & d_y & 0 \\ 1/v_x & T_r & T_q \end{bmatrix} \begin{bmatrix} r \\ n \\ k \end{bmatrix}, \quad r \in \mathbb{R}\,,\ (n,k) \in \mathbb{Z}^2$$

where the 3×3 matrix has the minimal form (8) with $p = 1$ and $q = 2$.

For lattices the minimization is less trivial. In the sublattice class of the orthogonal lattice $\mathbb{Z}(d_1,\ldots,d_m) \stackrel{\Delta}{=} \mathbb{Z}(d_1) \times \cdots \times \mathbb{Z}(d_m)$ the following result holds [25] [40].

Theorem 2. *The base* $\mathbf{J}_0$ *of any sublattice of* $\mathbb{Z}(d_1,\ldots,d_m)$ *can be written in the upper–triangular form*

$$\mathbf{J}_0 = \begin{bmatrix} d_1 & 0 & \ldots & 0 \\ 0 & d_2 & \ldots & 0 \\ \vdots & \vdots & \ddots & 0 \\ 0 & 0 & \ldots & d_m \end{bmatrix} \begin{bmatrix} a_{11} & a_{12} & \ldots & a_{1m} \\ 0 & a_{22} & \ldots & a_{2m} \\ \vdots & \vdots & \ddots & \vdots \\ 0 & 0 & \ldots & a_{mm} \end{bmatrix} \tag{10}$$

where the diagonal matrix is the base of $\mathbb{Z}(d_1,\ldots,d_m)$*. The triangular matrix consists of non–negative integers, with positive diagonal entries and non–diagonal entries that are smaller than the corresponding diagonal entries. A lower–triangular form with the same constraints is also possible.*

Example 1. The *quincunx* lattice $Z_2^1(d_1,d_2)$ is the set of pairs $(n_1 d_1, n_2 d_2)$ where n_1 and n_2 are either both odd, or both even integers. It is a sublattice of $\mathbb{Z}(d_1,d_2)$ with canonical bases

$$\begin{bmatrix} d_1 & 0 \\ 0 & d_2 \end{bmatrix} \begin{bmatrix} 2 & 1 \\ 0 & 1 \end{bmatrix}, \qquad \begin{bmatrix} d_1 & 0 \\ 0 & d_2 \end{bmatrix} \begin{bmatrix} 1 & 0 \\ 2 & 1 \end{bmatrix}.$$

A general sublattice of $\mathbb{Z}(d_x,d_y)$ will be denoted by $Z_i^b(d_1,d_2)$, where i and b are integers, with $0 < b < i$, and b relatively prime to i. The corresponding triangular bases are

$$\begin{bmatrix} d_1 & 0 \\ 0 & d_2 \end{bmatrix} \begin{bmatrix} i & b \\ 0 & 1 \end{bmatrix}, \qquad \begin{bmatrix} d_1 & 0 \\ 0 & d_2 \end{bmatrix} \begin{bmatrix} 1 & 0 \\ \tilde{b} & i \end{bmatrix} \tag{11}$$

where $\tilde{b}$ is the solution of the integer equation $mi + \tilde{b}b = 1$, with $m \in \mathbb{Z}$ and $0 < \tilde{b} < i$. □

Manipulation rules. The triangularization procedure of an arbitrary base and conversion from lower–triangular to upper–triangular form are, in general, not trivial, even if they can be mechanized [70].

We recall the following rules for lattice base transformations

1) a column multiplied by an arbitrary integer can be added to another column,
2) a column can be multiplied by -1.

The application of these rules, possibly repeated, to a given base $\mathbf{J}$ is equivalent to a left multiplication by an integer matrix $\mathbf{E}$ with $\det\mathbf{E} = \pm 1$, and therefore does not change the lattice. We give the following example of manipulation

$$\mathbf{J} = \begin{bmatrix} 3 & 7 & 4 \\ 2 & -5 & -3 \\ 0 & 0 & -1 \end{bmatrix} \to \begin{bmatrix} 3 & 16 & 4 \\ 2 & 1 & -3 \\ 0 & 0 & -1 \end{bmatrix} \to \begin{bmatrix} -29 & 16 & 4 \\ 0 & 1 & -3 \\ 0 & 0 & -1 \end{bmatrix}$$
$$\to \begin{bmatrix} -29 & 16 & 52 \\ 0 & 1 & 0 \\ 0 & 0 & -1 \end{bmatrix} \to \begin{bmatrix} 29 & 16 & -52 \\ 0 & 1 & 0 \\ 0 & 0 & 1 \end{bmatrix} \to \begin{bmatrix} 29 & 16 & 6 \\ 0 & 1 & 0 \\ 0 & 0 & 1 \end{bmatrix}$$

where the last is an upper–triangular form with the constraint of Theorem 2.

Determinant and density of a group. The absolute value of the base determinant, $d(\mathbf{J}) \stackrel{\Delta}{=} |\det \mathbf{J}|$, is the *determinant*, its reciprocal $\mu(\mathbf{J}) \stackrel{\Delta}{=} 1/|\det \mathbf{J}|$ is the *density* of the group $(\mathbf{J}, H) \mapsto J$. In general, $d(\mathbf{J})$ and $\mu(\mathbf{J})$ depend on the specific base of the group. For a lattice J they are independent of $\mathbf{J}$ and consequently denoted by $d(J)$ and $\mu(J)$; $\mu(J)$ effectively represents the lattice *density*, measured in number of points per unit volume of $\mathbb{R}^m$. In any case, referring to a canonical representation the above quantities become specific to the group.

Group transformations and improper representations. Let $(\mathbf{J}, H) \mapsto J$ and let $\mathbf{A}$ be a non singular $m \times m$ real matrix. The linear relationship $\mathbf{v} = \mathbf{At}$, $\mathbf{t} \in J$, defines the scanning point on a new group in $\mathbb{R}^m$

$$K = \{\mathbf{At} \mid \mathbf{t} \in J\} = \{\mathbf{AJh} \mid \mathbf{h} \in H\}$$

with representation $(\mathbf{AJ}, H)$. Comparison of the last relationship with (7) shows that any group J can be thought of as a linear transformation of its signature H. The pair $(\mathbf{A}, J)$, which uniquely determines the group K, may be regarded as an *improper representation* of K, with *improper base* $\mathbf{A}$ and *improper signature* J.

As an example, the lattice $Z_i^b(d_1, d_2)$ has a *proper representation* $(\mathbf{J}, \mathbb{Z}^2)$, where $\mathbf{J}$ may be one the matrices given by (11). The same lattice has the *improper representation*

$$\begin{bmatrix} d_1 & 0 \\ 0 & d_2 \end{bmatrix}, \qquad Z_i^b(1,1). \tag{12}$$

2.3 Regular pairs and unit cells

Unit cells play a fundamental role in an advanced signal theory.

Definition 2. Let I_0 be a group in $\mathbb{R}^m$ and S a subgroup of I_0. This will be called a *group pair* in $\mathbb{R}^m$ and denoted by $I_0 : S$. The pair is said to be *regular* if I_0 is full–dimensional and S_0 is a lattice.

Definition 3. Let $I_0 : S$ be a group pair in $\mathbb{R}^m$. Any subset C of I_0 is a *unit cell of* I_0 *modulo* S if the sets[4] $C+\mathbf{s}$, $\mathbf{s} \in S$ form a *partition* of I_0, i.e. $\bigcup_{\mathbf{s}\in S}[C+\mathbf{s}] = I_0$ and $(C+\mathbf{s}) \cap (C+\mathbf{t}) = \emptyset$, $\mathbf{s} \neq \mathbf{t}$.

Group pairs will be used in signal and Fourier transform specifications. The standard definition of unit cells usually refers to the case $I_0 = \mathbb{R}^m$ and S given by a full–dimension lattice [39], but the definition given here it is general.

Note that any member of the class $C+\mathbf{s}$, $\mathbf{s} \in S$, is itself a unit cell, so that the class represents *a partition of* I_0 *into unit cells*. We shall denote a unit cell determined by the pair $I_0 : S$ in the form[5] $[I_0 : S)$; hence, the partition of I_0 can be written as

$$[I_0 : S) + S = I_0 \,. \tag{13}$$

Fig.4 illustrates two examples of 2D unit cells for the standard case where $I_0 = \mathbb{R}^2$

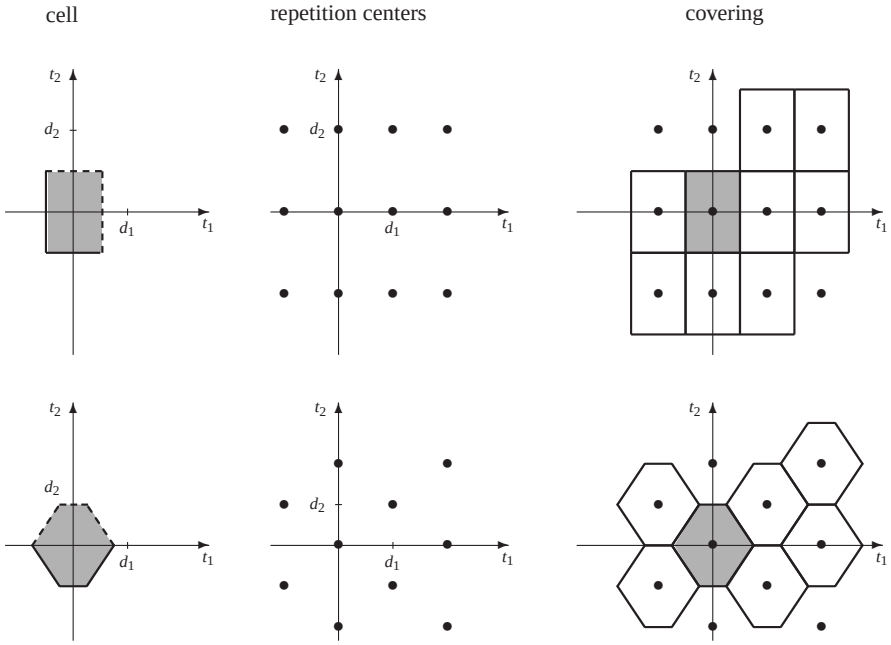

Fig. 4 Examples of cells of $\mathbb{R}^2$ modulo $\mathbb{Z}(d_1, d_2)$ and of $\mathbb{R}^2$ modulo $\mathbb{Z}_2^1(d_1, d_2)$

and S is a lattice. Fig.5 illustrates four examples of 2D discrete unit cells where both I_0 and S are lattices.

Proposition 1. $[I_0 : \mathbb{O}^m) = I_0$ *and* $[I_0 : I_0) = \mathbb{O}^m$ *for an arbitrary group* I_0.

[4] $C+\mathbf{s}$ denotes the *translated* set $\{\mathbf{c}+\mathbf{s} \mid \mathbf{c} \in C\}$.

[5] This notation recalls that right open intervals, such as [0,1) or $[-\frac{1}{2}, \frac{1}{2})$, are unit cells of $\mathbb{R}$ modulo $\mathbb{Z}$. More generally, $[a+d, d) = [\mathbb{R} : \mathbb{Z}(d))$ for any $d \in \mathbb{R}$.

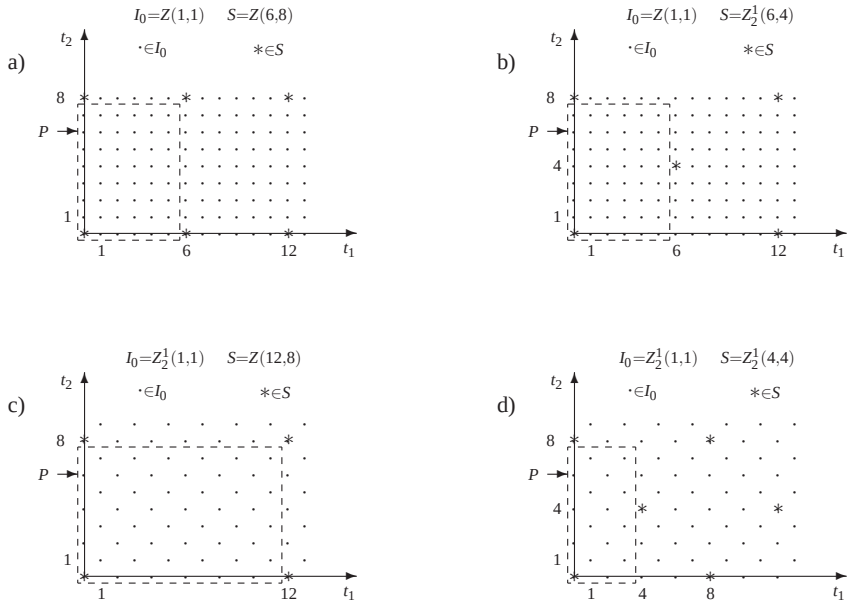

Fig. 5 Examples of 2D discrete unit cells P: cell points are enclosed in a dashed box.

Proposition 2. *If I_0 and S are full–dimensional lattices, the unit cell $[I_0 : S)$ is a finite set whose number of points is given by $d(S)/d(I_0) = \mu(I_0)/\mu(S)$.*

Proposition 3. *Let $(\mathbf{S}, \mathbb{Z}^m) \mapsto S$. The set $P_0 = \{\mathbf{Sh} \mid \mathbf{h} \in [0,1)^m\}$ is the fundamental parallelepiped of the lattice S [39]. It follows that $P_0 = [\mathbb{R}^m : S)$. This result still holds if the m–dimensional cube $[0,1)^m$ is replaced by $[-\frac{1}{2}, \frac{1}{2})^m$ so that P_0 becomes a centered fundamental parallelepiped. Note that P_0 depends on the basis $\mathbf{S}$ of S and different bases yield different parallelepipeds.*

Proposition 4. *The previous result is thus generalized. Let $(\mathbf{S}, \mathbb{R}^p \times \mathbb{Z}^q \times \mathbb{O}^s) \mapsto S$. The set $P_0 = \{\mathbf{Sh} \mid \mathbf{h} \in \mathbb{O}^p \times [0,1)^q \times \mathbb{R}^s\}$ may be regarded as the generalized fundamental parallelepiped of the group S. Then $P_0 = [\mathbb{R}^m : S)$.*

Proposition 5. *If $C = [\mathbb{R}^m : S)$, then $C \cap I_0$ is $[I_0 : S)$.*

The last two propositions let us identify unit cells for an arbitrary group pair in two steps. However, the variety of unit cells is very wide [39], [61] and goes beyond the class identified by this procedure.

2.4 Signal specification by a group pair

A (deterministic) signal may be conveniently defined as a mapping $s : I_0 \to \mathbb{C}$, where I_0 is an Abelian group and $\mathbb{C}$ is the set of complex numbers. Signals will be denoted

in the form $s(\mathbf{t})$, where $\mathbf{t}$ denotes an m–tuple of arguments $(t_1,\ldots,t_m)$ and m is the dimensionality.

The nature of a signal is essentially determined by its domain I_0, which may be one–dimensional as well as multi–dimensional; it may be continuous, discrete (*lattice*) or mixed (*grating*).

It is desirable to complete the signal specification in terms of a regular group pair $I_0 : S$, where S represents the invariance property

$$s(\mathbf{t}-\mathbf{p}) = s(\mathbf{t}), \qquad \mathbf{p} \in S, \tag{14}$$

which generalizes *periodicity*. If S is a full–dimensional lattice, (14) expresses standard periodicity. If S is n–dimensional, with $0 < n < m$, the invariance on S states that the signal is periodic in n directions and aperiodic in the rest. If $S = \mathbb{O}^m$ the invariance becomes irrelevant, on the other hand, if $S = I_0$ the signal is constant.

For a given signal, the choice of the invariance subgroup is not unique. In fact, if S_0 is the largest subgroup that satisfies condition (14), the signal is S invariant for any subgroup S of S_0. For example, a continuous–time signal having period T_0 can be specified not only as $s(t)$, $t \in \mathbb{R} : \mathbb{Z}(T_0)$, but also by the pair $\mathbb{R} : \mathbb{Z}(2T_0)$ or by $\mathbb{R} : \mathbb{Z}(3T_0)$ and, as a limiting case, by $\mathbb{R} : \mathbb{O}$. The specific choice will depend on the context.

A signal with the property (14) will be denoted in the form $s(\mathbf{t})$, $\mathbf{t} \in I_0 : S$ and simplified to $s(\mathbf{t})$, $\mathbf{t} \in I_0$, as $S = \mathbb{O}^m$ (in most respects the degenerate pair $I_0 : \mathbb{O}^m$ is equivalent to the group I_0).

Remark. The idea of group pairs is strictly related to *quotient groups*. Indeed, a one–to–one correspondence (isomorphism) can be established between the class of signals specified by a pair $I_0 : S$ and the class of signals (complex function) defined on the corresponding quotient group I_0/S [67]. Our preference for group pairs is mainly because quotient groups, which are sets of sets, are too cumbersome for a Signal Theory.

2.5 The Haar integral

To continue with the unified approach a linear operator that enables the introduction of convolution, Fourier transformation, etc., is required. The appropriate operator is the Haar integral [54], here denoted by

$$\int_I d\mathbf{t}\, s(\mathbf{t}), \tag{15}$$

where $I = I_0 : S$ is a regular pair in $\mathbb{R}^m$. The construction of the Haar integral, starting from the Haar measure, is covered in many treatises on Topological Groups [57][59]

[58] [55]. Within the class of Abelian groups in $\mathbb{R}^m$, the *definition* of (15) can be given in three steps.[6]

1) For the cases $I = \mathbb{R}$ and $I = \mathbb{Z}$ the Haar integral is, respectively, the Lebesgue integral

$$\int_{\mathbb{R}} dt\; s(t) \stackrel{\Delta}{=} \int_{-\infty}^{+\infty} s(t)\, dt\,, \tag{16a}$$

and the series summation:

$$\int_{\mathbb{Z}} dt\; s(t) \stackrel{\Delta}{=} \sum_{t\in\mathbb{Z}} s(t)\,. \tag{16b}$$

2) If $I = J$ is a full–dimensional group in $\mathbb{R}^m$, the Haar integral is given by

$$\begin{aligned}\int_J d\mathbf{t}\; s(\mathbf{t}) &\stackrel{\Delta}{=} d(\mathbf{J}) \int_H d\mathbf{h}\; s(\mathbf{J}\mathbf{h}) \\ &= d(\mathbf{J}) \int_{H_1} dh_1 \ldots \int_{H_m} dh_m\; s(h_1\mathbf{j}_1 + \ldots + h_m\mathbf{j}_m)\,,\end{aligned} \tag{17}$$

where $\mathbf{J} = [\mathbf{j}_1, \ldots, \mathbf{j}_m]$ is the base and $H = H_1 \times \cdots \times H_m$ is the signature of the group J. Since H_i may be $\mathbb{R}$ or $\mathbb{Z}$, the one–dimensional integrals $\int_{H_i} dh_i$ on the second line turn out to be defined according to (16). For example, if $J = \mathbb{R} \times \mathbb{Z}(d_y) \times \mathbb{Z}(T_q)$ is the 3D grating of the 1:1 scanning format, considering the representation

$$\mathbf{J} = \begin{bmatrix} 1 & 0 & 0 \\ 0 & d_y & 0 \\ 0 & 0 & T_q \end{bmatrix}, \qquad H = \mathbb{R} \times \mathbb{Z} \times \mathbb{Z}$$

from (17) we obtain

$$\begin{aligned}\int_{\mathbb{R}\times\mathbb{Z}(d_y)\times\mathbb{Z}(T_q)} d\mathbf{t}\; s(\mathbf{t}) &= d_y T_q \int_{\mathbb{R}} dh_1 \int_{\mathbb{Z}} dh_2 \int_{\mathbb{Z}} dh_3\; s(h_1, h_2 d_y, h_3 T_q) \\ &= d_y T_q \int_{-\infty}^{+\infty} dh_1 \sum_{h_2\in\mathbb{Z}} \sum_{h_3\in\mathbb{Z}} s(h_1, h_2 d_y, h_3 T_q)\,.\end{aligned}$$

3) If $I = I_0 : S$ is a regular group pair, the Haar integral is the integral *limited to a unit cell* $[I_0 : S)$, namely

$$\int_{I_0:S} d\mathbf{t}\; s(\mathbf{t}) \stackrel{\Delta}{=} \int_{[I_0:S)} d\mathbf{t}\; s(\mathbf{t}) = \int_{I_0} d\mathbf{t}\; s(\mathbf{t})\; \eta_{[I_0:S)}(\mathbf{t})\,, \tag{18}$$

[6] In the author's opinion the abstract definition of Haar measure and integral falls outside the scope of a Signal Theory.

where $\eta_{[\cdot]}$ denotes the indicating function, and the last integral is evaluated according to (17). When the pair degenerates to $I_0 : \mathbb{O}^m$, the integral (18) becomes the integral *over the whole group* I_0 given by (17).

We note that the Haar integral is unique within a multiplicative constant [58]. In the above definition the constant is set equal to the group determinant $d(\mathbf{I})$ so that any ambiguity is removed. There are several reasons for this choice, one being that it achieves a perfect symmetry between the signal domain and the frequency domains.

Properties. The Haar integral has the following properties[7]

a) It is independent of the specific representation $(\mathbf{J}, H)$ of the group.

b) It is shift–invariant, so that for any $\mathbf{p} \in J$

$$\int_J d\mathbf{t}\, s(\mathbf{t}-\mathbf{p}) = \int_J d\mathbf{t}\, s(\mathbf{t}), \qquad \mathbf{p} \in J. \tag{19}$$

c) It is invariant to coordinate inversion, that is,

$$\int_J d\mathbf{t}\, s(-\mathbf{t}) = \int_J d\mathbf{t}\, s(\mathbf{t}). \tag{20}$$

d) If J is a Cartesian product $J_1 \times \cdots \times J_m$, then

$$\int_J d\mathbf{t}\, s(\mathbf{t}) = \int_{J_1} dt_1 \ \ldots \int_{J_m} dt_m\, s(t_1, \ldots, t_m). \tag{21}$$

Specific cases. From (17) it follows that

1) The Haar integral on 1D groups is the Lebesgue integral, if $J = \mathbb{R}$, while on the lattice $\mathbb{Z}(d)$ it becomes

$$\int_{\mathbb{Z}(d)} dt\, s(t) = d \sum_{n=-\infty}^{+\infty} s(nd). \tag{22}$$

2) The Haar integral on $\mathbb{R}^m$ is an m–dimensional Lebesgue integral

$$\int_{\mathbb{R}^m} d\mathbf{t}\, s(\mathbf{t}) = \int_{-\infty}^{+\infty} \ldots \int_{-\infty}^{+\infty} s(t_1, \ldots, t_m)\, dt_1 \ldots dt_m. \tag{23}$$

3) If J is a lattice

$$\int_J d\mathbf{t}\, s(\mathbf{t}) = d(J) \sum_{\mathbf{t} \in J} s(\mathbf{t}) \tag{24}$$

i.e., the Haar integral is given by the weighted sum of the signal values, where the weight $d(J)$ is independent of the group representation.

4) If J is a grating specified by canonical representation (8)

[7] These properties hold for the groups in $\mathbb{R}^m$, but more generally on any *locally compact Abelian group* [60].

$$\int_J d\mathbf{t}\, s(\mathbf{t}) = d(F) \int_{\mathbb{R}^p} d\mathbf{r} \sum_{\mathbf{n}\in F} s(\mathbf{r}, \mathbf{E}\mathbf{r}+\mathbf{n})\,. \tag{25}$$

Haar measure. The integral extended over any (Haar measurable) subset A of a group J can be defined by

$$\int_A d\mathbf{t}\, s(\mathbf{t}) \stackrel{\Delta}{=} \int_J d\mathbf{t}\, s(\mathbf{t})\, \eta_A(\mathbf{t})\,, \tag{26}$$

where $\eta_A(\mathbf{t})$ is the indicating function of A. The Haar measure of A can then be introduced[8] as

$$\mathrm{mis}\,(A) = \int_A 1\, dt \;= \int_J d\mathbf{t}\, \eta_A(\mathbf{t})\,. \tag{27}$$

Use of (17) in (27) yields the particular result: if $J = \mathbb{R}^m$ the Haar measure is the same as the Lebesgue measure; if J is a lattice the Haar measure is $d(J)$ times the number of points of the set A. In all case the Haar measure is shift invariant, i.e. $\mathrm{mis}\,(A+\mathbf{p}) = \mathrm{mis}\,(A)$ for any $\mathbf{p} \in J$.

2.6 Convolution and impulse

Let $I = I_0 : S$ be regular group pair in $\mathbb{R}^m$ and $0 < p < \infty$; then $L_p(I)$ denotes the class of signals for which the norm $\|s\|_p \stackrel{\Delta}{=} [\int_I d\mathbf{t}\, |s(\mathbf{t})|^p]^{1/p}$ exists and is finite. For any pair of signals $x(\mathbf{t})$, $y(\mathbf{t})$ in $L_1(I)$ the convolution is defined as

$$x * y(\mathbf{t}) = \int_I d\mathbf{u}\, x(\mathbf{t}-\mathbf{u})\, y(\mathbf{u})\,, \qquad \mathbf{t} \in I\,. \tag{28}$$

This definition unifies many definitions, such as ordinary convolution on the real line $\mathbb{R}$, cyclic convolution for periodic signals, etc..

Definition 4. The *impulse* on a regular pair I is the unitary element of convolution, i.e. a signal $\delta_I(\mathbf{t})$, such that $x = \delta_I * x$ for any $x(\mathbf{t})$, $\mathbf{t} \in I$.

The existence of such a unitary element is predicted by [60].

Theorem 3. *The convolution in $L_1(I)$ has a unitary element, if and only if I is discrete.*

Hence, the existence of the impulse in $L_1(I)$ is assured whenever the group I_0 in the pair $I = I_0 : S$ is a lattice. In the other cases, i.e. when I_0 is $\mathbb{R}^m$, or a grating, the impulse must be treated as a distribution [60] rather than an ordinary function. We illustrate this in the 1D case (Fig.6). For $I = \mathbb{Z}(T)$ the impulse is an ordinary function: $\delta_{\mathbb{Z}(T)}(t) = 1/T$ for $t = 0$, and 0 otherwise; hence it is essentially a Kronecker

[8] The Haar measure is a preliminary to the Haar integral. In the present approach the roles are reversed.

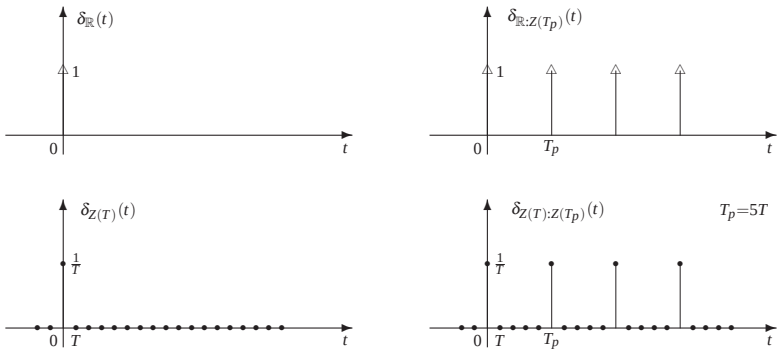

Fig. 6 The 1D impulses (delta functions are represented by arrows).

delta. For $I = \mathbb{R}$ the impulse is a delta distribution (denoted by an arrow in Fig. 6). For $I = \mathbb{Z}(T) : \mathbb{Z}(T_p)$ and $I = \mathbb{R} : \mathbb{Z}(T_p)$ the impulses are periodic repetitions of the previous ones.

We note the following properties of the impulse

$$x(\mathbf{p}) = \int_I d\mathbf{t}\, x(\mathbf{t})\, \delta_I(\mathbf{t}-\mathbf{p}), \qquad \mathbf{p} \in I_0 \tag{29a}$$

$$\delta_{I_0:S}(\mathbf{t}) = 0, \qquad \mathbf{t} \notin S \tag{29b}$$

$$\delta_{I_0:S}(\mathbf{t}) = \mu(I_0), \qquad \mathbf{t} \in S \qquad (I_0 \text{ lattice}) \tag{29c}$$

$$\int_I d\mathbf{t}\, \delta_I(\mathbf{t}) = 1 \tag{29d}$$

$$\delta_{I_0:S}(\mathbf{t}) = \sum_{\mathbf{p}\in S} \delta_{I_0}(\mathbf{t}-\mathbf{p}). \tag{29e}$$

a) is known as the *recovery* property; b) and c) state that the support of $\delta_I(\mathbf{t})$ is given by the periodicity S, in particular, in the aperiodic case the support is limited to the origin; e) relates the impulse on a pair $I_0 : S$ to the impulse on I_0.

2.7 Frequency domain and Fourier transform

A preliminary to the introduction of the Fourier transform is the identification of the *frequency domain*. If the signal is specified by the pair $I = I_0 : S$, then the Fourier transform is specified by the *dual pair*, which has the form

$$\widehat{I} = S^\star : I_0^\star, \tag{30}$$

where $\star$ denotes the *reciprocal* group. Hence, the frequency domain is the reciprocal of the signal periodicity S and the frequency periodicity is the reciprocal of the signal domain I_0.

Definition 5. The *reciprocal* group $J^\star$ of a given group J in $\mathbb{R}^m$ is the set of all m–tuples $\mathbf{f} = (f_1, \ldots, f_m)$ such that[9] $\mathbf{f}'\mathbf{t} = f_1 t_1 + \ldots + f_m t_m$ is an integer for all $\mathbf{t} = (t_1, \ldots, t_m) \in J$, i.e. $J^\star = \{\mathbf{f} \mid \mathbf{f}'\mathbf{t} \in \mathbb{Z}\ ,\ \mathbf{t} \in J\}$.

Proposition 6. *If J is a subgroup of K, then $J^\star$ is a subgroup of $K^\star$.*

Proposition 7. *For the 1D groups in $\mathbb{R}$ it follows that*

$$\mathbb{R}^\star = \mathbb{O}, \quad \mathbb{Z}^\star = \mathbb{Z}, \quad \mathbb{O}^\star = \mathbb{R}. \qquad \square \tag{31}$$

Proposition 8. *If the group J is the Cartesian product $J_1 \times \cdots \times J_m$, the reciprocal group is $J_1^\star \times \cdots \times J_m^\star$.*

From Propositions 7 and 8, the reciprocal $H^\star$ of any signature H can be evaluated. As an example, the reciprocal of $H = \mathbb{R} \times \mathbb{Z}^2$ is $H^\star = \mathbb{O} \times \mathbb{Z}^2$.

Theorem 4. *For a general group $(\mathbf{J}, H) \mapsto J$ the reciprocal group is $(\mathbf{J}^\star, H^\star) \mapsto J^\star$, where the matrix $\mathbf{J}^\star = (\mathbf{J}')^{-1}$ is the inverse transpose of $\mathbf{J}$.*

Considering a proper signature written in the form $H = \mathbb{R}^p \times \mathbb{Z}^q \times \mathbb{O}^s$, we find $H^\star = \mathbb{O}^p \times \mathbb{Z}^q \times \mathbb{R}^s$. Hence, if J has dimensions $p+q$, the reciprocal $J^\star$ has dimensions $q+s$. In particular

a) If J is a full–dimensional lattice, $J^\star$ is a full–dimensional lattice.
b) If $J = \mathbb{R}^m$, $J^\star = \mathbb{O}^m$.
c) If J is a full–dimensional grating with signature $\mathbb{R}^p \times \mathbb{Z}^q$, then $J^\star$ is a q–dimensional lattice with signature $\mathbb{O}^p \times \mathbb{Z}^q$.
d) The reciprocal of the general 1D lattice $\mathbb{Z}(d)$ is $\mathbb{Z}(1/d)$.

The evaluation of a reciprocal group requires finding the *reciprocal* of a square matrix. Note the simple rule $\mathbf{J} = \mathbf{AB} \xrightarrow{\star} \mathbf{J}^\star = \mathbf{A}^\star\mathbf{B}^\star$. Also, matrix partitioning is often useful. Specifically, the following *block triangular* forms will be used:

$$\begin{bmatrix} \mathbf{A} & \mathbf{B} \\ \mathbf{0} & \mathbf{D} \end{bmatrix} \xrightarrow{\star} \begin{bmatrix} \mathbf{A}^\star & \mathbf{0} \\ \mathbf{B}_1 & \mathbf{D}^\star \end{bmatrix}, \qquad \mathbf{B}_1 = -\mathbf{D}^\star \mathbf{B}' \mathbf{A}^\star \tag{32a}$$

$$\begin{bmatrix} \mathbf{A} & \mathbf{0} \\ \mathbf{C} & \mathbf{D} \end{bmatrix} \xrightarrow{\star} \begin{bmatrix} \mathbf{A}^\star & \mathbf{C}_1^\star \\ \mathbf{0} & \mathbf{D}^\star \end{bmatrix}, \qquad \mathbf{C}_1 = -\mathbf{A}^\star \mathbf{C}' \mathbf{D}^\star. \tag{32b}$$

Hence, the reciprocal to an upper triangular base is lower triangular, and vice versa. Using (32) in Theorem 1 and in (11) yields.

[9] $'$ denotes matrix transposition.

Proposition 9. *The reciprocal of a grating with signature $\mathbb{R}^p \times \mathbb{Z}^q$ and canonical base (8) is a p–dimensional lattice in $\mathbb{R}^{p+q}$, with base*

$$\mathbf{J}_\delta^\star = \begin{bmatrix} \boldsymbol{\delta} & -\mathbf{E}'\mathbf{F}^\star \\ \mathbf{0} & \mathbf{F}^\star \end{bmatrix}. \tag{33}$$

To find the reciprocal base of the lattice $Z_i^b(d_1,d_2)$ consider the second of (11).

Proposition 10. *The reciprocal of the 2D lattice $Z_i^b(d_1,d_2)$ is the 2D lattice with base*

$$\begin{bmatrix} \frac{1}{i}F_1 & 0 \\ 0 & \frac{1}{i}F_2 \end{bmatrix} \begin{bmatrix} i & i-\tilde{b} \\ 0 & 1 \end{bmatrix}, \qquad F_1 = \frac{1}{d_1}\,,\ F_2 = \frac{1}{d_2}\,,$$

where $\tilde{b}$ is related to b as in (11). Hence, it is a sublattice of $Z\left(\frac{1}{i}F_1, \frac{1}{i}F_2\right)$.

In particular, the reciprocal to the quincunx lattice $Z_2^1(d_1,d_2)$ is the quincunx lattice $Z_2^1\left(\frac{1}{2}F_1, \frac{1}{2}F_2\right)$. Other explicit results will be seen in the scanning theory.

Proposition 11. *If $I = I_0 : S$ is a regular group pair, then $\widehat{I} = S^\star : I_0^\star$ is a regular group pair.*

The last result is fundamental to Signal Theory since it permits transferring to the frequency domain all the definitions introduced in the signal domain (Haar integral, convolution, impulses, etc.).

Having identified the frequency domain, the Haar integral allows us to introduce the Fourier transform in a unitary form.

Definition 6. Let $I = I_0 : S$ be a regular group pair in $\mathbb{R}^m$ and $\widehat{I} = S^\star : I_0^\star$ the dual pair. The Fourier transform of a signal $s(\mathbf{t})$, $\mathbf{t} \in I$, is given by

$$S(\mathbf{f}) = \int_I d\mathbf{t}\, s(\mathbf{t})\, e^{-j2\pi\mathbf{f}'\mathbf{t}}, \qquad \mathbf{f} \in \widehat{I} \tag{34}$$

and the inverse Fourier transform by

$$s(\mathbf{t}) = \int_{\widehat{I}} d\mathbf{f}\, S(\mathbf{f})\, e^{j2\pi\mathbf{f}'\mathbf{t}}, \qquad \mathbf{t} \in I\,. \tag{35}$$

The relevant point is that both the signal and its Fourier transform are complex functions specified on regular group pairs in $\mathbb{R}^m$, as the integral definitions (17) and (19) apply to both (34) and (35).

The Fourier transform defined above has essentially the same properties as the familiar Fourier transform on $\mathbb{R}$. For instance, the signal $s(\mathbf{t}-\mathbf{p})$ has Fourier transform $S(\mathbf{f})\exp(-j2\pi\mathbf{f}'\mathbf{p})$, the convolution $x*y(\mathbf{t})$ has Fourier transform $X(\mathbf{f})\,Y(\mathbf{f})$, and so on. In particular, the following perfectly symmetrical form of the Parseval's theorem holds

$$\int_I d\mathbf{t}\, x(\mathbf{t})\, y^*(\mathbf{t}) = \int_{\widehat{I}} d\mathbf{f}\, X(\mathbf{f})\, Y^*(\mathbf{f})\,. \tag{36}$$

The following *orthogonal conditions* link the impulse function to the Fourier transform kernel

$$\int_I d\mathbf{t}\, e^{j2\pi\mathbf{f}'\mathbf{t}} = \delta_{\widehat{I}}(\mathbf{f}), \qquad \int_{\widehat{I}} d\mathbf{f}\, e^{j2\pi\mathbf{f}'\mathbf{t}} = \delta_I(\mathbf{t}). \tag{37}$$

Examples. Elementary examples of Fourier transforms are related to impulses. Using orthogonality conditions and impulse properties in (34) or (35) gives

$$\begin{aligned} \delta_I(\mathbf{t}) &\xrightarrow{\mathcal{F}} 1, \qquad 1 \xrightarrow{\mathcal{F}} \delta_{\widehat{I}}(\mathbf{f}) \\ \delta_I(\mathbf{t}-\mathbf{p}) &\xrightarrow{\mathcal{F}} \exp(-j2\pi\mathbf{f}'\mathbf{p}). \end{aligned}$$

The Fourier transforms of some indicating functions will be useful in what follows. Let

$$\begin{aligned} \operatorname{sinc}(x) &= \frac{\sin \pi x}{\pi x}, \qquad \operatorname{sinc}_M(x) = \frac{\sin \pi x}{M \sin \frac{\pi}{M} x} \\ \operatorname{Sinc}(x) &= \operatorname{sinc}(x)\, e^{-j\pi x}, \qquad \operatorname{Sinc}_M(x) = \operatorname{sinc}_M(x)\, e^{-j\pi x(N-1)/N} \end{aligned} \tag{38}$$

where sinc is the Woodward function [3] and sinc_M is its periodic version. Let $w_1(x)$, $x \in \mathbb{R}$, be the indicating function of the interval $[0, D)$ and $w_{1M}(x)$, $x \in \mathbb{Z}(d)$, its discrete version, with $M = D/d$. Then, the corresponding Fourier transforms are

$$\begin{aligned} W_1(f) &= D \operatorname{Sinc}(fD), \\ W_{1d}(f) &= D \operatorname{Sinc}_M(fD). \end{aligned} \tag{39}$$

Suitable combinations yield the Fourier transforms of the indicating functions of the frame and of its sampled versions.

2.8 Linear transformations

Definition 7. Let $I = I_0 : S_1$ and $U = U_0 : S_2$ be regular group pairs. A linear transformation $I \to U$ is specified by the input–output relationship

$$y(\mathbf{t}) = \int_I d\mathbf{u}\, h(\mathbf{t}, \mathbf{u})\, x(\mathbf{u}), \qquad \mathbf{t} \in U \tag{40}$$

where $x(\mathbf{u})$, $\mathbf{u} \in I$ is the *input signal*, $y(\mathbf{t})$, $\mathbf{t} \in U$ is the *output signal* and the *kernel* $h(\mathbf{t}, \mathbf{u})$, $(\mathbf{t}, \mathbf{u}) \in U \times I$ characterizes the transformation.

This definition is completely general: the input and output domains may be equal $(I_0 = U_0)$ or different $(I_0 \neq U_0)$ and they may also have different dimensions. Furthermore, the input and output periodicities S_1 and S_2 may be different.

Definition 8. The *dual* of a linear transformation $I \to U$ is the linear transformation $\widehat{I} \to \widehat{U}$, linking the Fourier transform of the input signal and the output signal,

namely

$$Y(\mathbf{f}) = \int_{\widehat{I}} d\boldsymbol{\lambda}\ \hat{h}(\mathbf{f},\boldsymbol{\lambda})\, X(\boldsymbol{\lambda})\,, \qquad \mathbf{f} \in \widehat{U} \tag{41}$$

where $\hat{h}(\mathbf{f},\boldsymbol{\lambda})$ is the dual kernel.

It is easily shown that the dual kernel is given by

$$\hat{h}(\mathbf{f},\boldsymbol{\lambda}) = H(\mathbf{f},-\boldsymbol{\lambda})\,, \tag{42}$$

where $H(\mathbf{f},\boldsymbol{\lambda})$ is the Fourier transform of $h(\mathbf{t},\mathbf{u})$.

A linear transformation may be the model of a very simple linear system or that of a very complicated one, e.g. the whole scanning process. However, for the purpose of analysis it is generally convenient to split complicated transformations into "simple" ones.

2.9 Simple linear transformations

The scanning and reproduction processes (and perhaps most of linear signal processing) can be expressed in terms of a small number of simple linear transformations, which are now discussed together with the corresponding dual transformations.

Filters and windows. An $I \to I$ linear filter is governed by a convolution: $y(\mathbf{t}) = g * x(\mathbf{t})$, $\mathbf{t} \in I$, where $g(\mathbf{t})$, $\mathbf{t} \in I$ is the impulse response. An $I \to I$ window is governed by a product: $y(\mathbf{t}) = w(\mathbf{t})\, x(\mathbf{t})$, $\mathbf{t} \in I$, where $w(\mathbf{t})$ is the window *shape*. Clearly, the dual of a filter is a window and the vice versa.

Coordinate change. This $I \to I_A$ linear transformation is governed by the relationship

$$y(\mathbf{v}) = x(\mathbf{A}\mathbf{v})\,, \qquad \mathbf{v} \in I_A \tag{43}$$

where both x and y are m–dimensional and $\mathbf{A}$ is an $m \times m$ non–singular real matrix. If $I = I_0 : S$ is the input pair, then the output pair $I_A = I_{0A} : S_A$ is given by

$$I_{0A} = \left\{ \mathbf{A}^{-1}\mathbf{t} \mid \mathbf{t} \in I_0 \right\}, \qquad S_A = \left\{ \mathbf{A}^{-1}\mathbf{s} \mid \mathbf{s} \in S \right\}.$$

Hence, in general, a coordinate change acts on both domain and periodicity.

The dual $\widehat{I} \to \widehat{I}_A$ transformation is a coordinate change described by the relationship

$$Y(\mathbf{u}) = d(\mathbf{A}^\star)\, X(\mathbf{A}^\star\mathbf{u})\,, \qquad \mathbf{u} \in \widehat{I}_A\,. \tag{44}$$

impulsive transformations. The next four linear transformations are characterized by a kernel of the form $h(\mathbf{t},\mathbf{u}) = \delta_D(\mathbf{t}-\mathbf{u})$, where δ_D is the *impulse* on an appropriate pair D and we will call then *impulsive* transformations. Each of these is characterized by a specific ordering of the pairs $I = I_0 : S_1$ and $U = U_0 : S$ (see below). The object of these transformations is that they do nothing other than modify the signal domain or periodicity "in the simplest possible way". The specific

input–output relationship is obtained from the general relationship (40), giving

$$y(\mathbf{t}) = \int_I d\mathbf{u}\, \delta_D(\mathbf{t}-\mathbf{u})\, x(\mathbf{u})\,, \qquad \mathbf{t} \in U \tag{45}$$

to then use impulse properties.

The frequency domain relationships condensed into the following powerful result [22].

Duality Theorem. The dual of the impulsive transformation $I \to U$ is the impulsive transformation $\widehat{I} \to \widehat{U}$. □

Considering the specific ordering of $I \to U$, with the aid of Proposition 6, we find the correspondence of Tab. 1. We now examine the four impulsive transformations

Table 1 Impulsive transformations and their duals.

impulsive transformation	*dual transformation*
sampling $(I_0 \supset U_0)$	*periodization* $(I_0^\star \subset U_0^\star)$
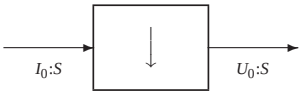	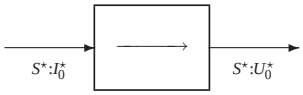
domain interpolation $(I_0 \subset U_0)$	*aperiodization* $(I_0^\star \supset U_0^\star)$
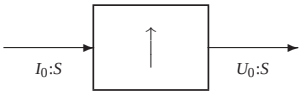	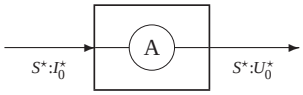
periodization $(S_1 \subset S_2)$	*sampling* $(S_1^\star \supset S_2^\star)$
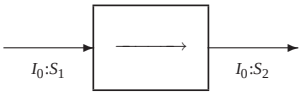	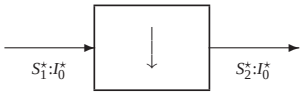
aperiodization $(S_1 \supset S_2)$	*domain interpolation* $(S_1^\star \subset S_2^\star)$
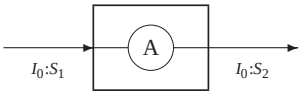	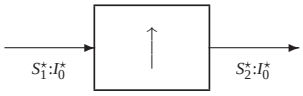

in some detail.[10]

[10] In multirate system literature the usual terms are *up–sampling* for sampling and *down–sampling* for domain–interpolation. In agreement to this, periodization and deperiodization should be called *up–periodization* and *down–periodization*, respectively.

1) *Sampling.* $I_0 \supset U_0$, $S_1 = S_2 = S$, $D = I$. Since $h(\mathbf{t},\mathbf{u}) = \delta_I(\mathbf{t}-\mathbf{u})$, the impulse property (29a) yields the simple relationship

$$y(\mathbf{t}) = x(\mathbf{t}), \qquad \mathbf{t} \in U,$$

which states that x and y take on the same values, since the equality is confined to the output domain (periodicity is preserved). In the frequency domain the above ordering yields $\widehat{I} = S^\star : I_0^\star$, $\widehat{U} = S^\star : U_0^\star$, with $I_0^\star \subset U_0^\star$. Hence, the duality theorem states the following periodic repetition (*periodization*)

$$Y(\mathbf{f}) = \sum_{\mathbf{p}\in[U_0^\star/I_0^\star)} X(\mathbf{f}-\mathbf{p}), \qquad \mathbf{f} \in \widehat{U}. \tag{46}$$

In most applications the sampling operation has the form $\mathbb{R}^m \to U_0$, where U_0 is a lattice or a grating and signal periodicity is neglected. In this case (46) simplifies to

$$Y(\mathbf{f}) = \sum_{\mathbf{p}\in U_0^\star} X(\mathbf{f}-\mathbf{p}), \qquad \mathbf{f} \in \widehat{U}. \tag{46a}$$

2) *Domain interpolation.* $I_0 \subset U_0$, $S_1 = S_2 = S$, $D = U$. The input–output relationship

$$y(\mathbf{t}) = \int_I d\mathbf{u}\ \delta_U(\mathbf{t}-\mathbf{u})\, x(\mathbf{u}), \qquad \mathbf{t} \in U \tag{47}$$

cannot be simplified as in the previous case because the integral and the impulse are on different pairs. The increase of the signal domain could be achieved by inserting zeros at points of U_0 that are not present in I_0. However, the structure of the operation is less trivial since ,it requires an amplification (possibly infinite) of the original signal values, as shown in the following examples.

Example 2. Let I_0 be a lattice, $U_0 = \mathbb{R}^m$ and $S = \mathbb{O}^m$. Then, (47) yields:

$$y(\mathbf{t}) = \begin{cases} Ax(\mathbf{t}) & , \quad \mathbf{t} \in I_0 \\ 0 & , \quad \mathbf{t} \notin I_0 \end{cases}$$

where $A = d(I_0)/d(U_0)$ is the amplification. This relationship is illustrated for a two–dimensional case in Fig.7.

Example 3. Let $I_0 = \mathbb{Z}(d)$, $U_0 = \mathbb{R}$, and $S = \mathbb{O}$. Then, (47) yields

$$y(t) = \sum_{n=-\infty}^{+\infty} d\, x(nd)\ \delta(t-nd)$$

which corresponds to Woodward *comb* operation [3]. In this case amplification is infinite.

3) *Periodization.* $I_0 = U_0$, $S_1 \subset S_2$, $D = U$. In this transformation the periodicity is increased, whereas the signal domains remain unchanged. The impulse property (29e) yields

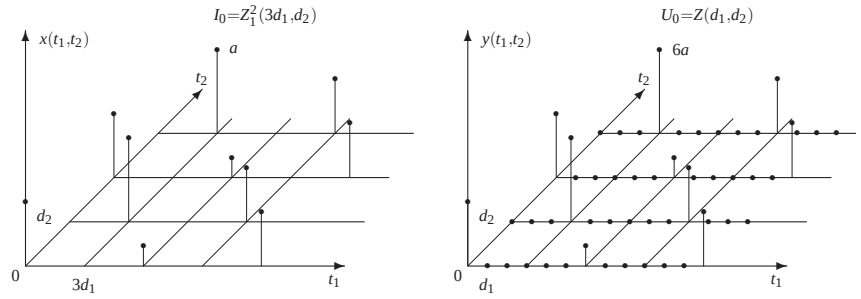

Fig. 7 Illustration of domain interpolation from one lattice into a denser lattice. The amplification is $A = 6$.

$$y(\mathbf{t}) = \sum_{\mathbf{p}\in[S_2:S_1)} x(\mathbf{t}-\mathbf{p}), \qquad \mathbf{t}\in U$$

which represent a periodic repetition, with repetition centers given by the unit cell $[S_2 : S_1)$. In the limiting case $S_1 = \mathbb{O}^m$ the periodization acts on an aperiodic signal, to produce a periodic signal, whose repetition centers are given by S_2.

4) *Deperiodization.* $I_0 = U_0$, $S_1 \supset S_2$, $D = I$. In this case, the relationship can be simplified to $y(\mathbf{t}) = x(\mathbf{t})$, $\mathbf{t}\in U$. Both signals are defined on the same domain so that they really are equal. However, the original signal is considered S_1–invariant and the final signal S_2–invariant. For instance in the case $I_0 = U_0 = \mathbb{R}$, $S_1 = \mathbb{Z}(5)$, $S_2 = \mathbb{Z}(20)$, a continuous–time signal with period 5 is taken to have period 20 at the output.

Deperiodization would appear to be an irrelevant transformation, but it has a concrete meaning in the frequency domain, where it becomes a domain interpolation.

Elementary changes of dimensionality. The linear transformations of Tab. 2 provide a *reduction* or an *increase* of signal dimensionality. They are akin to impulsive transformations in that dimensionality changes are achieved in the "simplest possible way", and their kernels are appropriate impulses.

Dimensionality *reductions* take the form $U\times V\to U$, where U is p–dimensional and V q–dimensional. In *zero–reduction* the last q coordinates of a $(p+q)$–dimensional signal are set to zero, i.e.

$$y(\mathbf{u}) = x(\mathbf{u},\mathbf{0}), \qquad \mathbf{u}\in U.$$

In *integral–reduction* the signal is integrated with respect to the last q coordinates, i.e.

$$y(\mathbf{u}) = \int_V d\mathbf{v}\, x(\mathbf{u},\mathbf{v}), \qquad \mathbf{u}\in U. \tag{48}$$

In the frequency domain, zero–reduction becomes integral–reduction, and vice versa.

Table 2 Elementary changes of dimensionality.

change of dimensionality	*dual change of dimensionality*
zero–reduction	*integral–reduction*
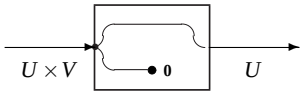	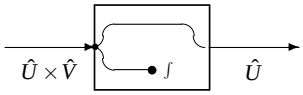
integral–reduction	*zero–reduction*
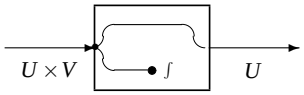	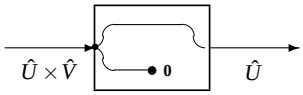
sum–reduction	*zero–reduction*
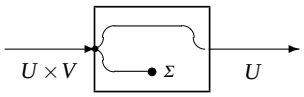	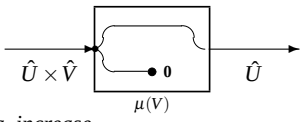
hold–increase	*delta–increase*
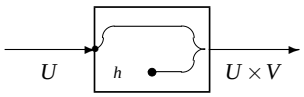	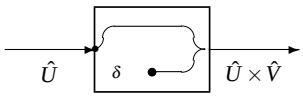
delta–increase	*hold–increase*
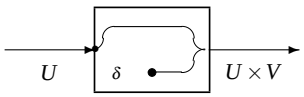	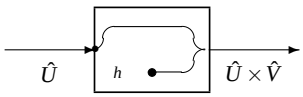

Dimensionality *increases* take the form $U \to U \times V$. In *hold increase* the relationship is

$$y(\mathbf{u},\mathbf{v}) = x(\mathbf{u}), \qquad (\mathbf{u},\mathbf{v}) \in U \times V$$

which states that the p–dimensional signal $x(\mathbf{u})$ is spread to the $(p+q)$–domain by a hold operation. In *delta–increase* the relationship is

$$y(\mathbf{u},\mathbf{v}) = x(\mathbf{u})\ \delta_V(\mathbf{v}), \qquad (\mathbf{u},\mathbf{v}) \in U \times V$$

i.e. an impulse is attached as a factor to the original signal. In the frequency domain, hold increase becomes delta–increase, and vice versa.

Tab. 2 lists a third kind of dimensionality reduction, *sum–reduction*, with the relationship

$$y(\mathbf{u}) = \sum_{\mathbf{v}\in V} x(\mathbf{u},\mathbf{v}) = \frac{1}{d(V)} \int_V d\mathbf{v}\, x(\mathbf{u},\mathbf{v}),$$

where V is a lattice. The dual of a sum–reduction is a zero–reduction followed by a multiplication by $1/d(V)$.[11]

2.10 Sampling Theorem

The possibility of signal recovery after a *sampling operation* is linked to *the limitation of the Fourier transform support*. Unit cells provide the appropriate tool. Consider a sampling of the form $\mathbb{R}^m \to I_s$, where I_s is an m–dimensional lattice or grating. The sampling relationship $x_s(\mathbf{t}) = x(\mathbf{t})$, $\mathbf{t} \in I_s$ in the frequency domain becomes the periodization $\mathbb{R}^m \to \mathbb{R}^m / I_s^\star$, with the relationship

$$X_s(\mathbf{f}) = \sum_{\mathbf{p} \in I_s^\star} X(\mathbf{f} - \mathbf{p}) \,.$$

Now, if the support of $X(\mathbf{f})$ is limited within a unit cell, say

$$\sigma(X) \subset C \qquad \text{with } C = [\mathbb{R}^m{:}I_s^\star) \,, \tag{49}$$

the terms of the periodic repetition do not overlap (non–aliasing condition). The original Fourier transform $X(\mathbf{f})$, $\mathbf{f} \in \mathbb{R}^m$ can thus be recovered as $X(\mathbf{f}) = X_s(\mathbf{f})\ \eta_C(\mathbf{f})$, where η_C is the indicating function of C. The latter is the frequency domain relationship of an interpolating filter with frequency response $\eta_C(\mathbf{f})$.

Theorem 5. *Let $x(\mathbf{t})$, $\mathbf{t} \in \mathbb{R}^m$, have a limited frequency support according to (49). Then, $x(\mathbf{t})$ can be perfectly recovered after a sampling $\mathbb{R}^m \to I_s$ by an interpolating filter $I_s \to \mathbb{R}^m$ with frequency response $\eta_C(\mathbf{f})$.*

This theorem summarizes and extends several results available in the literature [35] [36].

2.11 Dimensionality reduction theorem

The possibility of signal recovery after a dimensionality reduction is linked to *the limitation of the signal support* and to the nature of the signal domain.

Let U be a p–dimensional group and V a q–dimensional lattice. In a zero–reduction $U \times V \to U$ the condition for the signal support is $\sigma(x_0) \subset U \times \mathbb{O}^q$. For instance in a 2D→1D reduction of the form $\mathbb{R} \times \mathbb{Z}(d) \to \mathbb{R}$ the 2D signal support must be confined to the $\mathbb{R}$ line.

In a *sum–reduction* the condition is less trivial, and is stated in terms of lines and projections. The $U \times V$ *lines* are the subsets

[11] In the symbolism of Tab. 2 multiplication factors are indicated below the block.

$$(U\times V)_{\mathbf{v}} = \Big\{(\mathbf{u},\mathbf{v}) \mid \mathbf{u}\in U\Big\}, \qquad \mathbf{v}\in V,$$

which form a partition in unit cells of $U\times V$ modulo $U\times\mathbb{O}^q$. For a signal $x_0(\mathbf{u},\mathbf{v})$, $(\mathbf{u},\mathbf{v})\in U\times V$, the *support lines* are

$$\sigma(x_0)_{\mathbf{v}} = \sigma(x_0)\cap(U\times V)_{\mathbf{v}}, \qquad \mathbf{v}\in V,$$

and their *projections* are the subsets of U,

$$\pi(x_0)_{\mathbf{v}} = \Big\{\mathbf{u} \mid (\mathbf{u},\mathbf{v})\in\sigma(x_0)_{\mathbf{v}}\ ,\ \mathbf{u}\in U\Big\}, \qquad \mathbf{v}\in V.$$

Such lines are illustrated in Fig.8b for $U\times V=\mathbb{R}\times\mathbb{Z}(d)$. After a sum–reduction,

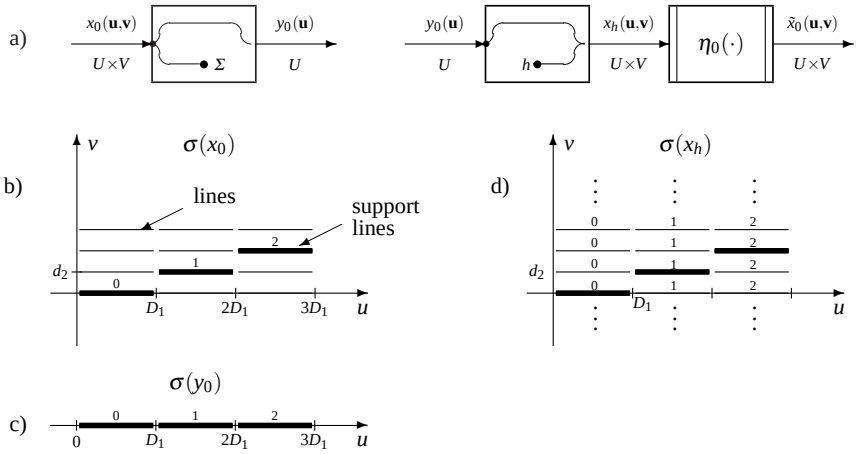

Fig. 8 Illustration of Dimensionality Reduction Theorem: b) shows the support of a 2D signal $x_0(u,v)$, $(u,v)\in\mathbb{R}\times Z(d_2)$ that meets the *disjoint projection condition*, c) support of the 1D signal $y_0(u)$ obtained by a sum–reduction, d) lines obtained after an $\mathbb{R}\to\mathbb{R}\times Z(d_2)$ hold–increase.

i.e.

$$y_0(\mathbf{u}) = \sum_{\mathbf{v}\in V} x_0(\mathbf{u},\mathbf{v}), \qquad \mathbf{u}\in U,$$

the y_0 support is given by the union of the x_0 projections $\pi(x_0)_{\mathbf{v}}$. If $\pi(x_0)_{\mathbf{v}}$ do not overlap as in Fig.8c, the original signal can be recovered by a *hold–increase* $U\to U\times V$, which spreads the $y_0(\mathbf{u})$ values to the whole domain $U\times V$ (Fig.8d), followed by a window that confines the signal values to the original support, as illustrated in Fig.8a.

Theorem 6. *(Dimensionality Reduction Theorem) Let U be a p–dimensional group and V a q–dimensional lattice. A signal $x_0(\mathbf{u},\mathbf{v})$, $(\mathbf{u},\mathbf{v})\in U\times V$ that satisfies the disjoint projection condition*

$$\pi(x_0)_{\mathbf{v}_1} \cap \pi(x_0)_{\mathbf{v}_2} = \emptyset\,, \qquad \mathbf{v}_1 \neq \mathbf{v}_2\,,$$

can be perfectly recovered from a $U \times V \to V$ sum–reduction by a $U \to U \times V$ hold–increase, followed by a window with the shape $\eta_{\sigma(x_0)}(\mathbf{u},\mathbf{v})$.

The *disjoint projection condition* is unlikely for a signal support since a signal, e.g. an image, rarely meets this requirement. However, this condition can be obtained from signals with a more interesting support limitation. In general we can start from a $(p+q)$–dimensional signal $x(\mathbf{t})$, $\mathbf{t} \in I$, with a suitably limited support $\sigma(x)$. If an $I \to U \times V$ transformation exists, typically a coordinate change, such that the signal $x_0(\mathbf{u},\mathbf{v})$ has disjoint projections after the transformation, then the original signal $x(\mathbf{t})$, $\mathbf{t} \in I$, can be perfectly recovered, provided that the $I \to U \times V$ transformation possesses an inverse $U \times V$ transformation.

In conclusion, dimensionality reduction (zero– or sum–) may be of little interest. A more interesting scheme for signal recovery results from a "composite" dimensionality reduction (*reading*) with a consequent "composite" dimensionality increase (*writing*) (Fig. 9). A reading reduction consists of an invertible $I \to U \times V$ transformation followed by a elementary $U \times V \to U$ reduction. A writing increase consists of a elementary $U \to U \times V$ increase, followed by a window, followed in turn by the inverse $U \times V \to I$ transformation. The order of two last transformations can be changed with the appropriate modification of the indicating function. Typically the $I \to U \times V$ transformation is provided by a coordinate change, in which case the composite reduction scheme will be called *standard reading*.

Fig. 9 illustrates a standard reading of a 2D signal $x(t_1,t_2)$ on a grating to give a 1D signal $y_0(u)$, $u \in \mathbb{R}$. The 2D signal $x(t_1,t_2)$ is first converted into a signal $x_0(u,v)$, $(u,v) \in \mathbb{R} \times \mathbb{Z}(d_2)$, by means of a coordinate change with a matrix of the form

$$\mathbf{A} = \begin{bmatrix} 1 & -\dfrac{D_1}{d_2} \\ 0 & 1 \end{bmatrix}.$$

The support of $x(t_1,t_2)$ is such that, after the coordinate change the signal $x_0(u,v)$ meets the disjoint projection condition. Then, according to Theorem 6 $x_0(u,v)$ can be perfectly recovered from $y_0(u)$ so that $x(t_1,t_2)$ is finally restored by the inverse coordinate change.

The above ideas, applied to a 3D→1D reduction, are the essential basis of television scanning.

Remark. The topic of dimensionality changes of multi–dimensional signals has not received much attention in the literature [69] [71]. Sometimes dimensionality reduction is considered as a degenerate form of sampling [39]. However, sampling and dimensionality reduction are different in nature. This becomes more evident when comparing the corresponding dual transformations and, more particularly, the corresponding fundamental theorems. (In Theorem 4 the assumption is on the Fourier transform support, in Theorem 5 it is on the signal support).

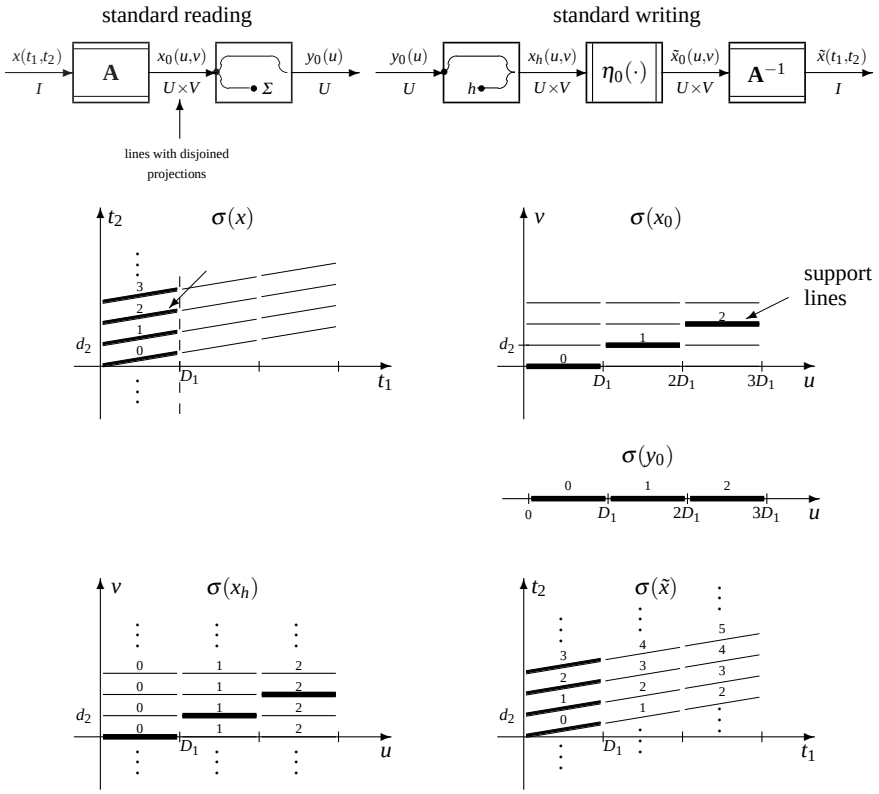

Fig. 9 *Reading* mD $\rightarrow$ nD and *writing* nD $\rightarrow$ mD operations illustated for $m = 2$ and $n = 1$ by signal supports. The support of the original signal is such that it satisfies the *disjoint projection condition* after the coordinate change.

3 Scanning Principles

A scanning process is essentially a 3D→1D conversion of a time–varying source image into a video signal. It can be conceptually subdivided into three parts: 1) framing, which performs a 2D limitation of the 3D source signal, 2) a sampling operation, which makes the signal discrete in two or three coordinates, and 3) a reading operation, which performs the 3D→1D reduction. Parts 1) and 2) are essential to make the subsequent reading operation invertible according to the dimensionality–reduction theorem.

Correct recovery by the reproduction process of the image within the frame requires that both 2) and 3) be invertible. From Theorems 4 and 5, the required conditions are non–aliasing and disjoint projections, respectively.

The scanning and reproduction models presented in the next sections originate in appropriate formulations of operations 1), 2), and 3).

Main symbols relating to scanning process

- D_x : horizontal frame dimension
- D_y : vertical frame dimensionality
- N : number of lines per frame
- M : number of pixels per line (in the full format)
- $d_y = D_y/N$: line separation (in the full format)
- $d_x = D_x/M$: pixel separation on a line (in the full format).
- T_q : frame period
- i : interlace factor
- $T_f = T_q/i$: field period
- $T_r = T_q/N$: line period
- $v_x = D_x/T_r$: scanning horizontal velocity
- $v_y = id_y/T_r$: scanning vertical velocity
- $Z_i^b(d_y, T_f)$: vertical–temporal lattice
- I_S : scanning group

4 The Scanning Group

The scanning group I_S, i.e. the 3D subset on which the time–varying image is scanned, must be discrete in at least two directions. It may be a 3D grating with signature $\mathbb{R} \times \mathbb{Z}^2$ (continuous scanning) or a 3D lattice (discrete scanning). Its general representation is therefore

$$\mathbf{I}_S = [\mathbf{i}_1\ \mathbf{i}_2\ \mathbf{i}_3] = \begin{bmatrix} i_{11} & i_{12} & i_{13} \\ i_{21} & i_{22} & i_{23} \\ i_{31} & i_{32} & i_{33} \end{bmatrix}, \qquad H_S = \mathbb{H} \times \mathbb{Z}^2, \tag{50}$$

where $\mathbb{H} = \mathbb{R}$ or $\mathbb{H} = \mathbb{Z}$. The scanning point on I_S has the form

$$(x_S, y_S, t_S) = h\mathbf{i}_1 + n\mathbf{i}_2 + k\mathbf{i}_3, \qquad h \in \mathbb{H},\ (n,k) \in \mathbb{Z}^2. \tag{51}$$

In principle, I_S may be arbitrary, but in practical applications *periodicity in the time coordinate* is always required. This means, that if $(x,y,t) \in I_S$, then also $(x,y,t + kT_q) \in I_S$, where T_q is the *frame period*. In the specification of a scanning group the natural references are the frame dimensions D_x and D_y and the frame period T_q, where usually $D_x = 1$ w and $D_y = 1$ h.[12]

We now introduce the concepts of *lines* and *fields*, which are essential in scanning theory, and then consider the fundamental classes of scanning groups.

[12] In theoretical considerations it is convenient to use distinct units for horizontal and vertical dimensions. Having chosen $D_x = 1$ w and $D_y = 1$ h, the aspect ratio D_x/D_y, which in practice is a fundamental parameter, disappears from scanning relationships.

4.1 Field and line decompositions

Reconsider Fig. 2, which refers to very particular scanning procedures, namely the **M** and **I** models of the continuous progressive 1:1 format. In that figure *lines* and *fields* are clearly recognized; the former are 1D sets of $\mathbb{R}^3$, the latter 2D sets of $\mathbb{R}^3$, both delimited by the frame. However, lines and fields may have different meanings depending on the context. They may denote either the unlimited objects, when extended outside the frame region, or their projections on the x,y plane. To obtain general definitions it is convenient to follow the order:

1) fields and lines in $\mathbb{R}^3$ as partition objects of the scanning group I_S,
2) fields and lines in $\mathbb{R}^2$ as projections of 1),
3) frame–limited versions of 1) and 2).

Referring to the general representation (50) and the scanning point expression (51), we state

Definition 1. Fields of the scanning group I_S in $\mathbb{R}^3$ are sets

$$C_k^{(3)} = C_0^{(3)} + k\mathbf{i}_3\,, \qquad k \in \mathbb{Z}\,, \tag{52}$$

where $C_0^{(3)} = \{h\mathbf{i}_1 + n\mathbf{i}_2\}$. Lines in $\mathbb{R}^3$ are sets

$$c_{nk}^{(3)} = c_{00}^{(3)} + n\mathbf{i}_2 + k\mathbf{i}_3\,, \qquad (n,k) \in \mathbb{Z}^2\,, \tag{53}$$

where $c_{00} = \{h\mathbf{i}_1 \mid h \in H\}$.

Note that $C_0^{(3)}$ is a 2D group in $\mathbb{R}^3$ and $c_{00}^{(3)}$ is a 1D group in $\mathbb{R}^3$. Also, (52) and (53) represent *partitions* of I_S, and $C_0^{(3)}$ and $c_{00}^{(3)}$ are unit cells of I_S.

Definition 2. Fields and lines of the scanning group I_S in $\mathbb{R}^2$ are projections on the x,y plane of the corresponding objects in $\mathbb{R}^3$.

To find the projections in terms of vectors, the last row of the base $\mathbf{I}_S$ must be dropped, to get

$$\mathbf{I}_S^{(2)} = [\mathbf{j}_1\ \mathbf{j}_2\ \mathbf{j}_3] = \begin{bmatrix} i_{11} & i_{12} & i_{13} \\ i_{21} & i_{22} & i_{23} \end{bmatrix} \quad ;$$

thus the scanning point in the projection is $h\mathbf{j}_1 + n\mathbf{j}_2 + k\mathbf{j}_3$. The fields of I_s in $\mathbb{R}^2$ are then given by

$$C_k = C_0 + k\mathbf{j}_3\,, \qquad k \in \mathbb{Z}\,, \tag{54}$$

where $C_0 = \{h\mathbf{j}_1 + n\mathbf{j}_2 \mid h \in \mathbb{H}\,,\ n \in \mathbb{Z}\}$, and the lines of I_s in $\mathbb{R}^2$ are given by

$$c_{nk} = c_{00} + n\mathbf{j}_2 + k\mathbf{j}_3\,, \qquad (n,k) \in \mathbb{Z}^2\,, \tag{55}$$

where $c_{00} = \{h\mathbf{j}_2 \mid h \in \mathbb{H}\}$.

The x,y projection of the whole scanning group will be called the *mosaic* of I_S and denoted by $\mathcal{M}(I_S)$. The mosaic is a group, but not a standard one in the sense of Definition 1; it can be shown that $\mathcal{M}(I_S)$ becomes a standard group in $\mathbb{R}^2$, with signature $\mathbb{H}\times\mathbb{Z}$, if and only if I_S is periodic in t. In this case, it is given by the union of the fields in a period,

$$\mathcal{M}(I_S) = \bigcup_{k=0}^{L-1} (C_0 + k\,\mathbf{j}_3)\,, \tag{56}$$

where L is the period (in fields) determined by the smallest positive integer k, such that $k\,\mathbf{j}_3 \in C_0$.

Finding, the mosaic and the period from a general representation may be cumbersome. However, it becomes straightforward when we start from a lower–triangular base, and use the following theorem [25].

Theorem 1. *The lower–triangular base of a periodic scanning group has the interpretation*

$$\mathbf{I}_S = \begin{bmatrix} i_{11} & 0 & 0 \\ i_{21} & i_{22} & 0 \\ i_{31} & i_{32} & i_{33} \end{bmatrix} \triangleq \begin{bmatrix} \mathbf{K}_0 & \mathbf{0} \\ \mathbf{d} & T_q \end{bmatrix} \tag{57}$$

where $\mathbf{K}_0$ *is a base of the mosaic and* $T_q = i_{33}$ *is the period (in seconds).*

The proof follows after writing out the scanning point coordinates (x,y,t) and observing that x,y are independent of t. A remarkable fact is that *the fields in a period* $C_0, C_1, \ldots, C_{L-1}$ *represent a partition of the mosaic*. In practice, this means that during one period of the scanning process the time–varying image is read on the mosaic pattern, *without repetition*. This situation would not be guaranteed in an arbitrary scanning process that is not governed by the geometric laws of groups.

Lines and fields are finally delimited by the frame, i.e., $Q = [0, D_x) \times [0, D_y)$ for $\mathbb{R}^2$ objects, and $Q^{(3)} = Q \times \mathbb{R}$ for $\mathbb{R}^3$ objects. Objects thus delimited will be denoted by Q_k, $Q_k^{(3)}$, q_{nk}, and $q_{nk}^{(3)}$.

4.2 Continuous scanning with memory

To introduce the scanning parameters it is convenient to begin with this simple scanning type. We take as reference the progressive 1:1 format, whose scanning group is

$$I_{S\,1:1} = \mathbb{R} \times \mathbb{Z}(d_y, T_f)\,. \tag{58}$$

The *vertical line spacing* d_y is assumed to be an integer submultiple of D_y, so that $N = D_y/d_y$ is the *number of lines per frame*; the frame period T_q is equal to the *field period* T_f. The grating $I_{S\,1:1}$ is illustrated in Fig.10 (top left) by means of its y,t projection $\mathbb{Z}(d_y, T_f)$, which represents the *vertical–temporal lattice*.

In 2:1 interlace scanning the grating can be expressed in terms of the quincunx lattice (Fig.10 top center)

$$I_{S2:1} = \mathbb{R} \times Z_2^1(d_y, T_f)\,,$$

where the line spacing becomes $2d_y$, the frame period $2T_f$ and the N lines of a full frame are shared in two fields.

In multiply i : 1 interlace scanning, the scanning group becomes a subgrating of $I_{S1:1}$, which can be written in the form

$$I_S = \mathbb{R} \times Z_i^b(d_y, T_f) \tag{59}$$

where the *vertical–temporal lattice* is a sublattice of $\mathbb{Z}(d_y, T_f)$, with Hermitian bases (see Example 5)

$$\begin{bmatrix} d_y & 0 \\ 0 & T_f \end{bmatrix} \begin{bmatrix} i & b \\ 0 & 1 \end{bmatrix}, \qquad \begin{bmatrix} d_y & 0 \\ 0 & T_f \end{bmatrix} \begin{bmatrix} 1 & 0 \\ \tilde{b} & i \end{bmatrix}. \tag{60}$$

Here i and b are positive integers, with $b < i$ and b prime relatively to i. The *interlace factor* i represents a reduction in line density, with respect to the full format $I_{S1:1}$. In fact, the line spacing becomes $i\,d_y$ and the N lines of a full frame are shared among i fields; the frame period is $T_q = i\,T_f$. The integer b represents the index of the first line in the first field. Note that for $i \geq 3$ multiple choices of b are possible, as illustrated in Fig.10.

The scanning grating (59) represents the general format for scanning with memory, since it includes the 1:1 progressive format (with $i = 1$, $b = 0$), and the 2:1 interlace format (with $i = 2$, $b = 1$) as particular cases. We denote this scanning format by $\mathbf{M}(1{:}1)$ and $\mathbf{M}(2{:}1)$ for the first two orders, and by $\mathbf{M}(i : 1|b)$ for $i \geq 3$.

Two base–signature representations of I_S are given in Tab. 3. In the first repre-

Table 3 The gratings for memory scanning $\mathbf{M}(i{:}1|b)$.

General form: $I_S = \mathbb{R} \times Z_i^b(d_x, T_f)$	
upper–triangular representation	
$\mathbf{I}_S = \begin{bmatrix} D_x & 0 & 0 \\ 0 & id_y & bd_y \\ 0 & 0 & T_f \end{bmatrix}$	$H_S = \mathbb{R} \times \mathbb{Z}^2$
lower–triangular representation	
$\mathbf{I}_S = \begin{bmatrix} D_x & 0 & 0 \\ 0 & d_y & 0 \\ 0 & \tilde{b}T_f & iT_f \end{bmatrix}$	$H_S = \mathbb{R} \times \mathbb{Z}^2$

sentation, the coordinates of I_S are expressed in the *proper* form

$$x_S = r\,D_x\,,\; y_S = (n'i + kb)\,d_y\,,\; t_S = k\,T_f \qquad \text{with} \qquad r \in \mathbb{R}\,,\; (n', k) \in \mathbb{Z}^2\,. \tag{61}$$

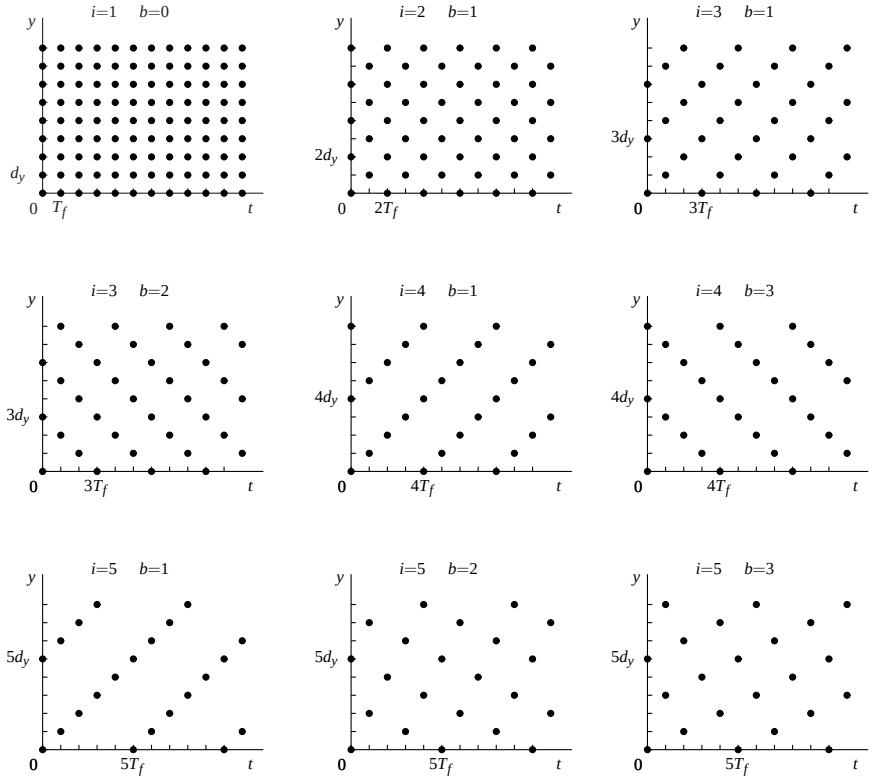

Fig. 10 Vertical–temporal lattices $Z_i^b(d_y, T_f)$ of the first interlace orders.

By the writing

$$n = n'i + kb \tag{62}$$

they take on the *improper* form

$$x_S = r D_x \, , \, y_S = n d_y \, , \, t_S = k T_f \qquad \text{with} \qquad r \in \mathbb{R} \, , \, (n,k) \in Z_i^b \, , \tag{63}$$

which yields the *improper* I_S representation (see Sect. 2–B)

$$\mathbf{I}_S = \begin{bmatrix} D_x & 0 & 0 \\ 0 & d_y & 0 \\ 0 & 0 & T_f \end{bmatrix} , \qquad H_S = \mathbb{R} \times Z_i^b \, .$$

In $\mathbf{M}(i:1|b)$ scanning the zeroth field is $C_0 = \mathbb{R} \times \mathbb{Z}(i d_y)$ and the k–th field can be written as $C_k = C_0 + k(0, b d_y)$. The mosaic is

$$\mathcal{M}(I_S) = \mathbb{R} \times \mathbb{Z}(d_y) \, , \tag{64}$$

for any order i. Lines can be written in the form

$$c_{nk} = c_{00} + (0, nd_y)\,, \qquad (n,k) \in Z_i^b\,, \tag{65}$$

where $c_{00} = \mathbb{R} \times \{0\}$ is the zeroth line of the zeroth field. When frame–limited they become

$$q_{nk} \stackrel{\Delta}{=} c_{nk} \cap Q = q_{00} + (0, nd_y)\,, \qquad n \in \mathcal{N}_k\,, \tag{66}$$

where $q_{00} = [0, D_x) \times \{0\}$ and $\mathcal{N}_k$ gives the indexes n for field k, disregarding empty lines. $\mathcal{N}_k$ has the form

$$\mathcal{N}_k = \Big\{ n_k\ ,\ n_{k+i}\ ,\ \ldots\ ,\ n_k + (N_k - 1)\, i \Big\} \tag{67a}$$

where n_k is the index of the first line and N_k is the number of lines in field k. Specifically,

$$n_k = \rho_i(kb)\,, \qquad N_k = \nu_i(N - 1 - n_k) + 1\,, \tag{67b}$$

where $\rho_i(x)$ denotes the remainder of the integer division of x by i, and $\nu_i(x)$ the integer part of x/i. Fig. 11 shows examples of lines and fields for $i = 1$, $i = 2$ and

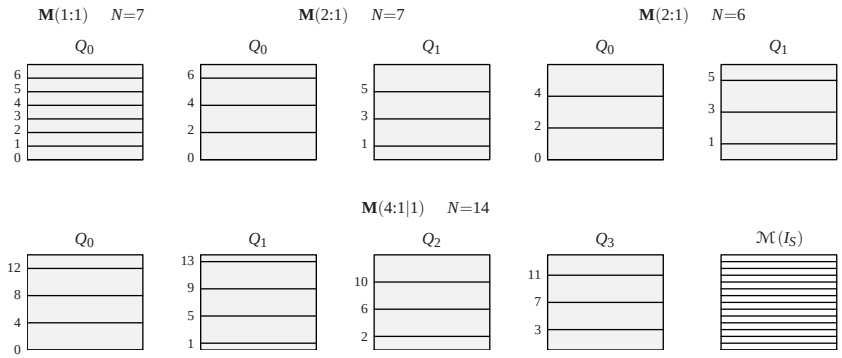

Fig. 11 Illustration of the picture–limited fields in the $\mathbf{M}(i{:}1|b)$ continuous scanning.

$i = 4$.

We finally clarify the meaning of the "periods" is this peculiar kind of scanning. The field period T_f represents the time separation between two consecutive fields. It does not represents the acquisition time of one field, which is zero. The *line period* defined as $T_r = T_q/N$ has no meaning as a scanning parameter, as all lines of the k–th field are read at the same instant kT_f. It represents the time available for a line to be read.

4.3 Instantaneous continuous scanning

For this type of scanning we follow a different approach. We start with a general 3D grating represented in the minimal form

$$\mathbf{I}_S = \begin{bmatrix} D_x & 0 & 0 \\ i_{21} & i_{22} & i_{23} \\ i_{31} & i_{32} & i_{33} \end{bmatrix}, \qquad H'_S = \mathbb{R} \times \mathbb{Z}^2 ,$$

and discuss possible solutions. Without loss of generality, we assume $i_{rs} \geq 0$ and $0 \leq i_{23} < i_{22}$. The coordinates of I_S are

$$\begin{aligned} x_S &= r\, D_x \\ y_S &= r\, i_{21} + i_{22}\, n' + i_{23}\, k \\ t_S &= r\, i_{31} + i_{32}\, n' + i_{33}\, k , \qquad r \in \mathbb{R} ,\ (n', k) \in \mathbb{Z}^2 . \end{aligned} \tag{68}$$

We first impose the time–periodicity condition. Considering that $(0,0,0) \in I_S$, this condition can be confined to the form $(0,0,T_q) \in I_S$, for some $T_q > 0$. In terms of (68) we find: $r = 0$ and $i_{22}\, n' + i_{23}\, k = 0$ for some integers n', k. The solution is possible if and only if i_{23}/i_{22} is rational. In this case i_{22} and i_{23} must be $i_{22} = i\, d_y$ and $i_{23} = b\, d_y$, with i and b relatively prime, and $d_y = \mathrm{mcm}\,(i_{22}, i_{23})$. This holds for $i_{23} > 0$. For $i_{23} = 0$ let $i = 1$, $b = 0$, and $d_y = i_{22}$. By virtue of these results and the relationship $n = n' i + kb$, (68) can be rearranged in the *improper* form

$$\begin{aligned} x_S &= r\, D_x \\ y_S &= r\, i_{21} + n\, d_y \\ t_S &= r\, i_{31} + \frac{n}{i}\, T_r + \frac{k}{i}\, T_q , \qquad r \in \mathbb{R} ,\ (n, k) \in Z_i^b , \end{aligned} \tag{69}$$

where $T_r = i_{32}$, and $T_q = i\, i_{33} - b\, i_{32}$. T_q is just the frame period, whereas T_r represents the temporal separation between two consecutive lines. In principle, these parameters are not constrained by the grating structure. However, correct scanning requires $T_q \geq N\, T_r$, to guarantee that all the N lines are really scanned (as before, $N = D_y/d_y$ is assumed to be integer). For $T_q > N\, T_r$ an image fraction is captured outside the frame (vertical blanking).

We now discuss the parameters i_{21} and i_{31}. Letting $r = 1$, $n = 0$ and $k = 0$ in (69) we find that line 0 of field 0 terminates at the point (D_x, i_{21}, i_{31}). Then, the time i_{31} must satisfy the condition $T_r \geq i_{31}$. For $T_r > i_{31}$ again an image fraction is captured outside the frame (horizontal blanking). The vertical parameter i_{21} determines the line slope. It has no theoretical constraint, although if it is convenient to assume $i_{21} = i\, d_y$, which means that each line terminates at a level at which the next line begins.

To work with a clearly defined format, we neglect *blanking* by assuming

$$T_q = N\, T_r , \qquad i_{31} = T_r , \qquad i_{21} = i\, d_y . \tag{70}$$

Hence, the grating representation takes the *improper* form

$$\mathbf{I}_S = \begin{bmatrix} D_x & 0 & 0 \\ i\,d_y & d_y & 0 \\ T_r & \frac{1}{i}\,T_r & T_f \end{bmatrix}, \qquad H_S = \mathbb{R} \times Z_i^b\,. \tag{71}$$

The corresponding scanning format will be denoted by $\mathbf{I}(i:1|b)$. To find *proper* representations for I_S (with signature $\mathbb{R} \times \mathbb{Z}^2$), the reference lattice Z_i^b itself must be expressed in terms of a proper representation, e.g. by means of (60). This gives the *proper* I_S representations of Tab. 4.

Table 4 Gratings for instantaneous scanning $\mathbf{I}(i{:}1|b)$.

upper–triangular representation

$$\mathbf{I}_S = \begin{bmatrix} D_x & 0 & 0 \\ id_y & id_y & bd_y \\ iT_r & T_r & bT_r + T_f \end{bmatrix} \qquad H_S = \mathbb{R} \times \mathbb{Z}^2$$

lower–triangular representation

$$\mathbf{I}_S = \begin{bmatrix} D_x & 0 & 0 \\ id_y & d_y & 0 \\ iT_r & \frac{1}{i}\,T_r + \tilde{b}T_f & iT_f \end{bmatrix} \qquad H_S = \mathbb{R} \times \mathbb{Z}^2$$

The field C_0 consists of tilted lines vertically spaced by id_y, a 2D grating with representation

$$\mathbf{C}_0 = \begin{bmatrix} D_x & 0 \\ id_y & id_y \end{bmatrix}, \qquad \mathbb{R} \times \mathbb{Z}\,. \tag{72}$$

As in the $\mathbf{M}(i:1|b)$ scanning, the fields C_k are replicas of C_0, vertically shifted by $kb\,d_y$. From the lower–triangular representation of Tab. 4 and Theorem 1 it follows that the mosaic $\mathcal{M}(I_S)$ is the 2D grating with representation

$$\mathbf{K}_0 = \begin{bmatrix} D_x & 0 \\ id_y & d_y \end{bmatrix}, \qquad \mathbb{R} \times \mathbb{Z}\,. \tag{73}$$

The lines c_{nk} can be expressed as in (65) where now c_{00} is the line determined by the points (0,0) and (D_x, id_y). However, for framed lines the q_{nk} relationship (66) is no longer true due to the presence of "fractional" lines, as illustrated in Fig. 12. In $\mathbf{I}(1{:}1)$ scanning all N lines are "full", but in $\mathbf{I}(2{:}1)$ scanning we find "half" lines giving different partitions between fields Q_0 and Q_1 (two "half" lines in Q_1 for N even, and one "half" line in both Q_0 and Q_1, for N odd). With multiple interlace the partition of lines into fields depends on i and N, as well as on b.

Considering that all lines have the same slope id_y/D_x, we only need to list the lines in terms of their horizontal projections p_{nk}. The general result, which follows

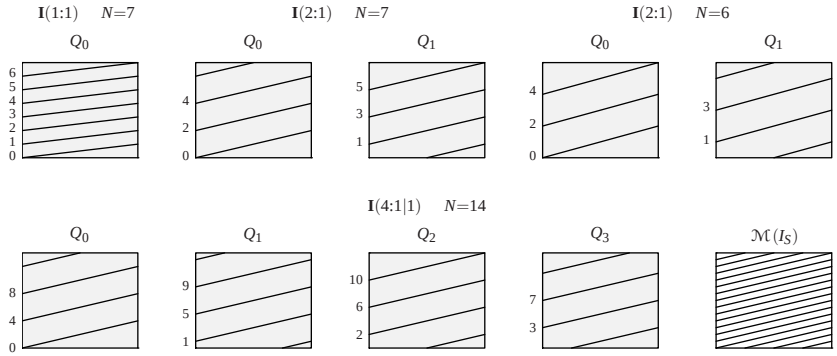

Fig. 12 Illustration of the picture–limited fields in the $\mathbf{I}(i\!:\!1|b)$ continuous scanning.

from geometrical considerations, is

$$p_{nk} = \begin{cases} [\alpha_k D_x, D_x) & n = n_k - i \\ [0, D_x) & n = n_k, n_k + i, \ldots, n_k + (N'_k - 1)\, i \\ [0, \beta_k D_x) & n = n_k + N'_k i \end{cases} \tag{74}$$

where $n_k = \rho_i(kb)$ gives the position of the first full line, $N'_k = \nu_i(N - n_k)$ is the number of full lines, and $\alpha_k = 1 - n_k/i$ and $\beta_k = (N - n_k - iN'_k)/i$. In general, a field Q_k has two fractional lines, one at the top and one at the bottom, and N'_k full lines in the middle. In field Q_0 the lower fractional line is absent ($\alpha_0 = 1$) and in another field of the period the upper fractional line is missing (see lower half of Fig. 12). Note that in each case the number of lines per field is exactly $N_f = N/i$, for all fields, provided that fractional lines are suitably weighted in the count.

4.4 Discrete scanning with memory

The reference scanning lattice is

$$I_{S\,1:1} = \mathbb{Z}(d_x, d_y, T_f)\,, \tag{75}$$

where $d_y = D_y/N$ is the vertical spacing and $d_x = D_x/M$ is the horizontal spacing with M the number of pixels per line.

In the general case, the scanning lattice becomes an arbitrary sublattice of $I_{S\,1:1}$, whose base has the Hermitian form

$$\mathbf{I}_S = \begin{bmatrix} d_x & 0 & 0 \\ 0 & d_y & 0 \\ 0 & 0 & T_f \end{bmatrix} \begin{bmatrix} a & p & q \\ 0 & i & b \\ 0 & 0 & 1 \end{bmatrix}. \tag{76}$$

As in $\mathbf{M}(i:1|b)$ continuous scanning, the integers i and b describe the vertical–temporal interlace. The values a, p and q are integers, with $0 \leq p$ and $q < a$, where a specifies the horizontal pixel spacing as ad_x, and p and q complete the interlace specification of the lattice. A similar lower–triangular representation applies, as listed in Tab. 5.

Table 5 Lattices of memory scanning.

upper triangular representation

$$\mathbf{I}_S = \begin{bmatrix} \mathbf{C}_0 & \mathbf{c} \\ \mathbf{0} & T_f \end{bmatrix} \qquad \mathbf{I}_S = \begin{bmatrix} d_x & 0 & 0 \\ 0 & d_y & 0 \\ 0 & 0 & T_f \end{bmatrix} \begin{bmatrix} a & p & q \\ 0 & i & b \\ 0 & 0 & 1 \end{bmatrix} \qquad H = \mathbb{Z}^3$$

lower triangular representation

$$\mathbf{I}_S = \begin{bmatrix} \mathbf{K}_0 & \mathbf{0} \\ \mathbf{d} & T_q \end{bmatrix} \qquad \mathbf{I}_S = \begin{bmatrix} d_x & 0 & 0 \\ 0 & d_y & 0 \\ 0 & 0 & T_f \end{bmatrix} \begin{bmatrix} b_{11} & 0 & 0 \\ b_{21} & b_{22} & 0 \\ b_{31} & b_{33} & L \end{bmatrix} \qquad H = \mathbb{Z}^3$$

The reduction of pixel density with respect to the reference case (*reduction factor*) is given by $r(I_S) \stackrel{\Delta}{=} \mu(I_S)/\mu(I_{S1:1}) = ai$, where a and i represent the horizontal and the vertical reductions, respectively. In terms of the lower–triangular base this gives $r(I_S) = b_{11}b_{22}b_{33}$, where $b_{33} = L$ is the field period.

The scanning point of I_S has the coordinates

$$\begin{aligned} x_S &= (ma + n'p + kq)\, d_x \\ y_S &= (n'i + kb)\, d_y \\ t_S &= k\, T_f \end{aligned} \qquad\qquad m, n', k \in \mathbb{Z}\,.$$

The fields C_k can be written in the form

$$C_k = C_0 + k\,\mathbf{c}\,, \qquad \mathbf{c} = (qd_x, bd_y)\,,$$

where $C_0 = Z_a^p(d_x, id_y)$. The lines are given by

$$c_{n'k} = c_{00} + n'(pd_x, id_y) + k(qd_x, bd_y)\,,$$

where $c_{00} = \mathbb{Z}(ad_x) \times \{0\}$. The field period, which determines the frame period as $T_q = L\,T_f$, is the smallest integer L such that $L\,\mathbf{c} \in C_0$; L is always a submultiple of ia. The mosaic $\mathcal{M}(I_S)$ is a sublattice of $\mathbb{Z}(d_x, d_y)$, which is immediately identified from the lower–triangular base (see Theorem 1).

Example 1. A sufficiently general example of a discrete scanning group is illustrated in Fig. 13. The reduction factor is $r(I_S) = 10$ and the period is $L = 5$. The fields are

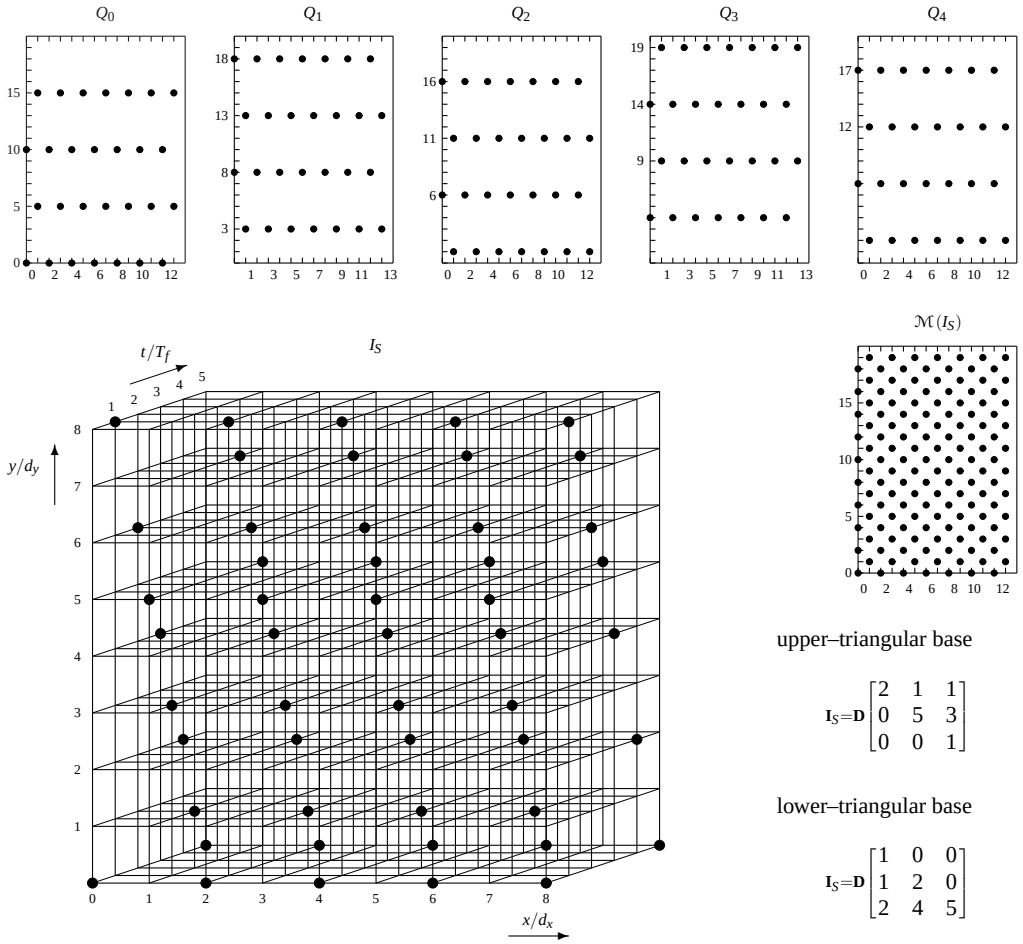

Fig. 13 Example of a scanning lattice I_S with field period $L = 5$. The top row represents the framed fields, with $M = 14$ and $N = 20$, below are the perspective view and the mosaic. **D** is the diagonal matrix diag$[d_x, d_y, T_f]$.

$C_0 + k(d_x, 3d_y)$, with $C_0 = Z_2^1(d_x, 5d_y)$. The mosaic is $\mathcal{M}(I_S) = Z_2^1(d_x, d_y)$.

In the framed fields Q_k the problem is to evaluate of the number of lines for fields N_k and the number of pixels per line $M_{n'k}$. N_k is the same as in continuous scanning (see (67)). The evaluation of $M_{n'k}$ is not trivial, as it depends on the position $m_{n'k}$ of the first pixel in the line (n', k) (Fig.14), which in turn depends on m_{0k}; the result is [25]

$$\begin{aligned} m_{0k} &= \rho_a\Big(kq - v_i(kb)\, p\Big) \\ m_{n'k} &= \rho_a(m_{0k} + n' p) \\ M_{n'k} &= v_a(M - 1 - m_{n'k}) + 1\,, \end{aligned} \tag{77}$$

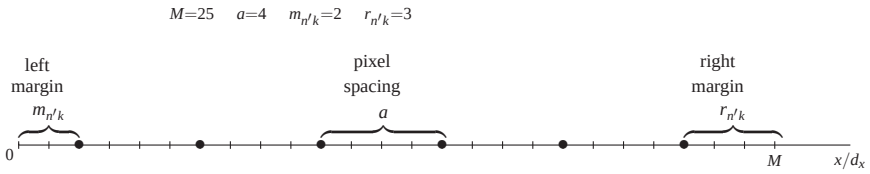

Fig. 14 Line structure in the discete scanning.

where the functions $\rho_a(\cdot)$ and $v_a(\cdot)$ were defined earlier. The number of pixels in field Q_k can be obtained by summing $M_{n'k}$ over $n' = 0, 1, \ldots, N_k - 1$ to then obtain the number of pixels per frame by summing over k in a period. The latter can be more directly evaluated from the mosaic, considering that fields do not overlap in a period. Recall that in the full format the number of pixels per frame is MN. This result still holds with a unit pixel spacing ($a = 1$), and more generally when the mosaic is $\mathbb{Z}(d_x, d_y)$. The *periods* are thus related

$$T_r = MT_0\,, \qquad T_q = T_f = NT_r = NMT_0\,,$$

where T_0 is the pixel period. In the general case, the pixel period becomes $T_e = aT_0$, whereas the line period remains $T_r = MT_0$, the field period is $T_f = NT_r/i$ and the frame period becomes

$$T_q = L\,T_f = \frac{LN}{i}\,T_r = \frac{LNM}{i}\,T_0 = \frac{LNM}{ai}\,T_e\,. \tag{78}$$

5 Aperiodic Scanning Model

The aperiodic model is illustrated in Fig. 15. It consists of the three parts outlined

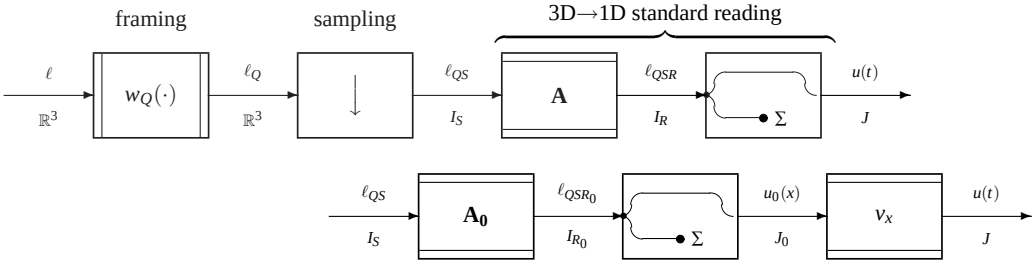

Fig. 15 *Aperiodic* scanning model with two forms of *standard* reading.

above, which are represented by appropriate "simple" transformations.

1) *Framing*

$$\ell_Q(x,y,t) = w_Q(x,y)\,\ell(x,y,t)\,, \qquad (x,y,t) \in \mathbb{R}^3\,, \tag{79}$$

where w_Q is the indicating function of the frame.

2) $\mathbb{R}^3 \to I_S$ *sampling*

$$\ell_{QS}(x,y,t) = \ell_Q(x,y,t)\,, \qquad (x,y,t) \in I_S\,, \tag{80}$$

where I_S is the *scanning group*, which is a 3D grating in continuous scanning and a 3D lattice in discrete scanning.

3) 3D→1D *reading*, which provides the final video signal $u(t)$, $t \in J$, where $J = \mathbb{R}$ is continuous scanning and $J = \mathbb{Z}(aT_0)$ in discrete scanning (aT_0 is the pixel period). This operation is a dimensionality reduction. It consists of a *composite shift* with relationship

$$\ell_{QSR}(t, nd_y, kT_f) = \ell_{QS}\Big(\mathbf{A}(t, nd_y, kT_f)\Big)\,, \quad t \in J\,,\ (n,k) \in Z_i^b\,, \tag{81}$$

where the 3×3 matrix $\mathbf{A}$ provides the composite shifts, followed by a 3D→1D sum–reduction

$$u(t) = \sum_{(n,k)\in Z_i^b} \ell_{QSR}(t, nd_y, kT_f)\,, \qquad t \in J\,. \tag{82}$$

After the composite shift the image domain becomes the *reading group*

$$I_R = J \times Z_i^b(d_y, T_f)\,,$$

where J is the domain of the video signal and $Z_i^b(d_y, T_f)$ is the *vertical–temporal lattice*.

Combining of (81) and (82) gives the video signal in terms of the framed sampled image ℓ_{QS}:

$$u(t) = \sum_{(n,k)\in Z_i^b} \ell_{QS}\Big(\mathbf{A}(t, nd_y, kT_f)\Big)\,, \qquad t \in J\,. \tag{83}$$

A slight rearrangement of the reading operation helps this analysis. In (81) the change of coordinates has the structure

$$(x_S, y_S, t_S) \in I_S \longrightarrow (t, y_R, t_R) \in I_R\,,$$

where the horizontal coordinate x_S becomes time t. The reason is that the matrix $\mathbf{A}$ not only does provide line shifts, but also a scale change in the first coordinate. This twofold operation can be split as in the lower half of Fig.15. This replaces (81) by

$$\ell_{QSR_0}(x, nd_y, kT_f) = \ell_{QS}\Big(\mathbf{A}_0(x, nd_y, kT_f)\Big)\,, \qquad (x, nd_y, kT_f) \in I_{R_0} \tag{84}$$

and the sum–reduction yields the "horizontal" video signal

$$u_0(x) = \sum_{(n,k)\in Z_i^b} \ell_{QSR_0}(x, nd_y, kT_f)\,, \qquad x \in J_0\,, \tag{85}$$

which is related to the "temporal" video signal by $u(t) = u_0(v_x t)$, $t \in J$. In this relationship v_x is the horizontal reading velocity, $J_0 = \mathbb{R}$ for continuous scanning and $J_0 = \mathbb{Z}(ad_x)$, with $ad_x = v_x aT_0$, for discrete scanning. The reading group becomes $I_{R_0} = J_0 \times Z_i^b(d_y, T_f)$, and the new matrix $\mathbf{A}_0$ is related to the original matrix by $\mathbf{A} = \mathrm{diag}\,[v_x, 1, 1]\,\mathbf{A}_0$.

5.1 Model Specification

With minor changes in the line shifts given below, the above model unifies a variety of scanning procedures, namely, continuous and discrete, progressive and interlaced including multiply–interlaced, instantaneous and with memory. A *specific type* from this variety is uniquely determined by the scanning group I_S. All the other parameters in the model, i.e. either $\mathbf{A}$, I_R, and J, or $\mathbf{A}_0$, I_{R_0}, and J_0, are obtained from I_S. In fact, the matrix $\mathbf{A}_0$, which provides the line shifts, is determined by imposing the disjoint projection condition in the final 3D→1D reduction. Then, I_{R_0} is given by

$$I_{R_0} = \left\{ \mathbf{A}_0^{-1}\,\mathbf{t}_S \mid \mathbf{t}_S \in I_S \right\} \tag{86}$$

and J_0 is the first factor of I_{R_0}.

In $\mathbf{M}(i:1|b)$ scanning the matrices $\mathbf{A}$ and $\mathbf{A}_0$ have the forms given in Tab. 6 in terms of the horizontal and vertical velocities v_x and v_y. In the continuous case the scanning group has the general form $I_S = \mathbb{R} \times Z_i^b(d_y, T_f)$, and the reading group I_{R_0} is still given by I_S. In the discrete case the scanning group I_S has the general form specified by (76) and the reading group becomes $I_{R_0} = \mathbb{Z}(ad_x) \times Z_i^b(d_y, T_f)$.

In $\mathbf{I}(i:1|b)$ scanning the matrices $\mathbf{A}$ and $\mathbf{A}_0$ have the forms listed in Tab. 6. They are more complex then the previous ones, as in this case line shifts also provide the removal of tilting. In continuous scanning the grating I_S has the general form specified in Tab. 4 and the reading group becomes $I_{R_0} = \mathbb{R} \times Z_i^b(d_y, T_f)$, the same as in $\mathbf{M}(i:1|b)$ scanning. Discrete scanning, where the scanning lattice would be a subgroup of the grating of Tab. 4, will be not considered.

Essential parameters. The scanning group I_S completely specifies the scanning format and hence the aperiodic model. However, some parameters in I_S are redundant. In continuous scanning essential parameters could be

$$i\,, \quad b\,, \quad N\,, \quad F_f\,, \tag{87}$$

which is in accordance with standard TV format specification, e.g. 1250/2:1/50 Hz, which means $N = 1250$, $i = 2$, $F_f = 50$ Hz. In fact, taking the frame dimension $D_x \times D_y$ as reference, from (87), one would obtain $d_y = D_y/N$, $T_r = iT_f/N$, etc., which identify the scanning grating in both $\mathbf{M}(i:1|b)$ and $\mathbf{I}(i:1|b)$ models.

Table 6 Composite–shift matrices.

memory scanning $\mathbf{M}(i{:}1|b)$

$$\mathbf{A} = \begin{bmatrix} v_x & -\dfrac{v_x}{v_y} & -v_x \\ 0 & 1 & 0 \\ 0 & 0 & 1 \end{bmatrix} \qquad \mathbf{A}_0 = \begin{bmatrix} 1 & -\dfrac{v_x}{v_y} & -v_x \\ 0 & 1 & 0 \\ 0 & 0 & 1 \end{bmatrix}$$

instantaneous scanning $\mathbf{I}(i{:}1|b)$

$$\mathbf{A} = \begin{bmatrix} v_x & -\dfrac{v_x}{v_y} & -v_x \\ v_y & 0 & -v_y \\ 1 & 0 & 0 \end{bmatrix} \qquad \mathbf{A}_0 = \begin{bmatrix} 1 & -\dfrac{v_x}{v_y} & -v_x \\ \dfrac{v_y}{v_x} & 0 & -v_y \\ \dfrac{1}{v_x} & 0 & 0 \end{bmatrix}$$

fundamental relationships (i: interlace order)

$$v_x = D_x N F_q \qquad v_x T_r = D_x$$
$$v_y = i D_y F_q \qquad v_y T_r = i\, d_y$$

In discrete scanning the integers M, a, p, and q must be added to (87) to identify the reference pixel spacing as $d_x = D_x/M$, the true pixel spacing $a d_x$, and the lattice interlace.

5.2 Reproduction

The *reproduction process* consists of recovering a replica of the continuous image from the video signal. It can be subdivided into two parts, as illustrated in Fig. 16,

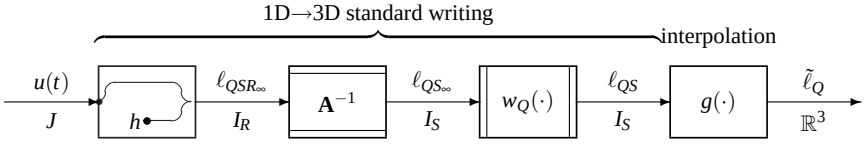

Fig. 16 Model of the reproduction process.

consisting of

1) recovery of the sampled image from the video signal (1D→3D conversion), according to the Dimensionality Reduction Theorem;
2) recovery of the continuous image from the sampled image (interpolation), according to the Sampling Theorem.

1) is governed by the Dimensionality Reduction Theorem via the *disjoint projection condition*, 2) is governed by the Sampling Theorem via the *non–aliasing condition* $\sigma(L_Q) \subset C_0$, where C_0 is a unit cell of $\mathbb{R}^3$ modulo $I_S^\star$. The indicating function of C_0 yields the frequency response of the interpolating filter.

We will now discuss the disjoint projection condition, which has consequences for the scanning model, in detail.

5.3 Disjoint projection condition. Adjustments

The scanning group I_S can be expressed in terms of the reading group I_{R_0} (see (86)), as follows

$$I_S = \left\{ \mathbf{A}_0 \mathbf{t}_R \mid \mathbf{t}_R \in I_{R_0} \right\},$$

where $I_{R_0} = J_0 \times Z_i^b(d_y, T_f)$, so that $\mathbf{t}_R$ has the form (x, nd_y, kT_f), with $x \in J_0$, $(n,k) \in Z_i^b$. The lines can then be written in the form

$$c_{nk}^{(3)} = \left\{ \mathbf{A}_0(x, nd_y, kT_f) \mid x \in J_0 \right\}, \qquad (n,k) \in Z_i^b\,, \tag{88}$$

and the framed lines as

$$q_{nk}^{(3)} = \left\{ \mathbf{A}_0(x, nd_y, kT_f) \mid x \in \pi_{nk} \right\}, \qquad n \in \mathcal{N}_k\,, \tag{89}$$

where π_{nk} are subsets of J_0, and $\mathcal{N}_k$ indexes the non–empty lines of the field Q_k. After the change of coordinates with matrix $\mathbf{A}_0$, (89) becomes

$$r_{nk}^{(3)} = \left\{ (x, nd_y, kT_f) \mid x \in \pi_{nk} \right\} = \pi_{nk} \times \left\{ (nd_y, kT_f) \right\}, \tag{90}$$

which shows that π_{nk} are just the x–projections of the shifted lines $r_{nk}^{(3)}$.

The condition for a correct recovery of the sampled image $\ell_{QS}(\cdot)$, from the video signal, is that π_{nk} do not overlap. We now check this condition for the different types of scanning. As we shall see, in some cases the condition is not satisfied.

$\mathbf{M}(i:1|b)$ continuous scanning. The line projections have the form $\pi_{nk} = [s_{nk}, s_{nk} + D_x)$, where

$$s_{nk} = (n + kN)\,\frac{D_x}{i}\,, \qquad n \in \mathcal{N}_k\,.$$

We note the following: a) all lines are full length with projection of length D_x, b) the beginning of the projection of field k is given by

$$\sigma_k = (n_k + kN)\,\frac{D_x}{i} \qquad \text{with} \qquad n_k = \mu_i(kb)$$

and its length is $N_k D_x$, c) the beginning of projection of the frame h is $\sigma_{ih} = hND_x$. Hence, in the projection frames are separated by ND_x, i.e. by the exact length needed

for N lines. Because line projections do not overlap within a field, the only condition is the projection at each field ends exactly at the beginning of the next, i.e.

$$\sigma_k + N_k D_x = \sigma_{k+1}\,. \tag{91}$$

We now verify this condition (in any case the verification can be limited to one period). For **M**(1:1) scanning verification is trivial. For **M**(2:1) scanning, we find $\sigma_0 = 0$, $\sigma_1 = \frac{1}{2}(1+N)D_x$ and $\sigma_2 = ND_x$. On the other hand $N_0 = N_1 = \frac{1}{2}N$ for N even, and $N_0 = \frac{1}{2}(n+1)$, $N_1 = \frac{1}{2}(N-1)$ for N odd (see Fig. 11). Hence, for N odd all the fields appear correctly, whereas for N even the odd fields have a $\frac{1}{2}D_x$ overlap with respect to even fields, so that a $-\frac{1}{2}D_x$ shift must be introduced to meet the disjoint projection condition.

Unfortunately, this offset cannot be achieved by modifying the shift matrix. Instead the aperiodic model of Fig. 15 must be complemented by introducing a horizontal offset $\varepsilon_k D_x$, where $\varepsilon_k = 0$ for k even, and $\varepsilon_k = -\frac{1}{2}$ for k odd. Hence, the aperiodic model takes the form of Fig. 17, where the sampled image is modified,

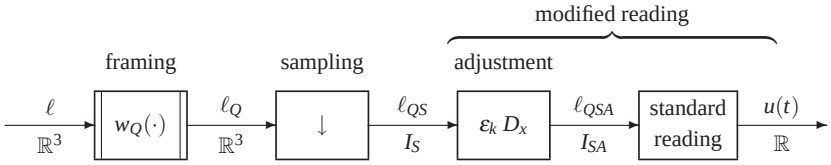

Fig. 17 *Aperiodic* model with *modified* reading.

before the coordinate change, as

$$\ell_{QSA}(x, nd_y, kT_f) = \ell_{QS}(x - \varepsilon_k D_x, nd_y, kT_f)\,. \tag{92}$$

This situation becomes quite frequent with multiple interlace, according to the following general result [25]:

Theorem 1. *In* $\mathbf{M}(i:1|b)$ *scanning the disjoint projection condition is assured by a coordinate change with a matrix* $\mathbf{A}_0$*, if the number of lines per frame has the form* $N = iZ - b$*, with* Z *integer. Otherwise, horizontal adjustments* $\varepsilon_k D_x$ *are needed, such that* $\varepsilon_0 = 0$ *and*

$$\varepsilon_k = \varepsilon_{k-1} + \frac{1}{i}\left[\mu_i(kb - N) - \mu_i(kb + b)\right], \qquad k \geq 1\,.$$

As an example, in **M**(3:1|1) scanning for $N = 3Z - 1$ no adjustment are not needed, whereas for $N = 3Z$ and $N = 3Z - 2$ adjustment $\varepsilon_k D_x$ are required, with $\varepsilon_1 = -1/3$, $\varepsilon_2 = 1/3$, and $\varepsilon_1 = 1/3$, $\varepsilon_2 = -1/3$, respectively.

I$(i:1|b)$ **continuous scanning.** The line projections are given by (see (74)):

$$\pi_{nk} = p_{nk} + \frac{n + kN}{i} D_x\,, \qquad n = n_k - i\,,\ n_k\,,\ n_k + i\,,\ \ldots\,,\ n_k + N'_k i\,,$$

where $p_{nk} = [\alpha_k D_x, D_x)$ for $n = n_k - i$, $p_{nk} = [0, \beta_k D_x)$ for $n = n_k + N'_k i$, and $p_{nk} = [0, D_x)$ for the N'_k full lines. Hence: a) within the same field k the line projections are consecutive, with a total length

$$(1-\alpha_k)\, D_x + N'_k D_x + \beta_k D_x = \frac{N}{i}\, D_x \quad ;$$

b) the projections of the beginning of the frames occur at hND_x, $h \in \mathbb{Z}$, so that they are separated by ND_x. It remains to check that the beginning of the projection σ_k of field k is kND_x/i . In fact, the projection of the first full line starts at $(n_k + kN)\, D_x/i$ and the beginning of the fractional line is shifted to the left by $(1-\alpha_k)\, D_x$. Hence

$$\sigma_k = \frac{n_k + kN}{i}\, D_x - (1-\alpha_k)\, D_x = \frac{kN}{i}\, D_x\,.$$

In conclusion, in $\mathbf{I}(i:1|b)$ scanning the disjoint projection condition is always verified so that the aperiodic model of Fig.15 is correct, without any introduction of horizontal adjustments.

$\mathbf{M}(i:1|b)$ **discrete scanning.** The same conclusion seen for the continuous scanning hold. In general if the number of lines does not have the form $N = iZ - b$ horizontal adjustments must be introduced according to Theorem 6. This guarantees that the shifted lines always have disjoint projections. In discrete scanning, however, there is the additional requirement that the video–signal domain J_0 consists of equally spaced points, i.e. J_0 must have the lattice form $\mathbb{Z}(ad_x)$. In general, this does not happen even introducing horizontal offsets $\varepsilon_k D_x$. In fact, re–examining the structure of a discrete line q_{nk} (see Fig.14), we find that the pixels are separated by ad_x, with a *left margin* $m_{nk}d_x$ and a *right margin* $r_{nk}d_x$. The condition for uniform spacing is that the right margin of one line plus the left margin of the next line equals the spacing ad_x, namely

$$r_{n'k} + m_{(n'+1)k} = a\,. \tag{93}$$

Theorem 2. *[25] Condition (93) holds if and only if M has the form $M = aV - p$, with V integer, i.e. if $p = \rho_a(-M)$. Otherwise, a horizontal offset of the form $\delta_{n'k}d_x$ must be introduced, where*

$$\delta_{n'k} = \rho_a(m_{0k} + n'p - M) - \rho_a(m_{0k} + n'p + p)\,, \tag{94}$$

with m_{0k} given by the first line of (77).

The situation is further complicated as the uniform spacing must be guaranteed in changes of fields: the right margin of the last line of field k plus the left margin of the first line of field $k+1$ must be equal to ad_x. Otherwise,

Theorem 3. *A horizontal adjustment of the form $\delta_k d_x$ is required, where*

$$\delta_k = \rho_a(kq - M - v_k p) - \rho_a(kq + q - z_{k+1}p)\,, \tag{95}$$

with

$$v_k = v_i(N-1-kb)\,, \qquad z_k = v_i(kb)\,. \tag{95a}$$

In conclusion, $\mathbf{M}(i:1|b)$ discrete scanning requires horizontal adjustments of the form

$$\Delta_{nk} = \varepsilon_k D_x + \delta_{n'k} d_x + \delta_k d_x\,. \tag{96}$$

If $b = \rho_i(-N)$ the first offset is not required. If $p = \rho_a(-M)$ the second is not required. Finally, if $q = \rho_a(-MZ)$, with $Z = (N+b)/i$, the last offset is not required. Hence, for any M, N, a and i we can choose integers b, p and q such that horizontal adjustments are not required at all. We shall illustrate this point after introducing of the periodic model.

6 Periodic Scanning Model

By an appropriate periodic repetition of the framed image it is possible to read the video–signal *along a single straight line*, as illustrated in Fig. 18 for $\mathbf{I}(1:1)$

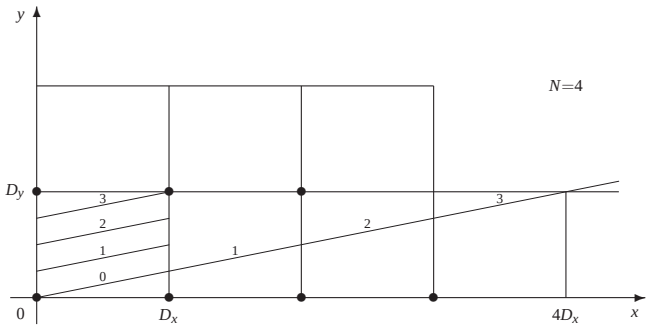

Fig. 18 Illustration of reading in the periodic model of **I**(1:1) scanning.

scanning. This possibility was first mentioned in a pioneering work by Mertz and Gray [41] for the elementary scanning types.

To derive the general periodic model, reconsider the video–signal expression (85) and set

$$(x, nd_y, kT_f) = (x,0,0) + (0, nd_y, kT_f)\,.$$

Then,

$$\begin{aligned} u_0(x) &= \sum_{(n,k)\in Z_i^b} \ell_{QS}\Big(\mathbf{A}_0(x,0,0) + \mathbf{A}_0(0,nd_y,kT_f)\Big) \\ &= \sum_{\mathbf{s}\in S} \ell_{QS}\Big(\mathbf{A}_0(x,0,0) - \mathbf{s}\Big)\,, \qquad\qquad x \in J_0 \end{aligned} \tag{97}$$

where S is the 2D lattice in $\mathbb{R}^3$ given by

$$S = \Big\{ -\mathbf{A}_0(0,nd_y,kT_f) \mid (n,k) \in Z_i^b \Big\}\,. \tag{98}$$

By the relationship

$$\ell_p(\mathbf{t}) = \sum_{\mathbf{s}\in S} \ell_{QS}(\mathbf{t}-\mathbf{s}), \qquad \mathbf{t} \in I_S : S \tag{99}$$

(97) yields

$$u_0(x) = \ell_p\Big(\mathbf{A}_0(x,0,0)\Big), \qquad t \in J_0. \tag{100}$$

The previous relationships lead to the *periodic model* depicted in Fig.19, where

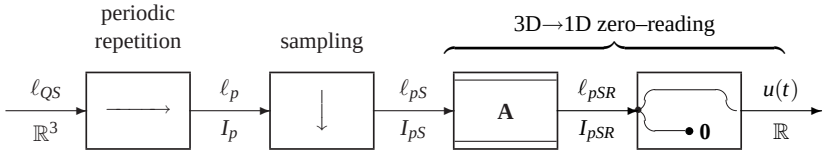

Fig. 19 Periodic model of continuous scanning.

1) the framed and sampled image $\ell_{QS}(\cdot)$ is periodically repeated according to (98);
2) the periodic image is read along a straight line with parametric equations

$$(x_S, y_S, t_S) = \mathbf{A}_0(x,0,0), \qquad x \in J_0,$$

which is just the line c_{00} of the scanning groups I_S (see (88)).

The last operation can be decomposed into a change of coordinates followed by a 3D→1D zero–reduction.

The same result is reached when starting from the temporal video signal (83), which after the periodic repetition takes the form

$$u(t) = \ell_{QSp}\Big(\mathbf{A}(t,0,0)\Big), \qquad t \in J. \tag{101}$$

6.1 Condition for correct recovery

In periodic model line shifts result from repetitions around the centers $\mathbf{s}_{nk} = \mathbf{A}_0(0, nd_y, kT_f)$ and the shifted lines take the form (see (90))

$$r^{(3)}_{nk} = q^{(3)}_{nk} + \mathbf{s}_{nk} = \Big\{\mathbf{A}_0(x,0,0) \mid x \in \pi_{nk}\Big\}, \tag{102}$$

so that they are displayed along the line $c^{(3)}_{00}$, i.e. the extension of $q^{(3)}_{00}$. The useful terms of the periodic repetition are limited to the centers $\mathbf{s}_{nk}$, $n \in \mathcal{N}_k$, $k \in \mathbb{Z}$, i.e. the centers whose terms fall on the line $c^{(3)}_{00}$.

The condition for correctly recovering the sampled image from the video signal is that the terms of the periodic repetition falling on the line $c_{00}^{(3)}$ do not overlap. This means the terms around the centers $\mathbf{s}_{nk}$, $n \in \mathcal{N}_k$, $k \in \mathbb{Z}$. Considering that the support of ℓ_{QS} is contained in the 3D frame $Q^{(3)}$, the condition implies that the sets

$$Q^{(3)} + \mathbf{s}_{nk}\,, \qquad n \in \mathcal{N}\,,\ k \in \mathbb{Z} \tag{103}$$

do not overlap.

In $\mathbf{I}(i:1|b)$ scanning, the nonoverlapping condition is satisfied for all the terms of the periodic repetition. In this case $Q^{(3)}$ is a unit cell of $\mathbb{R}^3$ modulo S. This, however, is not a necessary condition since according to (103), the useful terms are those falling along the line $c_{00}^{(3)}$.

If the sets (103) overlap, horizontal adjustments Δ_{nk} must be introduced, as in the aperiodic model. These adjustments can be combined with the *ordinary* repetition centers $\mathbf{s}_{nk}$ in the form $\tilde{\mathbf{s}}_{nk} = \mathbf{s}_{nk} + (\Delta_{nk}, 0, 0)$ to give *modified* repetition centers, and the *ordinary* periodic repetition (99) must be modified accordingly.

$\mathbf{I}(i:1|b)$ continuous scanning. The repetition centers are given by

$$\mathbf{s}_{nk} = -\mathbf{A}_0(0, nd_y, kT_f) = \left(\frac{n+kN}{i}D_x, kD_y, 0\right)\,, \qquad (n,k) \in Z_i^b\,, \tag{104}$$

which lie on the x,y plane and form the lattice

$$S_0 = Z_i^c\left(\frac{1}{i}D_x, D_y\right) \qquad \text{with} \qquad c = \rho_i(b+N)\,.$$

In particular, for $c = 0$, the lattice S_0 becomes the orthogonal lattice $\mathbb{Z}(D_x, D_y)$. According to (98) the video signal takes the form

$$u(t) = \ell_{QSp}(v_x t, v_y t, t)\,, \qquad t \in \mathbb{R}\,, \tag{105}$$

where the argument runs along the line $c_{00}^{(3)}$ of I_S.

It can be shown that the lattice of the repetition centers S have the right spacing for $Q^{(3)}$ to be a unit cell of $\mathbb{R}^3$. Then the condition of a correct recovery of the image from the video signal is always satisfied for this kind of scanning in accordance with the conclusion of the previous section.

Here are some examples to illustrate the periodic model. In $\mathbf{I}$(1:1) scanning the lattice S_0 is $\mathbb{Z}(D_x, D_y)$; reading along the line c_0 is depicted in Fig.18 for $N = 4$ lines per frame. In $\mathbf{I}$(2:1) scanning the lattice S_0 is still $\mathbb{Z}(D_x, D_y)$ for N odd (Fig.20a), but becomes the quincunx lattice $Z_2^1\left(\frac{1}{2}D_x, D_y\right)$ for N even (Fig.20b). Fig.20c illustrates $\mathbf{I}$(5:1|4) scanning for $N = 13$, where $S_0 = Z_5^2\left(\frac{1}{5}D_x, D_y\right)$. In these examples we can verify that $Q^{(3)}$ is a unit cell of $\mathbb{R}^3$ modulo S_0.

$\mathbf{M}(i:1|b)$ continuous scanning. The repetition centers are given by

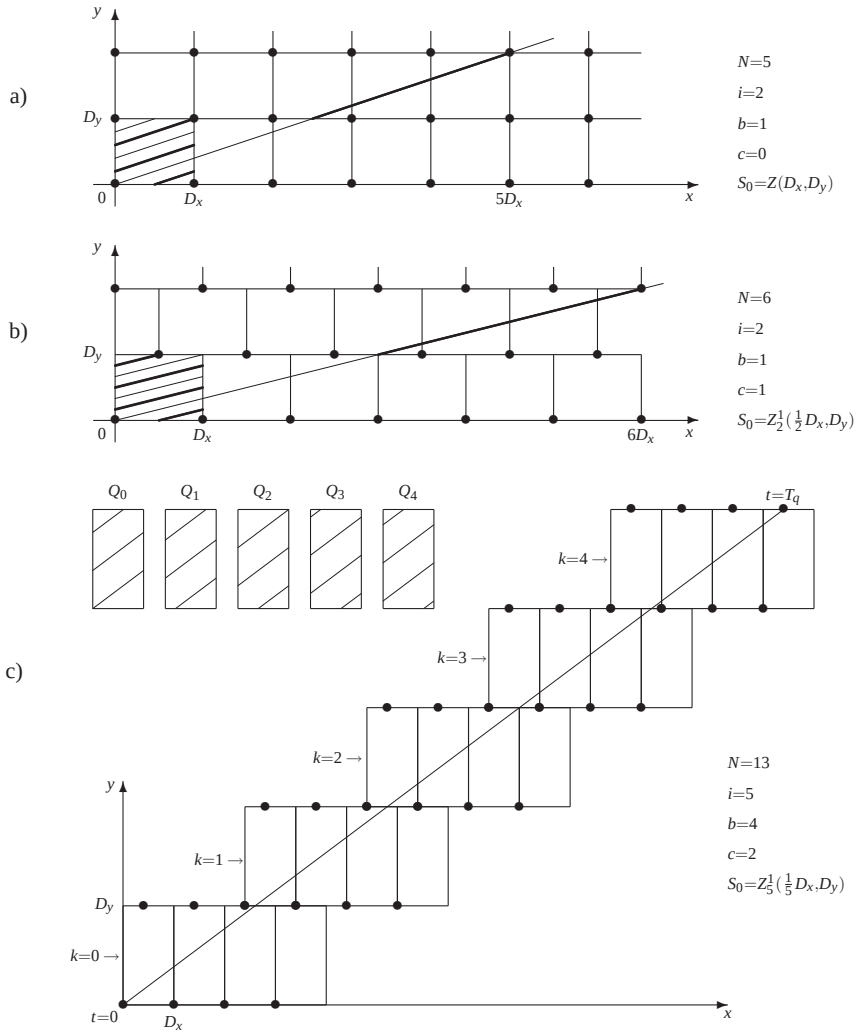

Fig. 20 Illustrations of periodic model for $\mathbf{I}(i{:}1|b)$ scanning, with $i=2$ and $i=5$.

$$\mathbf{s}_{nk} = -\mathbf{A}_0(0, nd_y, kT_f) = \left(-(n+kN)\,\frac{D_x}{i}, nd_y, kT_f\right) \tag{106}$$

which no longer lie on the x,y plane. Moreover, their x,y projections $\mathbf{s}_0 \in S_0$ do not assure that Q is a unit cell of $\mathbb{R}^2$, so that horizontal adjustments are generally required. The video signal is given by

$$u(t) = \ell_{QSp}(v_x t, 0, 0)\,, \qquad t \in \mathbb{R}\,, \tag{107}$$

and in this kind of scanning the line $c_{00}^{(3)}$ indeed coincides with the x axis.

We now illustrate the periodic model for **M**(2:1) scanning. With an odd number of lines the repetition centers (106) provide the exact spacing for $Q^{(3)}$ to be a unit cell, so that the line sequence forms a partition of the x axis, as illustrated for $N = 5$ in Fig. 21a. With an even number of lines this is no longer true, since the repetition

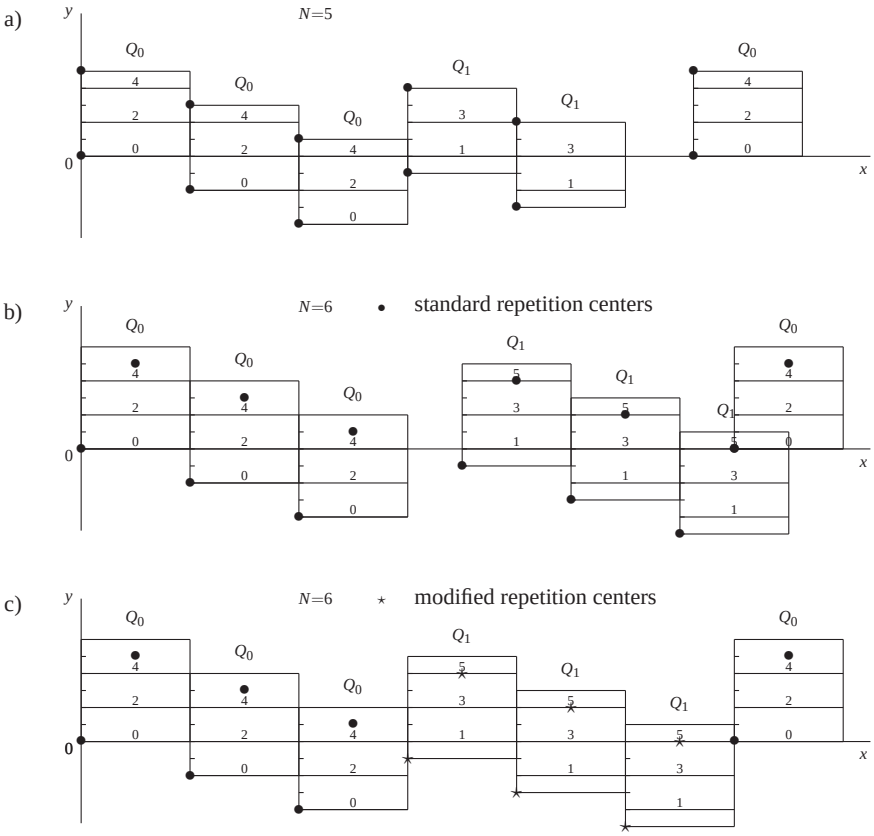

Fig. 21 Reading according to the periodic scanning model a) shows that the standard repetition centers work well for N odd, b) but they fail for N even and must be modified as in c).

of odd fields overlaps the repetition of even fields (Fig. 21b). This overlapping is avoided by horizontally offsetting the repetition centers of odd fields (Fig. 21c).

In general, according to Theorem 4, the ordinary repetition centers (106) are correct when $b = \rho_i(-N)$, otherwise they must be modified with horizontal adjustments $\varepsilon_k D_x$.

M$(i : 1|b)$ **discrete scanning.** The repetition centers and the reading line are the same as in continuous scanning, but *line* offsets are generally required to guarantee that the video signal has an equally spaced format. We illustrate this with a simple example of **M**(1:1) discrete scanning on a quincunx field, with $M = 6$ and $N = 4$

(Fig. 22). The ordinary repetition centers (106) provide the exact spacing for the

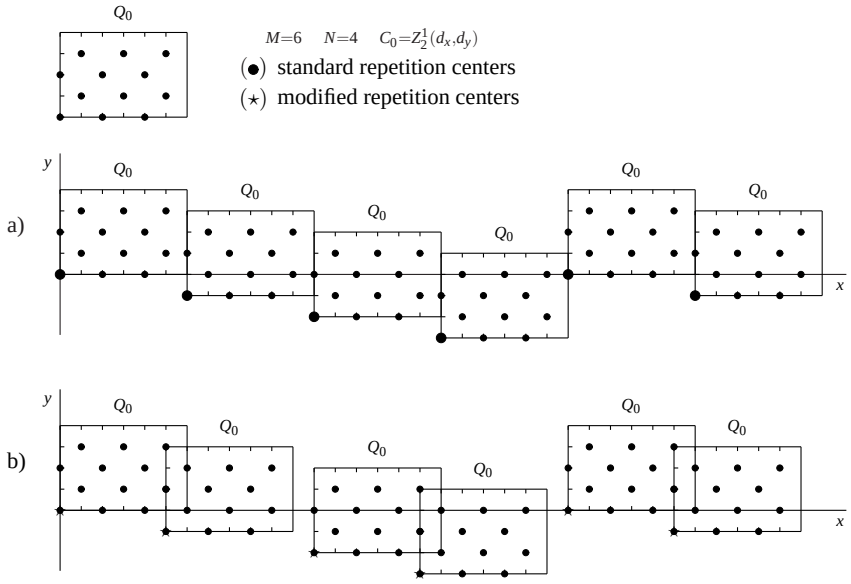

Fig. 22 Reading according to the periodic model in **M**(1:1) discrete scanning with a quincunx frame and $M = 5$, $N = 4$. a) The correct recovery condition is not assured with standard repetition centers; the repetition centers must be modified with line adjustments, as in b).

$Q^{(3)}$ repetition not to overlap so that horizontal *field* adjustments are not required (Fig.22a). This, however, does not guarantee an equally spaced format $\mathbb{Z}(2d_x)$ of the video signal as line 0 as a right margin $2d_x$ and line 1 has a left margin d_x, thus giving a $3d_x$ spacing. Line 1 has a right margin d_x and line 2 a left margin 0, thus giving a d_x spacing, etc. A correct $2d_x$ spacing is achieved by modifying the repetition centers by means of *line* adjustments $\delta_{n'k}d_x$, with $\delta_{0k} = 0$, $\delta_{1k} = -1$, $\delta_{2k} = 1$, $\delta_{3k} = -1$ (Fig. 22b). This is in accordance with Theorem 5 and, indeed, with $M = 6$, $a = 2$, $p = 1$, the condition $p = \mu_a(-M)$ fails.

Continuing the example for $M = 7$, and in general for M odd, one can see that line adjustments are not needed. Regarding *field end* in accordance with Theorem 6 these are not required as long as MN is even.

A more elaborate example is found by reconsidering Fig. 13, where it can be shown that adjustments of all three kinds are required.

7 Fourier Analysis of Scanning Process

The object of this section is to evaluate the Fourier transforms of the signals involved in the scanning and reproduction processes. The Fourier transform of a time–varying image $\ell(x,y,t)$ is a complex 3D function $L(f_x, f_y, f_t)$, where the frequencies have dimensions of cycles per width (cpw), cycles per height (cph), and cycles per second

(cps or Hz), respectively. For Fourier analysis a preliminary identification of the frequency domain is needed, in particular the dual $\widehat{I_S}$ of the scanning group I_S, which has the form

$$\widehat{I_S} = \mathbb{R}^3 : I_S^\star ,$$

where $I_S^\star$ is the reciprocal of I_S.

7.1 Reciprocal scanning group

If I_S is orthogonal, the evaluation of $I_S^\star$ is immediate. In particular, in *full format* discrete scanning we have

$$I_S = \mathbb{Z}(d_x, d_y, T_f) \xrightarrow{\star} I_S^\star = \mathbb{Z}(F_x, F_y, F_f)$$

where

$$F_x = \frac{1}{d_x} = \frac{M}{D_x} , \qquad F_y = \frac{1}{d_y} = \frac{N}{D_y} , \qquad F_f = \frac{1}{T_f} .$$

In **M**(1:1) continuous scanning

$$I_S = \mathbb{R} \times \mathbb{Z}(d_y, T_f) \xrightarrow{\star} I_S^\star = \mathbb{O} \times \mathbb{Z}(F_y, F_f) .$$

These cases apart, according to Proposition 6, $I_S^\star$ must be evaluated in matrix–signature representation, namely

$$(\mathbf{I}_S, H_S) \mapsto I_S \xrightarrow{\star} (\mathbf{I}_S^\star, H_S^\star) \mapsto I_S^\star . \tag{108}$$

The signature test shows that

- in continuous scanning ($H_S = \mathbb{R} \times \mathbb{Z}^2$), the reciprocal group is a 2D lattice in $\mathbb{R}^3$ ($H_S^\star = \mathbb{O} \times \mathbb{Z}^2$).
- in discrete scanning ($H_S = \mathbb{Z}^3$), the reciprocal group is a full 3D lattice ($H_S^\star = \mathbb{Z}^3$).

To evaluate the reciprocal base matrix $\mathbf{I}_S^\star$ (the inverse transpose of $\mathbf{I}_S$), according to (32), it is convenient to use *triangular* forms.

For both continuous and discrete $\mathbf{M}(i:1|b)$ scanning an upper triangular form for $\mathbf{I}_S$ can be written in terms of fields (see Tab. 3 and Tab. 4). Hence,

$$\mathbf{I}_S = \begin{bmatrix} \mathbf{C}_0 & \mathbf{c} \\ \mathbf{0} & T_f \end{bmatrix} \xrightarrow{\star} \mathbf{I}_S^\star = \begin{bmatrix} \mathbf{C}_0^\star & \mathbf{0} \\ \mathbf{c}_1 & F_f \end{bmatrix} \tag{109}$$

where $\mathbf{c}_1 = -F_f \, \mathbf{c}' \mathbf{C}_0^\star$.

For *all* types of scanning (see Tab. 3, Tab. 4, and Tab. 5) a lower triangular form can be written in terms of the mosaic and the frame period (see (57)). Hence,

$$\mathbf{I}_S = \begin{bmatrix} \mathbf{K}_0 & \mathbf{0} \\ \mathbf{d} & T_q \end{bmatrix} \xrightarrow{\star} \mathbf{I}_S^\star = \begin{bmatrix} \mathbf{K}_0^\star & \mathbf{d}_1 \\ \mathbf{0} & F_q \end{bmatrix} \tag{110}$$

where $\mathbf{d}_1 = -F_q \mathbf{K}_0^\star \mathbf{d}$.

Explicit results are collected in Tab. 7 for continuous scanning and in Tab. 8 for

Table 7 Reciprocals of scanning gratings.

M(i:1|b) *scanning: upper triangular representation*

$$\mathbf{I}_S^\star = \begin{bmatrix} \frac{1}{D_x} & 0 & 0 \\ 0 & \frac{1}{i}F_y & 0 \\ 0 & 0 & F_q \end{bmatrix} \begin{bmatrix} 1 & 0 & 0 \\ 0 & 1 & 0 \\ 0 & 0 & 1 \end{bmatrix} \qquad H_S^\star = \mathbb{O} \times Z_i^c$$

I(i:1|b) *scanning: upper triangular representation*

$$\mathbf{I}_S^\star = \begin{bmatrix} \frac{1}{D_x} & 0 & 0 \\ 0 & \frac{1}{i}F_y & 0 \\ 0 & 0 & F_q \end{bmatrix} \begin{bmatrix} 1 & -i & -c \\ 0 & i & c-\frac{1}{N} \\ 0 & 0 & 1 \end{bmatrix} \qquad H_S^\star = \mathbb{O} \times \mathbb{Z}^2$$

Table 8 Reciprocals of scanning lattices.

lower triangular representation

$$\mathbf{I}_S^\star = \begin{bmatrix} \mathbf{C}_0^\star & \mathbf{0} \\ \mathbf{c}_1 & F_f \end{bmatrix} \qquad \mathbf{c}_1 = -F_f \, \mathbf{c}' \, \mathbf{C}_0^\star$$

$$\mathbf{I}_S^\star = \begin{bmatrix} \frac{1}{r}F_x & 0 & 0 \\ 0 & \frac{1}{r}F_y & 0 \\ 0 & 0 & \frac{1}{r}F_f \end{bmatrix} \begin{bmatrix} i & 0 & 0 \\ a-p & a & 0 \\ e & a(i-b) & ai \end{bmatrix} \qquad H_S^\star = \mathbb{Z}^3$$

$$r = ai \quad , \qquad e = a(i-b) + i(a-q) + bp$$

upper triangular representation

$$\mathbf{I}_S^\star = \begin{bmatrix} \mathbf{K}_0^\star & \mathbf{d}_1 \\ \mathbf{0} & F_q \end{bmatrix} \qquad \mathbf{d}_1 = -F_q \mathbf{K}_0^\star \mathbf{d}_0'$$

$$\mathbf{I}_S^\star = \begin{bmatrix} \frac{1}{r}F_x & 0 & 0 \\ 0 & \frac{1}{Lb_{22}}F_y & 0 \\ 0 & 0 & F_q \end{bmatrix} \begin{bmatrix} Lb_{22} & (b_{22}-b_{21})L & h \\ 0 & L & L-b_{22} \\ 0 & 0 & 1 \end{bmatrix} \qquad H_S^\star = \mathbb{Z}^3$$

$$h = (b_{22}-b_{21})L + b_{22}(L-b_{31}) + b_{32}b_{21}$$

discrete scanning, and commented on below. Note that some results were manipulated according to the rules of Section II.B.

Decomposition of $I_S^\star$. In scanning with memory, I_S is a subset of the corresponding full–format group $I_{S\,1;1}$. Hence, from Proposition 6, $I_S^\star \supset I_{S\,1:1}^\star$, and from (13) we can write

$$I_S^\star = I_{S\,1:1}^\star + P\,, \qquad P = [I_S^\star : I_{S\,1:1}^\star)\,, \tag{111}$$

where the unit cell P is a finite set whit a number of points given by the *reduction factor* r ($r = i$ in continuous scanning and $r = ai$ in discrete scanning).

Continuous scanning. We first evaluate the vertical–temporal lattice $J_{vt} = Z_i^b(d_y, T_f)$. From the lower triangular representation (11) we have

$$\mathbf{J}_{vt}^\star = \begin{bmatrix} \frac{1}{i}F_y & 0 \\ 0 & \frac{1}{i}F_f \end{bmatrix} \begin{bmatrix} i & -\tilde{b} \\ 0 & 1 \end{bmatrix} \to \begin{bmatrix} \frac{1}{i}F_y & 0 \\ 0 & \frac{1}{i}F_f \end{bmatrix} \begin{bmatrix} i & i-\tilde{b} \\ 0 & 1 \end{bmatrix}. \tag{112}$$

For example, the reciprocal of $Z_4^1(d_y, T_f)$ is $Z_4^3\left(\frac{1}{i}F_y, F_q\right)$.

Now, in $\mathbf{M}(i:1|b)$ scanning the scanning group has the factored form $I_S = \mathbb{R} \times J_{vt}$, hence,

$$I_S^\star = \mathbb{O} \times J_{vt}^\star = \mathbb{O} \times Z_i^c\left(\frac{1}{i}F_y, F_q\right).$$

Since the points of $I_S^\star$ lie in the f_y, f_t plane, we use the decomposition (111) in the 2D form

$$J_{vt}^\star = J_{vt\,1:1}^\star + P\,, \qquad P = [J_{vt}^\star : J_{vt\,1:1}^\star)\,,$$

where $J_{vt\,1:1}^\star = \mathbb{Z}(F_y, F_f)$ is the reciprocal of the vertical–temporal lattice of $\mathbf{M}(1{:}1)$ scanning. The unit cell P contains i points, and can be written in the form (see (112))

$$\left(kc\frac{F_y}{i}, k\frac{F_f}{i}\right), \qquad k = 0, 1, \ldots, i-1\,.$$

These points can be placed within the rectangle $[0, F_y) \times [0, F_f)$ by replacing kc with $\rho_i(kc)$, as illustrated in Fig.23 for the first order of interlace i.

In $\mathbf{I}(i:1|b)$ scanning the grating is not factorisable and the 2D lattice $I_S^\star$ is tilted with respect to the f_y, f_t plane. For comparison, starting from the upper–triangular representation of $I_S^\star$ (see Tab. 8), we write the scanning point of $I_S^\star$ for $\mathbf{M}(i:1|b)$ scanning, given by

$$\left(0, \left(n + k\frac{c}{i}\right)F_y, kF_q\right), \qquad n, k \in \mathbb{Z}\,,$$

and for $\mathbf{I}(i:1|b)$ scanning, given by

$$\left(-(ni+kc)\frac{1}{D_x}, n + \frac{k}{i}\left(c - \frac{1}{N}\right)F_y, kF_q\right), \qquad n, k \in \mathbb{Z}\,.$$

Discrete scanning. Considering that both the scanning group I_S and its reciprocal $I_S^\star$ are full 3D lattices, symmetric considerations apply.

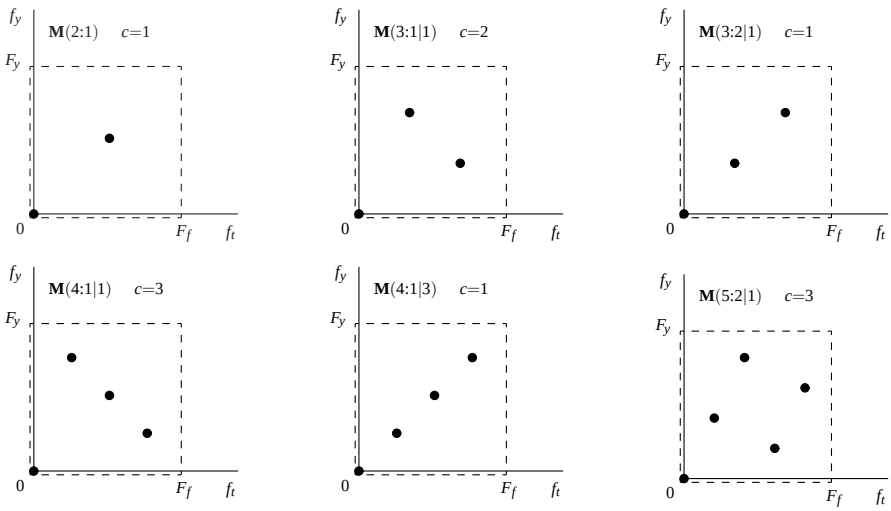

Fig. 23 Illustration of the unit cell of *additional centers* of $I_S^\star$ with respect to $I_{S\,1:1}^\star$ in $\mathbf{M}(i{:}1|b)$ scanning.

Comparing (109) and (110) we find

1) The upper–triangular form of I_S identifies the field sequence $C_k = C_0 + k\mathbf{c}$. Similarly, from the upper–triangular form of $I_S^\star$ we can identify the fields in the frequency domain
$$\hat{C}_k = \hat{C}_0 + k\hat{\mathbf{c}}\,,$$
which represent the 2D sets obtained from $I_S^\star$ by fixing the temporal frequency to the values kF_q.
2) The field $\hat{C}_0$ is the reciprocal of the mosaic $\mathcal{M}(I_S)$.
3) The lower–triangular form of I_S identifies the mosaic $\mathcal{M}(I_S)$ and the field period L as T_q/T_f. Similarly, the lower–triangular form of $I_S^\star$ identifies the mosaic $\mathcal{M}(I_S^\star)$ and the field period $\hat{L}$. We also conclude that (see Tab. 8) $\hat{L} = L$.
4) The mosaic $\mathcal{M}(I_S^\star)$ is the reciprocal of the zero–th field C_0.
5) The field decomposition in the frequency domain is of the form (111) with $I_{1:1}^\star = \mathbb{Z}(F_x, F_y, F_f)$ and
$$P = \left\{ \{h\hat{\mathbf{c}} \times \left\{ k\frac{1}{r}F_f \right\} \;\middle|\; k = 0,1,\ldots,r-1 \right\}. \tag{113}$$

We test these assertions in the following example.

Example 1. Consider a scanning lattice I_S with Hermitian bases
$$\mathbf{I}_S = \begin{bmatrix} d_x & 0 & 0 \\ 0 & d_y & 0 \\ 0 & 0 & T_f \end{bmatrix} \begin{bmatrix} 2 & 1 & 1 \\ 0 & 2 & 1 \\ 0 & 0 & 1 \end{bmatrix} \rightarrow \begin{bmatrix} d_x & 0 & 0 \\ 0 & d_y & 0 \\ 0 & 0 & T_f \end{bmatrix} \begin{bmatrix} 1 & 0 & 0 \\ 0 & 1 & 0 \\ 2 & 3 & 4 \end{bmatrix}. \tag{114}$$

Using (109) and (110), after some rearrangement, we obtain the following Hermitian bases for the reciprocal group $I_S^\star$

$$\mathbf{I}_S^\star = \begin{bmatrix} \frac{1}{4}F_x & 0 & 0 \\ 0 & \frac{1}{4}F_y & 0 \\ 0 & 0 & \frac{1}{4}F_f \end{bmatrix} \begin{bmatrix} 4 & 0 & 2 \\ 0 & 4 & 1 \\ 0 & 0 & 1 \end{bmatrix} \rightarrow \begin{bmatrix} \frac{1}{4}F_x & 0 & 0 \\ 0 & \frac{1}{4}F_y & 0 \\ 0 & 0 & \frac{1}{4}F_f \end{bmatrix} \begin{bmatrix} 2 & 0 & 0 \\ 1 & 2 & 0 \\ 1 & 2 & 4 \end{bmatrix}. \tag{115}$$

From (114) we identify the field sequence $C_0 + k\mathbf{c}$ with $C_0 = Z_2^1(d_x, 2d_y)$ and $\mathbf{c} = (d_x, d_y)$. The mosaic is $\mathcal{M}(I_S) = \mathbb{Z}(d_x, d_y)$ and the field period is $L = 4$ (Fig.24a).

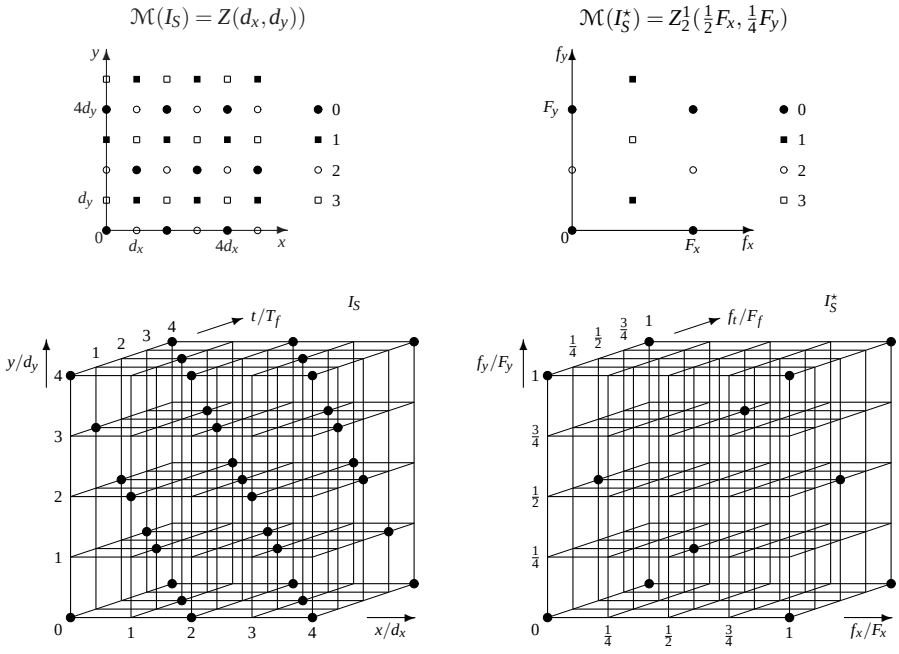

Fig. 24 Example of a scanning lattice I_S and its reciprocal $I_S^\star$: at the top are the mosaics, below the perspective views.

From (115) we identify the frequency domain field sequence $\hat{C}_0 + k\mathbf{c}$ with $\hat{C}_0 = \mathbb{Z}(F_x, F_y)$ and $\mathbf{c} = \left(\frac{1}{2}F_x, \frac{1}{4}F_y\right)$. The mosaic is $\mathcal{M}(I_S^\star) = Z_2^1\left(\frac{1}{2}F_x, \frac{1}{4}F_y\right)$ and the field period is $\hat{L} = 4$ (Fig.24b). Note that $\hat{C}_0$ is the reciprocal of $\mathcal{M}(I_S)$ and $\mathcal{M}(I_S^\star)$ is the reciprocal of C_0.

According to (113) the unit cell P is given by

$$P = \left\{ k\left(\frac{1}{2}F_x, \frac{1}{4}F_y, \frac{1}{4}F_f\right) \;\middle|\; k = 0, 1, 2, 3 \right\}.$$

7.2 Aperiodic model analysis

Assume that the Fourier transform $L(\mathbf{f})$, $\mathbf{f} = (f_x, f_y, f_t) \in \mathbb{R}^3$, of the source image is known. Following the aperiodic model of Fig. 15 we can determine the Fourier transform in each section and then combine them to find the overall relationship. For the moment we ignore horizontal adjustments.

1) *Framing.* The dual transformation is a 2D convolution given by

$$L_Q(\mathbf{f}) = \int_{\mathbb{R}^2} d\lambda_x\, d\lambda_y\, Q(\lambda_x, \lambda_y)\, L(f_x - \lambda_x, f_y - \lambda_y, f_t) \tag{116}$$

where (see (39))

$$Q(f_x, f_y) = D_x\, \mathrm{Sinc}\,(f_x D_x)\, D_y\, \mathrm{Sinc}\,(f_y D_y)\,.$$

2) $\mathbb{R}^3 \to I_S$ *sampling.* The dual transformation is a periodic repetition with *repetition centers* given by the reciprocal group $I_S^\star$

$$L_{QS}(\mathbf{f}) = \sum_{\mathbf{p}\in I_S^\star} L_q(\mathbf{f} - \mathbf{p})\,. \tag{117}$$

3) *3D→1D reading.* The first part of this operation is a coordinate change with matrix $\mathbf{A}$. The dual transformation is a coordinate change with matrix $\mathbf{A}^\star$ (see (81)), specifically

$$L_{QSR}(\mathbf{f}) = d(\mathbf{A}^\star)\, L_{QS}(\mathbf{A}^\star \mathbf{f})\,, \tag{118}$$

where $\mathbf{A}^\star$ is given in Tab. 9 for both scanning with memory and instantaneous scanning. The second part is a sum–reduction of the form (see (82))

$$u(t) = \sum_{(y_R, t_R)\in J_{vt}} \ell_{QSR}(t, y_R, t_R)\,.$$

The dual transformation is a zero–reduction (see Tab. 2), specifically

$$U(f) = \mu(J_{vt})\, L_{QSR}(f, 0, 0)\,. \tag{119}$$

Combining (118) and (119) yields:

$$\boxed{U(f) = \mu_0\, L_{QS}\Big(\mathbf{A}^\star (f, 0, 0)\Big)} \tag{120}$$

where $\mu_0 = d(\mathbf{A}^\star)\, \mu(J_{vt})$. It turns out that $\mu_0 = 1/(D_x D_y) = 1$ for all types of scanning (see (112) and Tab. 9). According to (120), the Fourier transform $U(f)$ of the video signal is obtained by "reading" the 3D function $L_{QS}(f_x, f_y, f_t)$ along the straight line described by the parametric equation

$$(f_x, f_y, f_t) = \mathbf{A}^\star (f, 0, 0)\,, \qquad f \in \mathbb{R}\,. \tag{121}$$

Table 9 Composite–shift matrices and their reciprocals.

memory scanning $\mathbf{M}(i{:}1|b)$

$$\mathbf{A} = \begin{bmatrix} v_x & -\dfrac{v_x}{v_y} & -v_x \\ 0 & 1 & 0 \\ 0 & 0 & 1 \end{bmatrix} \qquad \mathbf{A}^\star = \begin{bmatrix} \dfrac{1}{v_x} & 0 & 0 \\ \dfrac{1}{v_y} & 1 & 0 \\ 1 & 0 & 1 \end{bmatrix}$$

instantaneous scanning $\mathbf{I}(i{:}1|b)$

$$\mathbf{A} = \begin{bmatrix} v_x & -\dfrac{v_x}{v_y} & -v_x \\ v_y & 0 & -v_y \\ 1 & 0 & 0 \end{bmatrix} \qquad \mathbf{A}^\star = \begin{bmatrix} 0 & -\dfrac{v_y}{v_x} & 0 \\ 0 & 1 & -\dfrac{1}{v_y} \\ 1 & 0 & 1 \end{bmatrix}$$

fundamental relationships (*i*: interlace order)

$$v_x = D_x N F_q \qquad v_x T_r = D_x$$
$$v_y = i D_y F_q \qquad v_y T_r = i d_y$$

Considering the expression of $\mathbf{A}^\star$ given in Tab. 9, for $\mathbf{M}(i:1|b)$ scanning (120) becomes

$$U(f) = \mu_0 L_{QS}\left(\frac{f}{v_x}, \frac{f}{v_y}, f\right) \tag{122a}$$

so that the straight line is determined by the scanning velocities. In $\mathbf{I}(i:1|b)$ scanning

$$U(f) = \mu_0 L_{QS}(0,0,f) \tag{122b}$$

and the straight line is the f_t axis.

Illustrations of "reading" operations giving the Fourier transforms of video signals are given in Fig.25 for **M**(1:1) and **I**(1:1) scanning. In the first case the repetition centers are $(0, rF_y, sF_q)$, $r,s \in \mathbb{Z}$, so that they lie on the f_y, f_t plane. The reading line is *tilted* with respect to this plane and a typical point being $\left(\frac{1}{D_x}, F_y, NF_q\right)$. The Fourier transform $U(f)$ of the video signal depends on how the reading line intersects the periodic repetitions of $L_{QS}(\mathbf{f})$. Note that in the absence of the *tilt*, $U(f)$ would be periodic.

It is worth noticing that, using the periodicity of $L_{QS}(\mathbf{f})$, reading $U(f)$ from $L_{QS}(\mathbf{f})$ can be confined within the unit cell $\mathbb{R} \times [0,F_y) \times [0,F_q)$, provided that the segments of length F_q of the original reading line are placed within the unit cell, as illustrated in Fig.25. In this way, making suitable correspondences [25], in particular x,y,t coordinates with f_t, f_y, f_t coordinates, reading $U(f)$ from $L_{QS}(\mathbf{f})$ in **M**(1:1) scanning is perfectly analogous to **I**(1:1) image scanning, which produces $u(t)$ from $\ell_{QS}(x,y,t)$ (compare Fig.25a with Fig.18).

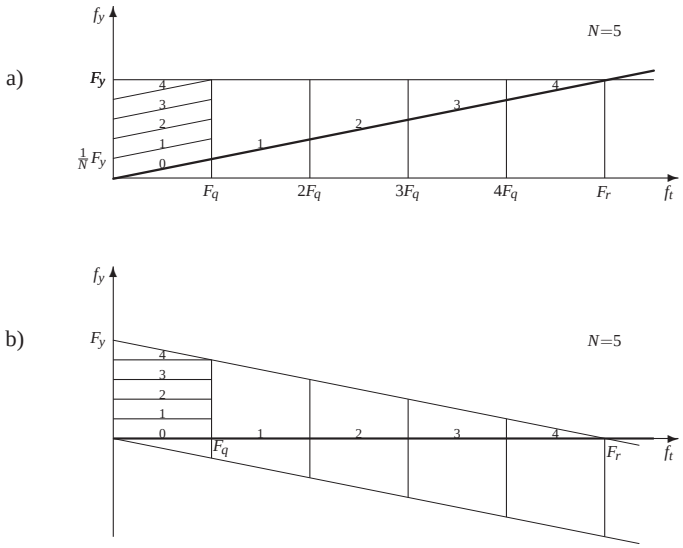

Fig. 25 Illustrations of "reading" operations giving the Fourier transforms of video signals: a) for **M**(1:1) scanning and in b) for **I**(1:1) scanning. In both cases the operation can be reduced to a scanning process.

Similar considerations hold for reading $U(f)$ in **I**(1:1) scanning, which becomes analogous to **M**(1:1) image scanning, as illustrated in Fig.25b.

Effect of framing. An evaluation of the convolution (116) can be avoided in most cases, since $Q(f_x, f_y)$ can be replaced by an impulse $\delta(f_x)\,\delta(f_y)$. However, in some special cases (see below) framing cannot be neglected.

7.3 Analysis in the presence of horizontal adjustments

The requirements of an *adjustment* in some types of $\mathbf{M}(i:1|b)$ scanning complicates the Fourier analysis. The reason is that a horizontal adjustment is not a standard shift, but a *coordinate–dependent* horizontal shift. This is made evident by rewriting (92) in the form

$$\ell'_{QS}(x,y,t) = \ell_{QS}\Big(x - \Delta(t), y, t\Big)$$

where $\Delta(t) = \varepsilon_k D_x$ is the adjustment needed at time $t = kT_f$. In the general case (see (96)), the adjustment has the form $\Delta(y,t)$.

The technique for dealing with such a coordinate–dependent shift may be the following: subdivide the image into *regions* in which $\Delta(y,t)$ is constant and then, within each region, apply the standard shift rule of Fourier analysis. We illustrate this technique for a very elementary case, namely **M**(2;1) continuous scanning with an even number of lines N. In this case a horizontal adjustment of $-\frac{1}{2}D_x$ is required

for odd fields. Let

$$\ell_i(x,y,t) = q_i(t)\,\ell_{QS}(x,y,t)\,, \qquad i = 0,1$$

where $q_0(t)$ and $q_1(t)$ are the indicating functions of even and odd fields, respectively. Then, the adjustment image can be written in the form

$$\ell'_{QS}(x,y,t) = \ell_0(x,y,t) + \ell_1\left(x - \frac{1}{2}D_x,y,t\right).$$

On the other hand, the indicating functions can be written as

$$q_0(t) = \frac{1}{2}\left[1 + e^{j\pi F_f t}\right], \qquad q_1(t) = \frac{1}{2}\left[1 - e^{j\pi F_f t}\right],$$

where the complex form is only apparent, since t runs on $\mathbb{Z}(T_f)$. Then,

$$\begin{aligned}\ell'_{QS}(x,y,t) = {} & \frac{1}{2}\left[\ell_{QS}(x,y,t) + \ell_{QS}\left(x - \frac{1}{2}D_x,y,t\right)\right] \\ & + \frac{1}{2}e^{j\pi F_f t}\left[\ell_{QS}(x,y,t) - \ell_{QS}\left(x - \frac{1}{2}D_x,y,t\right)\right].\end{aligned}$$

This is interpreted by the *filter–modulator model* of Fig.26, where the image $\ell_{QS}(\cdot)$

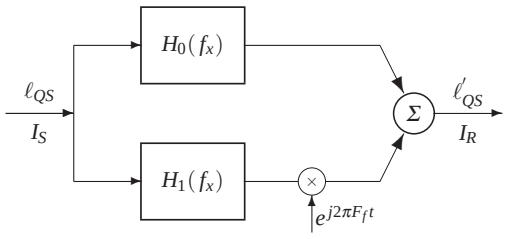

Fig. 26 *Filter–modulator* model of the horizontal adjustment of the field.

is filtered by two *horizontal filters* with frequency responses

$$H_0(f_x) = \frac{1}{2}\left[1 + e^{j\frac{1}{2}D_x f_x}\right], \qquad H_1(f_x) = \frac{1}{2}\left[1 - e^{j\frac{1}{2}D_x f_x}\right].$$

The output of $H_1(f_x)$ is multiplied by the *exponential time carrier* $\exp(j2\pi F_f t)$. This interpretation leads to the relationship

$$L'_{QS}(\mathbf{f}) = H_0(f_x)\,L_{QS}(f_x,f_y,f_t) + H_1(f_x)\,L_{QS}\left(f_x,f_y,f_t - \frac{1}{2}F_f\right).$$

In general $\mathbf{M}(i:1|b)$ continuous scanning the *field offsets* yield a filter–modulator model with i branches, each containing a horizontal filter and a temporal modulator with exponential carrier. In discrete scanning, due to *line–offsets* the number of branches becomes ai and the modulators have vertical–temporal carriers of the

form $\exp\left(j(2\pi F_{my}y+F_{mt}t)\right)$. In each case, once the filter–modulator model has been identified, the analysis becomes straightforward, and the Fourier transform of the adjusted image takes the form

$$L'_{QS}(\mathbf{f}) = \sum_{m=0}^{ai-1} H_m(f_x)\, L_{QS}(f_x, f_y - F_{my}, f_t - F_{mt})\,.$$

7.4 Analysis of reproduction

Using the scheme of Fig.16 it is possible to express the 3D Fourier transform $\tilde{L}_Q(\mathbf{f})$, $\mathbf{f}\in\mathbb{R}^3$, of a replica of the framed image in terms of the 1D Fourier transform $U(f)$, $f\in\hat{J}$, of the video signal. For the condition of correct reproduction (see Section V–B), this gives $L_Q(\mathbf{f})$ in terms of $U(f)$.

In the first part of the scheme (1D→3D *writing*) the sampled image ℓ_{QS} is recovered from $u(t)$ in the sequence 1a) 1D→3D hold dimensionality increase, 1b) coordinate change with matrix $\mathbf{A}^{-1}$, 1c) windowing with $w_{QS}(x,y,t)$, the indicating function of the support of the *framed and sampled image*, given by

$$I_S \cap Q^{(3)} = I_S \cap [0,D_x)\times[0,D_y)\times\mathbb{R}\,. \tag{123}$$

The Fourier analysis of this first part is not immediate, but gives result [25]:

$$L_{QS}(\mathbf{f}) = \int_{\hat{J}} d\lambda\; U(\lambda)\, W_{QS}\Big(\mathbf{f} - \mathbf{A}^{\star}(\lambda,0,0)\Big)\,. \tag{124}$$

The Fourier analysis of the interpolating filter is immediate, namely

$$L_Q(\mathbf{f}) = G(\mathbf{f})\, L_{QS}(\mathbf{f})\,, \qquad \mathbf{f}\in\mathbb{R}^3\,,$$

where $G(\mathbf{f})$ is the frequency response of the filter.

The formula (124) does not reveal the interpolating nature of writing operation. A more explicit result is obtained after evaluating $W_{QS}(\mathbf{f})$, the Fourier transform of the indicating function of the set (123). This result is

$$\boxed{L_{QS}(\mathbf{f}) = \sum_{k\in\mathbb{Z}} W_k(f_x, f_y, f_t - kF_q)\, U(f_t - kF_q)} \tag{125}$$

where the *interpolating function* is given by

$$W_k(\mathbf{f}) = Q_{\mathcal{M}}(f_x - kF_{13} - c_{11}f_t,\, f_y - kF_{23} - c_{21}f_t)\,. \tag{126}$$

Here, $Q_{\mathcal{M}}(f_x, f_y)$ is the Fourier transform of the indicating function of the framed mosaic $Q\cap\mathcal{M}(I_S)$ of the scanning group, (F_{13}, F_{23}, F_q) represents the third column

of the upper–triangular base of $I_S^\star$ (see Tab. 7 and Tab. 8), and $(c_{11}, c_{21}, 1)$ is the first column of the matrix $\mathbf{A}^\star$ (see Tab. 9).

As an example, using the lattice of Example 5 as the scanning group, we find

$$\mathcal{M}(I_S^\star) = Z_2^1\left(\frac{1}{2}F_x, \frac{1}{2}F_y\right), \quad F_{13} = \frac{1}{2}F_x\,,\ F_{23} = \frac{1}{4}F_y\,,\ F_{33} = \frac{1}{4}F_f\,,$$

$$c_{11} = \frac{1}{v_x} = \frac{4}{ND_xF_f} = \frac{4}{NM}\,\frac{F_x}{F_f}\,, \qquad c_{21} = \frac{1}{v_y} = \frac{1}{D_xNF_q} = \frac{2}{N}\,\frac{F_y}{F_f}\,,$$

$$Q_{\mathcal{M}}(f_x, f_y) = D_xD_y\,\Big[\mathrm{Sinc}_{\frac{1}{2}M}(f_xD_x)\,\mathrm{Sinc}_N(f_yD_y) + \mathrm{Sinc}_{\frac{1}{2}M}\left(f_xD_x - \frac{1}{2}M\right)\,\mathrm{Sinc}_N\left(f_yD_y - \frac{1}{4}N\right)\Big]\,.$$

The last function is illustrated in Fig.27.

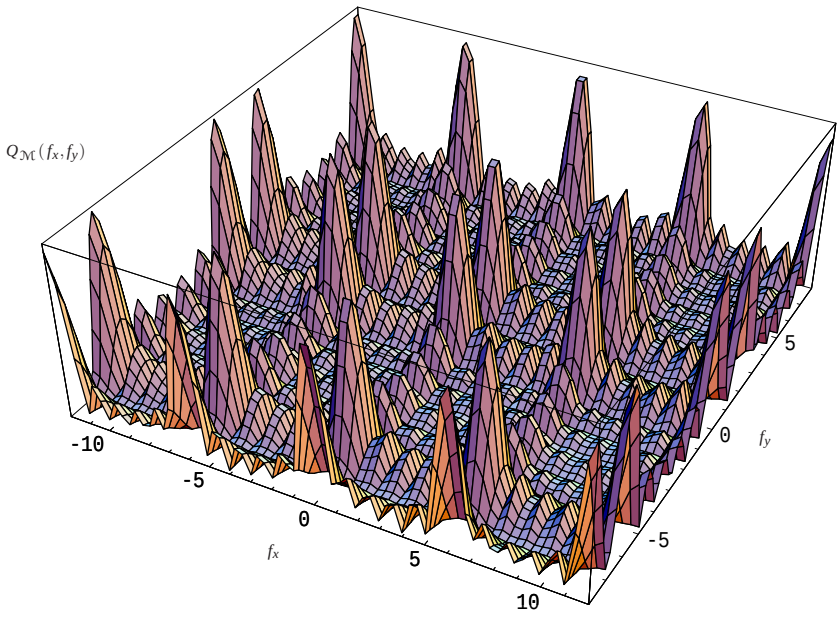

Fig. 27 Example of the Fourier transform $Q_{\mathcal{M}}(f_x, f_y)$ of the mosaic indicating function illustrated for $M = 12$ and $N = 8$.

8 Spectral Analysis of Scanning Process

The preceding theory is tacitly based on *deterministic signals* and corresponding Fourier transforms in the frequency domain (Fourier analysis). An alternative, more sophisticated, approach is based on *random processes* and corresponding spectral densities in the frequency domain (spectral analysis). The latter is usually performed under the assumption of (wide–sense) stationarity. For a time–varying image $\ell(x,y,t)$ stationarity requires that the correlation

$$r_\ell(\Delta x,\Delta y,\Delta t) \stackrel{\Delta}{=} \mathrm{E}\left[\ell(x+\Delta x,y+\Delta y,t+\Delta t)\,\ell(x,y,t)\right]$$

is independent of the reference point (x,y,t). In such case, the spectral density $R_\ell(\mathbf{f})$ is defined as the 3D Fourier transform of the correlation. Unfortunately, in the scanning process most of the operations are not shift invariant and, even starting with a stationary source image, stationarity is soon lost. Then, one must proceed with the tools of spectral analysis for nonstationary random processes, where correlation becomes dependent on the reference point. Correlations and spectral densities become 6D functions and spectral analysis becomes a formidable problem, which falls outside the scope of the present paper.

Here, we discuss only *average* spectral analysis of the video signal, which is quite simple and very similar to Fourier analysis. Assuming that the source image is stationary with given spectral density $R_\ell(f_x,f_y,f_t)$, $(f_x,f_y,f_t)\in\mathbb{R}^3$, it can be shown (by means of nonstationary spectral analysis) that the video signal $u(t)$ turns out to be *cyclostationary* with period T_q, the frame period. This means that the correlation $r_u(\tau,t) \stackrel{\Delta}{=} \mathrm{e}[u(t+\tau)\,u(t)]$ is periodic with respect to the reference time t, with period T_q. Then, the *average* correlation $\bar{r}_u(\tau)$ is obtained by averaging $r_u(\tau,t)$ in a period and, finally, the average spectral density results as the Fourier transform of $\bar{r}_u(\tau)$, namely

$$\bar{R}_u(f) = \int_J d\tau\,\bar{r}_u(\tau)\,e^{-j2\pi f\tau}, \qquad f\in\hat{J}.$$

Note that $\bar{r}_u(\tau)$ has the same domain J as the video signal, so that $\bar{R}_u(f)$ is a continuous–frequency function, aperiodic in continuous scanning ($\hat{J}=\mathbb{R}$) and periodic in discrete scanning ($\hat{J}=\mathbb{R}:\mathbb{Z}(F_e)$).

The *average* spectral density of $u(t)$ can be calculated following the steps [25]:

1) Evaluate the spectral density after $\mathbb{R}^3\to I_S$ sampling, as

$$R_{\ell_S}(\mathbf{f}) = \sum_{\mathbf{p}\in I_S^\star} R_\ell(\mathbf{f}-\mathbf{p})\,. \tag{127}$$

2) Evaluate the 2D convolution

$$\tilde{R}_{\ell_{QS}}(\mathbf{f}) = \int_{\hat{K}_0} da_x\,da_y\,|Q_{\mathcal{M}}(a_x,a_y)|^2\,R_{\ell_S}(f_x-a_x,f_y-a_y,f_t) \tag{128}$$

where $Q_{\mathcal{M}}(f_x,f_y)$ is the Fourier transform of the indicating function of the framed mosaic (see above) and K_0 is the mosaic.

3) Find the average spectral density of the video signal, given by

$$\bar{R_u}(\mathbf{f}) = \mu_0^2 \, \tilde{R}_{\ell_{QS}}\Big(\mathbf{A}^\star(f,0,0)\Big)\,, \tag{129}$$

i.e. by reading the 3D function[13] $\tilde{R}_{\ell_{QS}}(\mathbf{f})$ along the straight line in (f_x, f_y, f_t)–space

$$(f_x, f_y, f_t) = \mathbf{A}^\star(f,0,0)\,.$$

In (128) the integral extends to a unit cell $[\mathbb{R}^2 : K_0^\star)$, which may be $\mathbb{R}\times[0,F_y)$ in $\mathbf{M}(i:1|b)$ continuous scanning (see (64)) and $[0,F_x)\times[0,F_y)$ in discrete scanning, when the mosaic is $\mathcal{M}(I_S) = \mathbb{Z}(d_x,d_y)$.

In most applications the effect of framing is negligible, and (128) can be approximated as

$$\tilde{R}_{\ell_{QS}}(\mathbf{f}) = R_{\ell_S}(\mathbf{f})\,.$$

This result is obtained by replacing $|Q_{\mathcal{M}}(f_x,f_x)|^2$ (not $Q_{\mathcal{M}}(f_x,f_y)$) by the appropriate impulse. We note, however, that a correct formulation of spectral analysis in scanning theory requires the introduction of framing. Meaningless results would otherwise be achieved, in particular the cyclostationarity of the video signal would not be recognized. This does not exclude that framing may be neglected *a posteriori*.

8.1 Example

Consider a *sinusoidal* source image

$$\ell(x,y,t) = L_0 \, \cos\left[2\pi\Big(f_{x0}x + f_{y0}y + f_{yt}t\Big) + \varphi\right]$$

where $\mathbf{f}_0 = (f_{0x}, f_{0y}, f_{0t})$ are fixed frequencies and φ is a random phase uniformly distributed over $[0,2\pi)$. This image is stationary with spectral density

$$R_\ell(\mathbf{f}) = \frac{1}{4}L_0^2 \, \delta_{\mathbb{R}^3}(\mathbf{f}-\mathbf{f}_0) + \frac{1}{4}L_0^2 \, \delta_{\mathbb{R}^3}(\mathbf{f}+\mathbf{f}_0)\,.$$

Applying the above procedure yields the following result for the average spectral density of the video signal [25]

$$\bar{R_u}(\mathbf{f}) = \frac{1}{4}L_0^2 \sum_{k\in\mathbb{Z}} \Big[|A_k(+)|^2 \, \delta_{\mathbb{R}}(f - f_{0t} - kF_q) + |A_k(-)|^2 \, \delta_{\mathbb{R}}(f + f_{0t} + kF_q)\Big] \tag{130}$$

where

[13] The function $R_{\ell_S}(\mathbf{f})$ is an ordinary spectral density, since $\mathbb{R}^3 \to I_S$ sampling preserves stationarity. The function $\tilde{R}_{\ell_{QS}}(\mathbf{f})$ is a fictitious spectral density, useful in the final calculation.

$$A_k(\pm) = \mu_0\, Q_{\mathcal{M}}\Big(c_{11}(f_{0t}+kF_q) \mp f_{0x} - kF_{13}, c_{21}(f_{0t}+kF_q) \mp f_{0y} - kF_{23}\Big) \quad (130a)$$

and c_{11}, c_{21}, F_{13}, F_{23} are the same as in (126).

Note that in this example framing cannot be ignored, since it is essential for determining the amplitudes of the spectral lines in (130).

9 Application to HDTV

In principle, High Definition Television (HDTV) does not require a specific scanning theory since the process is the same as for ordinary television, i.e. a conversion of a time–varying image into a 1D signal. However, the enormous amount of information involved (four times than of standard TV) and the requirement to use conventional transmission channels and storage media requires some operations that may be regarded *as typical of HDTV*. One of these is the *subsampling* technique, used in both MUSE and HD–MAC standards, which essentially reduces the density of the $\mathbf{M}(2{:}1)$ lattice by a factor of four with a consequent reduction in signal bandwidth. Another typical HDTV operation is the *line–shuffling* technique, which converts a 1250–line format to a 625–line format, thus assuring the down–compatibility of HD–MAC with respect to the MAC standard. A signal theory approach to these techniques is presented in the final chapters of [25]. Here, we examine multiplexing of luminance and chrominance information as used in the HD–MAC standard.

9.1 Component multiplexing in HD–MAC

In the Multiplexed Analog Components (MAC) system, the luminance (Y) and chrominance (U and V) components are conveyed together in the video signal.[14] The technique is Time–Compression Multiplexing (TCM). Specifically, in each line period T_r, the components Y, U and V are compressed in such a way that a fraction of T_r, say 2/3, is devoted to Y leaving the remaining 1/3 to U and V. The latter are inserted alternatively, U in even lines, V in odd lines.

Conceptually this technique is very simple, although its formulation and analysis is quite complicated as in normal for TCM. This is because for each component the signal compression does not have the standard form $u(at)$, where $a > 1$ is the compression factor. Instead it is a *cyclic* compression, which (conceptually) works at follows: 1) subdivide each component into portions of length T_r, 2) compress each portion by the appropriate factor, and 3) shift the compressed portions to the appropriate time slot. Note that step 1) involves *windowing* the components, with the consequent complication of the frequency analysis.

It is possible to overcome the above difficulties by working at the image level rather than at the video signal level. The idea is to horizontally compress the image

[14] MAC also provides multiplexing of data, containing audio channels in digital form. Here, for simplicity, data are neglected.

signals of the Y, U, V components, thus creating a fictitious multiplexed image from which the scanning process produces the desired multiplexed video signal. The simplifying trick relies on the fact that working at the image level *windowing* is automatically assured by framing.

We now develop the MAC theory in two steps. First we combine U and V into a "color" component C, and then multiplex Y and C.

9.2 Alternating combination of U and V components

This combination does not represent multiplexing, but a *sampling* process, since half of the lines are dropped for each component U and V. Referring to **M**(2:1) continuous scanning, we examine the vertical–temporal lattice, i.e. $Z_2^1(d_y, T_f)$, where lines are represented by their y,t projections. Originally both U and V (as well as Y) fill all $Z_2^1(d_y, T_f)$ positions (Fig. 28). However, after thinning out and inter-

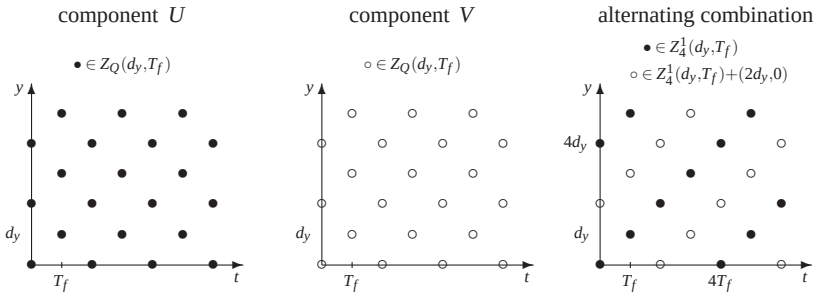

Fig. 28 Alternating components U and V from the images $\ell(\cdot)_U$ and $\ell(\cdot)_V$.

leaving, between them they fill this lattice. Inspection of Fig. 28c shows that in the end U fills the points of the sub–lattice $Z_4^1(d_y, T_f)$, which would correspond to the vertical–temporal lattice of the **M**(4:1|1) scanning, whereas V fills its shifted version $Z_4^1(d_y, T_f) + (2d_y, 0)$.

To correctly write the "virtual" combined image C, we must introduce the indicating functions $q_U(y,t)$ and $q_V(y,t)$ of the final subsets U and V (denoted by • and ○ in Fig. 28c). Then

$$\ell_{QS}(x,y,t) = q_U(y,t)\,\ell_{QS}(x,y,t)_U + q_V(y,t)\,\ell_{QS}(x,y,t)_V\,, \tag{131}$$

where $\ell_{QS}(\cdot)_U$ and $\ell_{QS}(\cdot)_V$ are U and V images and $\ell_{QS}(\cdot)_C$ is their alternating combination.

Consider in particular the sampling of the U component in the y,t plane (no changes take place in x). In this plane the original lattice is $J = Z_2^1(d_y, T_f)$, the final lattice $K = Z_4^1(d_y, T_f)$. Their reciprocals are (see (112)):

$$J^\star = Z_2^1\left(\frac{1}{2}F_y, \frac{1}{2}F_f\right), \qquad K^\star = Z_4^3\left(\frac{1}{4}F_y, \frac{1}{4}F_f\right) \tag{132}$$

The effects of sampling are illustrated in Fig.29 in terms of the spectral supports: in

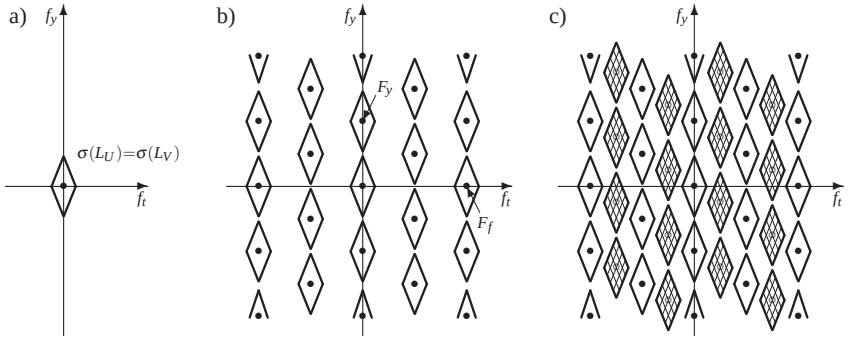

Fig. 29 a) Spectral support of components U and V, b) Periodic repetition due to $\mathbf{M}(2{:}1)$ scanning, and c) additional terms due to suppressing half the lines.

a) the original support $\sigma(L_U)$ of the unsampled component U, in b) the support after vertical–temporal sampling $\mathbb{R}^2 \to Z_2^1(d_y, T_f) = J$, which causes a periodic repetition with centers given by $J^\star$, and in c) the support after $Z_2^1(d_y, T_f) \to Z_4^1(d_y, T_f) = K$ sampling, which halves the number of lines. The latter causes *additional* repetitions. In fact, $K^\star$ is twice as dense as $J^\star$, and can be decomposed as

$$K^\star = J^\star + \left\{(0,0), \left(\frac{1}{4}F_y, \frac{3}{4}F_f\right)\right\}. \tag{133}$$

This means that $K^\star$ can be obtained from a replica of $J^\star$, with *additional* points given by the $\left(\frac{1}{4}F_y, \frac{3}{4}F_f\right)$–shifted version of $J^\star$.

Then, to ensure that the component U can be fully recovered (in the reproduction process) after having dropped half the lines, the original support $\sigma(L_U)$ must be small enough for additional repetitions not to cause aliasing (as shown in the figure). The correct condition is that the f_x, f_y projection of $\sigma(L_U)$ is contained in a unit cell of $\mathbb{R}^2$ modulo $K^\star$.

Similar considerations hold for dropping lines of the component V.

These results are confirmed by Fourier analysing the whole thinning–interleaving operation stated in (131). For such analysis it is convenient to use appropriate formulas for the indicating functions,[15] specifically

[15] The technique for finding these formulas is to recognize that the indicating functions are periodic and can be expressed by an appropriate impulse, and then to apply orthogonality conditions (37) (in the present case with $I = Z_2^1(d_y, T_f) : Z_4^1(d_y, T_f)$).

$$
\begin{aligned}
q_U(y,t) &= \frac{1}{2}\left[1+\exp j2\pi\left(\frac{1}{4}\frac{y}{d_y}+\frac{3}{4}\frac{t}{T_f}\right)\right] \\
q_V(y,t) &= \frac{1}{2}\left[1-\exp j2\pi\left(\frac{1}{4}\frac{y}{d_y}+\frac{3}{4}\frac{t}{T_f}\right)\right],
\end{aligned}
\tag{134}
$$

Then, (131) yields

$$
\begin{aligned}
L_{QS}(\mathbf{f})_C &= \frac{1}{2}\left[L_{QS}(\mathbf{f})_U + L_{QS}(\mathbf{f}-\mathbf{f}_0)_U + L_{QS}(\mathbf{f})_V - L_{QS}(\mathbf{f}-\mathbf{f}_0)_V\right] \\
\mathbf{f} &= (f_x, f_y, f_t), \quad \mathbf{f}_0 = \left(0, -\frac{1}{4}F_y, \frac{1}{4}F_t\right).
\end{aligned}
\tag{135}
$$

The result confirms the presence of *additional* repetitions via the frequency $\mathbf{f}_0$.

9.3 Image multiplexing

The combined color image $\ell_{QS}(\cdot)_C$ obtained by the above procedure can be multiplexed with the luminance image $\ell_{QS}(\cdot)_Y$ to form a "virtual" image, which scanned yields the correctly multiplexed video signal. The idea is illustrated in Fig.30, where

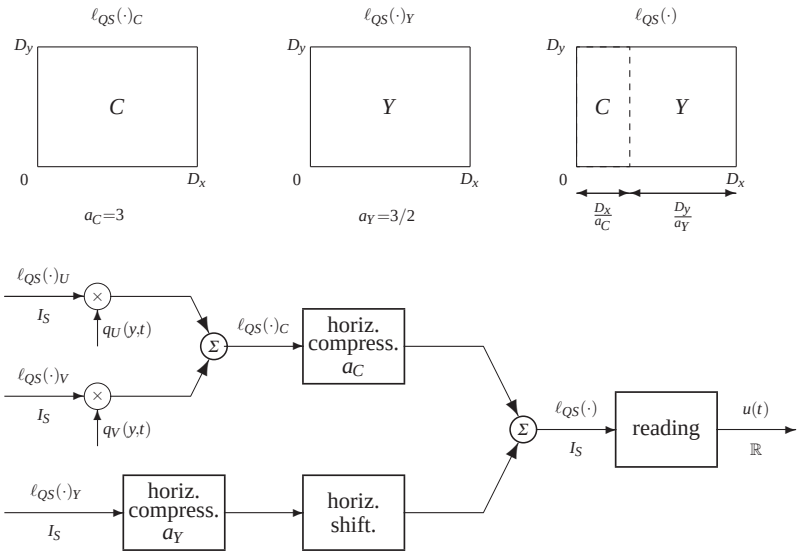

Fig. 30 MAC multiplexing performed on the image level by horizontally compressing the combined colour image C and the luminance image Y.

$\ell_{QS}(\cdot)_C$ and $\ell_{QS}(\cdot)_Y$ are limited to the ordinary frame dimension $[0,D_x)\times[0,D_y)$. They are then horizontally compressed according to the respective compression ra-

tios a_C and a_Y, namely

$$\ell_{QS}(a_C x, y, t)_C \qquad \text{and} \qquad \ell_{QS}(a_Y x, y, t)_Y$$

where

$$\frac{1}{a_C} + \frac{1}{a_Y} = 1\,. \tag{136}$$

In the HD–MAC standard these are either $a_C = 3$, $a_Y = 3/2$ or $a_C = 5$, $a_Y = 5/4$. After compression the horizontal frame dimensions become, respectively, D_x/α_C and D_y/α_Y. Then, the Y compressed image is horizontally shifted by D_x/α_C and summed with the C compressed image, to give the virtual image

$$\ell_{QS}(x,y,t) = \ell_{QS}(a_C x, y, t)_C + \ell_{QS}\left(a_Y\left(x - \frac{1}{a_C} D_x\right), y, t\right). \tag{137}$$

Note that 1) the *windowing* effect of framing, 2) the reciprocal aspect ratios according to (136), and 3) the horizontal shift of Y, ensure correct image multiplexing. It is straightforward to check that the **M**(2:1) reading process applied to the virtual image yields the correct MAC video signal.

Hence, formulating MAC *in the image domain* according to (137) is trivial and remains very easy even in the frequency domain. In fact, using elementary rules of Fourier analysis, from (137) we get

$$\begin{aligned} L_{QS}(f_x, f_y, f_t) = {} & \frac{1}{a_C} L_{QS}\left(\frac{f_x}{a_C}, f_y, f_t\right)_C \\ & + \frac{1}{a_Y} L_{QS}\left(\frac{f_x}{a_Y}, f_y, f_t\right)_Y e^{-j2\pi f_x (a_Y/a_C) D_x}\,. \end{aligned} \tag{138}$$

Then, to find the Fourier transform of the video signal, starting from $L_{QS}(\mathbf{f})$ we can use (122a), i.e.[16]

$$U(f) = \mu_0\, L_{QS}\left(\frac{f}{v_x}, \frac{f}{v_y}, f\right). \tag{139}$$

In conclusion, for Fourier analysis, starting from $L_{QS}(\mathbf{f})_U$, $L_{QS}(\mathbf{f})_V$ and $L_{QS}(\mathbf{f})_Y$, we first calculate $L_{QS}(\mathbf{f})_C$ according to (135), to then apply (138) and (139).

Similar results are obtained for *spectral analysis*, which, starting from the spectral densities of the luminance and the color images, leads to the average spectral density of the video signal.

References

1. E.C. Titchmarsh, *Introduction to the Theory of Fourier Integrals*, Oxford, Oxford University Press, 1937.

[16] Note that in HD–MAC standard the number of lines is even ($N = 1250$). Correct reading would then include a horizontal field offset (see Section V–C), here omitted.

2. H.S. Carslaw, *Introduction to the Theory of Fourier's Series and Integrals*, 3rd ed., Dover Publications, New York, 1952.
3. P.M. Woodward, *Probability and Information Theory, with Applications to Radar*, Pergamon Press, Macmillan, New York, 1953.
4. A. Papoulis, *The Fourier Integral and its Applications*, New York, McGraw–Hill, 1962.
5. G.R. Cooper, C.D. McGillem, *Methods of Signal and System Analysis*, Holt, Rinehart and Winston, New York, 1967.
6. L.E. Franks, *Signal theory*, Englewood Cliffs, Prentice–Hall, 1969.
7. W.R. Bennet, *Introduction to Signal Transmission*, New York: McGraw–Hill, 1970.
8. H. Dym, H.P. McKean, *Fourier Series and Integrals*, New York, Academic Press, 1972.
9. L.R. Rabiner, C.M. Rader, Eds., *Digital Signal Processing*, IEEE Press, New York, 1972.
10. R.A. Gabel, R.A. Roberts, *Signals and Linear Systems*, John Wiley and Sons, New York, 1973.
11. J.B. Cruz, M.E. Van Valkenburg, *Signals in Linear Circuits*, Houghton Mifflin Company, Boston, 1974.
12. G.R. Cooper, C.D. McGillem, *Continuous and Discrete Signal and System Analysis*, Holt, Rinehart and Winston, New York, 1974.
13. L.R. Rabiner, B. Gold, *Theory and Application of Digital Signal Processing*, Prentice–Hall, Englewood Cliffs, NJ, 1975.
14. A.V. Oppenheim, R.W. Schafer, *Digital Signal Processing*, Prentice–Hall, Englewood Cliffs, NJ, 1975.
15. A. Papoulis, *Signal Analysis*, New York, McGraw–Hill, 1977.
16. L.R. Rabiner, R.W. Schafer, *Digital Processing of Speech Signals*, Prentice–Hall, Englewood Cliffs, NJ, 1978.
17. L. Schwartz, *Information Transmission, Modulation and Noise: A Unified Approach to Communications Systems*, 3rd ed., McGraw–Hill Book Company, New York, 1980.
18. A. Papoulis, *Circuits and Systems*, Holt, Rinehart and Winston, New York, 1980.
19. A.V. Oppenheim, A.S. Willsky, I.T. Young, *Signals and Systems*, Prentice–Hall, Englewood Cliffs, NJ, 1983.
20. W.M. Siebert, *Circuits, Signals and Systems*, McGraw–Hill Book Company, New York, 1986.
21. J.S. Lim, A.V. Oppenheim, Eds., *Advanced Topics in Signal Processing*, Prentice–Hall, Englewood Cliffs, NJ, 1988.
22. G. Cariolaro, *Unified Signal Theory*, Springer–Verlag, 2011

23. G. Cariolaro, *A Unified Signal Theory (topological approach)*, *Proc. of Italy–USA Seminary on Digital Signal Processing*, Portovenere, Agost 1981.

24. P. Kraniauskas, *Transforms in Signals and Systems*. Wokingham, Addison–Wesley, 1992

25. G. Cariolaro, *Teoria dei Segnali Multidimensionali con applicazione alla HDTV*, Edizioni Scientifiche Telettra, 1995

26. A. Papoulis, *Systems and Transforms with Applications in Optics*, McGraw–Hill Book Company, New York, 1968.

27. D.E. Pearson, *Transmission and Display of Pictorial Information*, New York, Wiley, 1975.

28. W. Pratt, *Digital Image Processing*, John Wiley and Sons, New York, 1978.

29. R.E. Crochiere, L.R. Rabiner, *Multirate Digital Signal Processing*, Englewood–Cliffs, NJ, Prentice–Hall, 1983.

30. D.E. Dudgeon, R.M. Mersereau, *Multidimensional Digital Signal Processing*, Englewood–Cliffs, NJ, Prentice–Hall, 1984.

31. R.N. Bracewell, *The Fourier Transform and its Applications*, 2nd revised ed., McGraw–Hill Book Company, New York, 1986.

32. S.G. Tzafestas (Ed.), *Multidimensional Systems: Techniques and Applications*, New York, Marcel Dekker, 1986.

33. J.S. Lim, *Two–Dimensional Digital Signal Processing*, Prentice–Hall, Englewood Cliffs, 1989.

34. K.R. Rao, P. Yip, *Discrete Cosine Transform*, Academic Press, San Diego, 1990.

35. D.P. Petersen, D. Middleton, "Sampling and reconstruction of wave–number–limited functions in *N*–dimensional Euclidean spaces", *Informat. Contr.*, vol. 5, 1962, pp. 279–323.

36. N.T. Gaarder, "A note on the multidimensional sampling theorem", *Proc. IEEE*, vol. 60, February 1972, pp. 247–248.

37. A.H. Robinson, "Multidimensional Fourier transform and image processing with finite scanning apertures", *Appl. Opt.*, vol. 12, October 1973, pp. 2344–2352.

38. T.C. Chen, R.J.P. de Figueiredo, "Image decimation and interpolation techniques based on frequency domain analysis", *IEEE Trans. Commun.*, vol. COM–32, pp. 479–484, April 1984.

39. E. Dubois, "The Sampling and Reconstruction of Time–Varying Imagery with Application in Video Systems". *Proc. IEEE*, vol. 73, April 1985, pp. 502–523.

40. L. Vangelista, "Rappresentazione triangolare di un reticolo", Dipartimento di Elettronica e Informatica, Università di Padova, April 1990.

41. P. Mertz, F. Gray, "A Theory of Scanning and its Relation to the Characteristics of the Transmitted Signal in Telephotography and Television", *Bell Syst. Tech. J.*, vol. 13, 1934, pp. 464–515.

42. J.O. Drewery, “The filtering of luminance and chrominance signals to avoid cross–colour in a PAL colour system”, *BBC Eng.*, pp. 8–39, Sept. 1976.

43. G.J. Tonge, “The sampling of television images”, Independent Broadcasting Authority, Experimental and Development Rep. 112/81, Mayh 1981.

44. G.J. Tonge, ”Three–dimensional filters for television sampling”, Independent Broadcasting Authority, Experimental and Development Rep. 117/82, June1982.

45. G.J. Tonge, “The television scanning process”, *SMPTE J.*, vol. 93, pp. 657–666, July 1984.

46. G. Vannucchi, “Una nuova frontiera nella trasmissione delle immagini: la televisione ad alta definizione. Il perché di questo numero speciale della Rivista Telettra”, *Rivista Telettra* (edizione speciale dedicata all’HDTV), vol. 45, 1, pp. 3–8, 1990.

47. M. Fichera, “Un bel dì vedremo - L’avventura della RAI nell’alta definizione”, *Rivista Telettra* (edizione speciale dedicata all’HDTV), vol. 45, 1, pp. 9–16, 1990.

48. F. Cappuccini, M. Krivocheev, “Una panoramica sulla standardizzazione dell’HDTV”, *Rivista Telettra* (edizione speciale dedicata all’HDTV), vol. 45, 1, pp. 17–34, 1990.

49. D. Grandi, A. Riccomi, “I principali aspetti dello scenario tecnico–economico della televisione e i progetti EU–95 ed EU–256 per l’HDTV”, *Rivista Telettra* (edizione speciale dedicata all’HDTV), vol. 45, 1, pp. 35–56, 1990.

50. A.H. Zemanian, *Distribution Theory and Transform Analysis: An Introduction to Generalized Functions, with Applications*, McGraw–Hill Book Company, New York, 1965.

51. J. Arsac, *Fourier Transforms and the Theory of Distributions*, Heim, Prentice–Hall, Englewood Cliffs, NJ, 1966.

52. L. Schwartz, *Théorie des distributions*, Paris, Hermann, 1966.

53. I.M. Gelfand et al., *Generalized Functions*, (5 volumes), New York, Academic Press, 1968.

54. A. Haar, “Der Massbegriff in der Theory der kontinuierlichen Gruppen”, *Annals of Mathematics*, vol. 34, 1933, pp. 147–169.

55. A. Weil, *L’Integration dans les Groupes Topologiques*, Paris, Hermann P.C., 1940.

56. L. Pontriagin, *Topological Groups*, Princeton University Press, 1946.

57. P. Halmos, *Measure Theory*, Princeton, Van Nostrand, 1950.

58. L.H. Loomis, *An Introduction to Abstract Harmonic Analysis*, New York, Van Nostrand, 1953.

59. N. Bourbaki, *Integration*, Paris, Hermann, 1959.

60. W. Rudin, *Fourier Analysis on Groups*, New York, Interscience Publishers, 1962.

61. J.W.S. Cassels, *An Introduction to the Geometry of Numbers*, Berlin, Germany, Springer–Verlag, 1959.

62. E. Hewitt, K.A. Ross, *Abstract Harmonic Analysis*, Berlin, Springer–Verlag, vol. 1 and vol. 2, 1963.

63. L. Nachbin, *The Haar Integral*, Princeton, N.J., Van Nostrand Co., 1965.

64. N. Bourbaki, *General Topology*, Part 1 and Part 2, Paris, Hermann, 1966.

65. N. Bourbaki, *Theory of sets*, Reading: Addison–Wesley, Hermann, 1968.

66. J.M. Ziman, *Principles of the Theory of Solids*, Cambridge, UK, Cambridge Univ. Press, 1972.

67. P.J. Higgins, *Introduction to Topological Groups*, London, Cambridge University Press, 1974.

68. A. Orsatti, *Introduzione ai gruppi abeliani astratti e topologici*, Bologna, Pitagora Ed., 1979.

69. R.C. Singleton, "A Method for Computing the Fast Fourier Transform with Auxiliary Memory and Limited High–Speed Storage", *IEEE Trans. Audio Electroacoustics*, vol. AU–15, June 1967, pp. 91–97.

70. G. Cariolaro, *Trasmissione Numerica*, Padova, Cleup, 1985.

71. G. Cariolaro, *Modulazione*, Padova, Cleup, 1987.